

## *Chapter 17*

# *The Lax–Wendroff Family of Space-Centred Schemes*

The space-centred algorithms for the Euler equations were historically the first to be derived and still form the basis and the reference for all the other schemes derived since then.

The second-order accurate scheme of Lax and Wendroff is the most important of them, due to its uniqueness for linear equations (it is the unique second-order central explicit scheme for the linear convection equation on a three-point support) and its essential role as the guideline for all schemes attempting to improve certain of its deficiencies. Since all centred second-order accurate schemes refer to the Lax–Wendroff algorithm, its weaknesses, such as the generation of oscillations at discontinuities, play an essential role in the understanding of the behaviour of centrally discretized schemes.

The essential property of the Lax–Wendroff schemes lies in the combination of time and space-centred discretizations. This is required in order to achieve second-order accuracy with an explicit time integration on a three-point support, and the Lax–Wendroff schemes are therefore the simplest explicit schemes of second-order accuracy.

Although this scheme is unique for the one-dimensional linear convection equation, many variants can be defined for non-linear fluxes, even in one dimension. They all reduce to the same linear form and are generally structured as predictor–corrector algorithms with an explicit time integration. However, implicit extensions have been developed and will be presented in Section 17.4.

*We will consider in the following all centred explicit or implicit schemes of second-order accuracy with combined space–time discretization as belonging to the Lax–Wendroff family.*

We will generally present the various schemes in their one-dimensional form and after a one-dimensional analysis we will introduce their multi-dimensional formulations and illustrate some properties by examples of applications.

The one-dimensional scalar, non-linear conservative form will be considered as

$$\frac{\partial u}{\partial t} + \frac{\partial f}{\partial x} = q$$

or in quasi-linear form as

$$\frac{\partial u}{\partial t} + a(u) \frac{\partial u}{\partial x} = q \quad \text{with } a(u) = \frac{\partial f}{\partial u}$$

When written as a system we will use  $U$  as the basic set of variables and  $A(U)$  as the Jacobian matrix. Similar conventions apply to the multi-dimensional case.

The field of one-dimensional flows offers a wide test space for methods and algorithms for the numerical computation of inviscid, steady or unsteady flows. This is due to a combination of complexity of the one dimensional Euler equations, making them representative of the full non-linearity of real flows and of sufficient simplicity, allowing the existence of exact solutions for both stationary and time-dependent situations.

In addition, the idealized one-dimensional Burgers equation,  $u_t + uu_x = 0$ , and the even simpler case of the linearized, first-order wave equation,  $u_t + au_x = 0$ , offer non-trivial test cases for accuracy and convergence properties of numerical schemes for hyperbolic equations, particularly with regard to the extremely difficult problem of representing accurately propagating discontinuities such as shock waves or contact discontinuities; several examples were presented in Volume 1.

Nearly all existing schemes have initially been analysed and developed on a one-dimensional basis and a considerable literature on the properties of one-dimensional algorithms, including topics such as stability and dissipation properties, influence of boundary conditions on convergence and accuracy, treatment of discontinuities, etc., is available.

An existing scheme that behaves satisfactory on a one-dimensional basis might lead to difficulties in its extension to two- or three-dimensional flows. However, there is no example of a scheme that failed in the one-dimensional version and still worked well in its multi-dimensional extensions. It is therefore safe to say and to recommend that any scheme should first be tested on a one-dimensional basis before extending it to multi-dimensional problems.

An essential property of discretized schemes, already discussed in Section 6.1 in Volume 1, is the *conservative* property. Essentially, this property requires that the time derivative of the integral of  $U$  over a given space domain only depends on the boundary fluxes and not on the fluxes within this domain. This ensures that the discretization technique actually represents a discrete approximation to the integral form of the conservation laws.

The conservative property of a discretization leads to a unified formulation of a scheme by the introduction of a *numerical flux*  $\bar{F}^*$ , where  $\bar{F}^*$  is a function of mesh point values  $U$ , with components  $f^*$ ,  $g^*$  see Lax (1957). All conservative explicit schemes have to be expressed in the following form, written here in two dimensions:

$$U_{ij}^{n+1} - U_{ij}^n = \frac{-\Delta t}{\Delta x} (f_{i+1/2,j}^* - f_{i-1/2,j}^*) - \frac{\Delta t}{\Delta y} (g_{i,j+1/2}^* - g_{i,j-1/2}^*)$$

with the consistency condition

$$\begin{aligned} f^*(U_j, \dots, U_{j+k}) &= f(U) && \text{when all } U_j = U \\ g^*(U_j, \dots, U_{j+k}) &= g(U) && \text{when all } U_j = U \end{aligned}$$

In Section 17.1, we will introduce the first-order Lax–Friedrichs scheme which, although not belonging to the Lax–Wendroff family, has in common the combined space–time and space-centred discretization. Historically, it is the unsatisfactory behaviour of this scheme that has led Lax and Wendroff to search for a second-order discretization.

The other sections will be devoted to the analysis of the basic explicit Lax–Wendroff scheme in one and two dimensions, including the non-linear variant of MacCormack and their generalization by Lerat and Peyret.

Several properties of these schemes have already been introduced in Chapters 8 and 9 of Volume 1 for the linear scalar case and eventually for the Burgers equation, and we refer the reader to the appropriate sections for an introduction and stability analysis.

Section 17.3 will introduce the important concept of artificial viscosity or dissipation which plays an essential role in space-centred discretizations, particularly in the vicinity of strong gradients and discontinuities.

Section 17.4 will present the very interesting family of implicit variants of the Lax–Wendroff schemes developed by Lerat.

## 17.1 THE SPACE-CENTRED EXPLICIT SCHEMES OF FIRST ORDER

The family of schemes considered in this section are perhaps the first representatives of the modern developments in the field of numerical discretizations of the Euler equations. They are known as the schemes of Lax or Lax–Friedrichs (Lax, 1954).

They are not applied in their original form any longer, due to their poor first-order accuracy, but several variants with improved accuracy are still in use (see Section 17.1.3). They form, however, an interesting base for comparisons with other schemes, and can be used as intermediate step in higher-order schemes, as in the Richtmyer two-step variant of the second-order Lax–Wendroff method, to be discussed in Section 17.2.

### 17.1.1 The one-dimensional Lax–Friedrichs scheme

The basic idea behind this scheme is to stabilize the explicit, unstable central scheme obtained from a central differencing of the first derivative of the flux term.

When applied to the linearized convection equation  $u_t + au_x = 0$ , it has been shown in Chapter 7 in Volume 1 that the explicit scheme

$$u_i^{n+1} - u_i^n = -\frac{\sigma}{2}(u_{i+1}^n - u_{i-1}^n) \quad (17.1.1)$$

is unstable. The variable  $\sigma$  is the *Courant number*, also called the *CFL number*:

$$\sigma = \frac{a \Delta t}{\Delta x} \quad (17.1.2)$$

The stabilizing procedure consists of replacing  $u_i^n$  by  $(u_{i+1}^n + u_{i-1}^n)/2$ , leading to the scheme

$$u_i^{n+1} = \frac{1}{2}(u_{i+1}^n + u_{i-1}^n) - \frac{\sigma}{2}(u_{i+1}^n - u_{i-1}^n) \quad (17.1.3)$$

When applied to the conservative form  $U_t + f_x = 0$ , the Lax–Friedrichs scheme is

$$U_i^{n+1} = \frac{U_{i+1}^n + U_{i-1}^n}{2} - \frac{\tau}{2}(f_{i+1}^n - f_{i-1}^n) \quad (17.1.4)$$

where

$$\tau = \frac{\Delta t}{\Delta x} \quad (17.1.5)$$

Comparing equation (17.1.3) with equation (17.1.1) it is seen that the stabilization procedure of Lax corresponds to the addition of a *dissipative* term proportional to the second derivative of  $u$ . Equation (17.1.4) can also be written as

$$U_i^{n+1} = U_i^n - \frac{\tau}{2}(f_{i+1}^n - f_{i-1}^n) + \frac{1}{2}(U_{i+1}^n - 2U_i^n + U_{i-1}^n) \quad (17.1.6)$$

Since the last term between parentheses can be considered as the discretization of  $(\Delta x^2/2\Delta t) \cdot U_{xx}$ , the Lax–Friedrichs scheme can be viewed as being obtained from an explicit Euler time integration of an equation of the form

$$\frac{\partial U}{\partial t} + \frac{\partial f}{\partial x} = \alpha \frac{\partial^2 U}{\partial x^2} \quad (17.1.7)$$

which is a *dissipative equation* with the numerical viscosity  $\alpha$ .

This scheme has been analysed in Chapter 8 in Volume 1 for the linear convection equation and from the truncation error analysis, in the linearized case  $f = aU$ , with constant  $a$ :

$$\alpha = \frac{a}{2\sigma} \Delta x (1 - \sigma^2) = \frac{\Delta x^2}{2\Delta t} (1 - \sigma^2) \quad (17.1.8)$$

For a non-linear equation, one can deduce, from equations (9.4.21) and (9.4.24),

$$\alpha = \frac{\Delta x^2}{2\Delta t} (1 - \tau^2 a^2) + \frac{\Delta x^2}{2} (3\tau^2 a^2 - 1) a_u \cdot U_x \quad (17.1.9)$$

This shows that the system is first-order accurate at constant  $\sigma$ , that is for a fixed ratio  $\Delta t/\Delta x$ . For independent variations of  $\Delta x$  and  $\Delta t$ , one could consider the scheme to be second-order accurate in space and first-order accurate in time. In practice, however, one operates at a fixed Courant number, so that the Lax–Friedrichs scheme is to be considered as a first-order scheme in space and time. Equation (17.1.9) contains a non-linear contribution to the numerical

dissipation, under the form of a term proportional to  $a_x = a_u \cdot U_x$  (the subscripts indicate partial derivatives).

### *Linearized stability analysis*

It has been shown in Chapter 8 that the linearized, one-dimensional Lax–Friedrichs scheme is conditionally stable by a Von Neumann analysis, satisfying the Courant–Friedrichs–Lewy condition, in brief the *CFL condition*.

Applying the analysis to the linearized system  $U_t + AU_x = 0$ , for a finite Fourier mode  $k$ , with  $\phi = k \Delta x$  with  $I = \sqrt{-1}$ , one obtains

$$G = \cos \phi - I \tau A \sin \phi \quad (17.1.10)$$

The eigenvalues  $\lambda(G)$  of  $G$  are determined from

$$\lambda(G) = \cos \phi - I \frac{\Delta t}{\Delta x} \lambda(A) \sin \phi = |\lambda(G)| e^{I\Phi} \quad (17.1.11)$$

We define

$$\bar{\sigma} = \frac{\Delta t}{\Delta x} \lambda(A) \quad (17.1.12)$$

where  $\lambda(A)$  is an eigenvalue of the Jacobian matrix  $A$  and the Courant number of the system is

$$\sigma = \frac{\Delta t}{\Delta x} \lambda(A)_{\max} \equiv \tau \rho(A) \quad (17.1.13)$$

The stability condition  $\rho(G) \leq 1$  is satisfied for the CFL condition, since  $A$  has real eigenvalues:

$$\sigma = \frac{\Delta t}{\Delta x} \rho(A) = \frac{\Delta t}{\Delta x} |u + c| \leq 1 \quad (17.1.14)$$

where  $\rho(A)$  is the spectral radius of the matrix  $A$  equal to  $|u + c|$  for the system of one-dimensional Euler equations. This is a necessary and sufficient stability condition.

The dispersion and diffusion errors are obtained from the amplification matrix by separating the phase and the amplitude.

The error analysis can be performed on  $G$ , through the eigenvectors  $\lambda(G)$ , as shown in Chapter 8, where  $\sigma$  is defined by equation (17.1.13).

The phase  $\Phi$  of  $G$  is given by

$$\tan \Phi = +\sigma \tan \phi \quad (17.1.15)$$

and the error in phase is obtained by the ratio of  $\Phi$  and of the phase of the exact solution  $\sigma\phi$ . The relative phase error is

$$\varepsilon_\Phi = \frac{\tan^{-1}(\sigma \tan \phi)}{\sigma \phi} \quad (17.1.16)$$

Since  $\varepsilon_\Phi$  is mostly greater than 1, in particular for  $\phi = \pi/2$ ,  $\varepsilon_\Phi = 1/\sigma$ , the phase error is a leading error, namely the numerical computed waves propagate at a higher velocity than the physical waves, since the numerical phase speed  $a_{\text{num}} = \Phi/(\kappa \Delta t) = a\Phi/\sigma\phi$  and the ratio of propagation speeds is equal to  $a_{\text{num}}/a = \varepsilon_\Phi$ .

The dissipation error is defined by

$$\varepsilon_D = |G| = (\cos^2 \phi + \sigma^2 \sin^2 \phi)^{1/2} \quad (17.1.17)$$

The highest damping occurs for  $\phi = \pi/2$ , that is in the mid-range frequencies with  $|G|_{\min} = \sigma$ , and any discontinuity will be strongly smoothed out for low CFL numbers  $\sigma$  and therefore this scheme is not very accurate.

Observe that  $\sigma = 1$  reproduces the exact solution  $U_i^{n+1} = U_{i-1}^n$ , since it corresponds to  $G = 1$ . Note also that, since  $G(\pi) = 1$ , the scheme is not dissipative in the sense of Kreiss.

### *Non-linear formulations*

The general form of a conservative discretization is based on the introduction of numerical fluxes  $f^*$ , such that the scheme can be written under the form

$$U_i^{n+1} = U_i^n - \tau(f_{i+1/2}^{**} - f_{i-1/2}^{**}) \quad (17.1.18)$$

When compared to the formulation (17.1.4), one obtains

$$\begin{aligned} f_{i+1/2}^* &= \frac{1}{2}(f_i + f_{i+1}) - \frac{1}{2\tau}(U_{i+1} - U_i) \\ &= f_{i+1/2} - \frac{1}{2\tau}(U_{i+1} - U_i) \end{aligned} \quad (17.1.19)$$

as the numerical flux defining the Lax–Friedrichs scheme. Here  $f_{i+1/2}$  is defined as  $f_{i+1/2} = (f_i + f_{i+1})/2$ , which is distinct from  $f[(U_i + U_{i+1})/2]$  in the non-linear case.

In the steady-state limit, the numerical scheme solves for the balance of the numerical fluxes  $f_{i+1/2}^* = f_{i-1/2}^*$  as an approximation to the balance of the physical fluxes  $f_{i+1/2} = f_{i-1/2}$ . The resulting stationary solution satisfies  $f_{i+1/2} - f_{i-1/2} = (U_{i+1} - 2U_i + U_{i-1})/2\tau$  instead, and is dependent on the ratio  $\tau = \Delta t/\Delta x$ .

### **17.1.2 The two-dimensional Lax–Friedrichs scheme**

Applied to the two-dimensional system of Euler equations, written as

$$\frac{\partial U}{\partial t} + \frac{\partial f}{\partial x} + \frac{\partial g}{\partial y} = 0 \quad (17.1.20)$$

the generalization of the one-dimensional scheme (17.1.4) is

$$\begin{aligned} U_{ij}^{n+1} = & \frac{1}{4}(U_{i+1,j}^n + U_{i-1,j}^n + U_{i,j+1}^n + U_{i,j-1}^n) - \frac{\tau_x}{2}(f_{i+1,j}^n - f_{i-1,j}^n) \\ & - \frac{\tau_y}{2}(g_{i,j+1}^n - g_{i,j-1}^n) \end{aligned} \quad (17.1.21)$$

where

$$\tau_x = \frac{\Delta t}{\Delta x} \quad \tau_y = \frac{\Delta t}{\Delta y} \quad (17.1.22)$$

This scheme can be represented by the stencil in Figure 17.1.1.

The linearized stability condition is obtained from the constant coefficient quasi-linear form

$$\frac{\partial U}{\partial t} + A \frac{\partial U}{\partial x} + B \frac{\partial U}{\partial y} = 0 \quad (17.1.23)$$

Applying a standard Von Neumann analysis, with  $\phi_x = \kappa_x \Delta x$  and  $\phi_y = \kappa_y \Delta y$ , one obtains the amplification matrix

$$G = \frac{1}{2}(\cos \phi_x + \cos \phi_y) - IA\tau_x \sin \phi_x - IB\tau_y \sin \phi_y \quad (17.1.24)$$

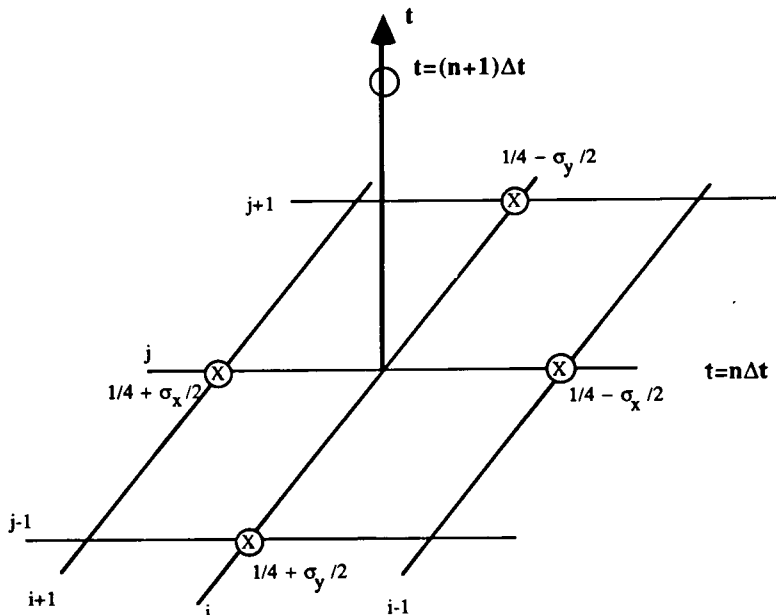


Figure 17.1.1 Computational stencil for the standard two-dimensional Lax-Friedrichs scheme applied to the linearized Euler equations

If the matrices  $A$  and  $B$  would commute (which is *not* the case for the Euler equations), they would have the same eigenvectors and one would obtain  $\lambda(G)$  for the eigenvalues of  $G$ :

$$\lambda(G) = \frac{1}{2}(\cos \phi_x + \cos \phi_y) - I \frac{\Delta t}{\Delta x} \lambda(A) \sin \phi_x - I \frac{\Delta t}{\Delta y} \lambda(B) \sin \phi_y \quad (17.1.25)$$

Defining

$$\sigma_x = \frac{\Delta t}{\Delta x} \lambda(A)_{\max} \equiv \tau \rho(A) \quad \sigma_y = \frac{\Delta t}{\Delta y} \lambda(B)_{\max} \equiv \tau \rho(B) \quad (17.1.26)$$

$\lambda(A)_{\max}$  and  $\lambda(B)_{\max}$  being the maximum eigenvalues of the Jacobians  $A$  and  $B$ , the necessary and sufficient stability condition, obtained in Chapter 8, Section 8.6.2, is

$$\sigma_x^2 + \sigma_y^2 \leq \frac{1}{2}$$

or

$$\frac{\Delta t^2}{\Delta x^2}(u+c)^2 + \frac{\Delta t^2}{\Delta y^2}(v+c)^2 \leq \frac{1}{2} \quad (17.1.27)$$

This is illustrated in Figure 17.1.2 in a diagram of  $\sigma_x$  and  $\sigma_y$ , where the stability region is inside a circle of radius  $\sqrt{2}/2$ .

When the matrices  $A$  and  $B$  do not commute, there are no general conditions known that are necessary and sufficient for the Von Neumann stability. However, some sufficient conditions can be obtained for  $A, B$  being *real symmetric* matrices. As seen in the previous chapter for the full system of Euler equations, the Jacobians  $A$  and  $B$  are not symmetric but a similarity trans-

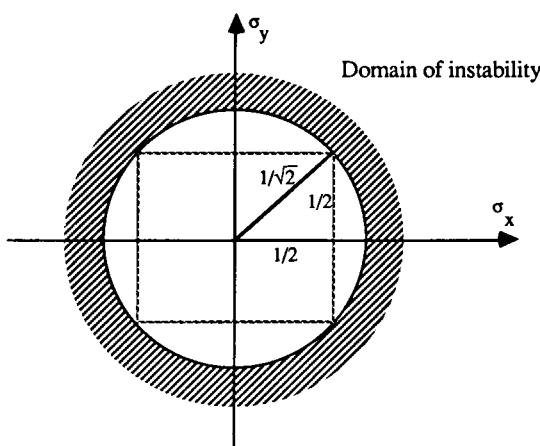


Figure 17.1.2 Two-dimensional Lax-Friedrichs scheme.  
Necessary and sufficient Von Neumann stability condition for commuting Jacobian matrices

formation  $S$  can be found, which simultaneously symmetrizes  $A$  and  $B$  (Turkel, 1973; Harten, 1983a); that is there exist non-singular matrices  $S$  such that

$$SAS^{-1} = A_0 \quad \text{and} \quad SBS^{-1} = B_0 \quad (17.1.28)$$

where  $A_0$  and  $B_0$  are symmetric matrices. In this case, the following conjecture has been made by Turkel (1977), which provides a guideline for obtaining sufficient conditions for stability in the non-commuting case:

*Turkel's conjecture:* If the amplification matrix  $G$  of a symmetric hyperbolic difference scheme is power bounded (that is the scheme is stable) for commuting matrices  $A, B, \dots$ , when their real eigenvalues are restricted to some subset  $R_s$ , then  $G$  is also power bounded for all real symmetric matrices having their eigenvalues restricted to the same subset  $R_s$ .

The scheme is said to be symmetric hyperbolic if  $G$  is symmetric, that is its real and imaginary parts are both real symmetric matrices. Within this conjecture, the above condition (17.1.27) can be considered as sufficient for stability of the Lax–Friedrichs scheme (17.1.21). Other sufficient conditions are summarized for a variety of explicit central schemes in Yanenko *et al.* (1984). For instance,

$$\sigma_x \leq \frac{1}{2} \quad \text{and} \quad \sigma_y \leq \frac{1}{2} \quad (17.1.29)$$

which is represented by the region inside the square of Figure 17.1.1.

A variant of the scheme (17.1.21) can be defined where the corner points of the mesh cell are used for the averaging term as in Figure 17.1.3 (Yanenko *et al.*, 1984):

$$\begin{aligned} U_{ij}^{n+1} = & \frac{1}{4}(U_{i+1,j+1}^n + U_{i+1,j-1}^n + U_{i-1,j+1}^n + U_{i-1,j-1}^n) \\ & - \frac{\tau_x}{4}(f_{i+1,j+1}^n + f_{i+1,j-1}^n - f_{i-1,j+1}^n - f_{i-1,j-1}^n) \\ & - \frac{\tau_y}{4}(g_{i+1,j+1}^n + g_{i-1,j+1}^n - g_{i+1,j-1}^n - g_{i-1,j-1}^n) \end{aligned} \quad (17.1.30)$$

or introducing the difference operators

$$\begin{aligned} \bar{\mu}_x U_{ij} &= \frac{1}{2}(U_{i+1,j} + U_{i-1,j}) & \bar{\mu}_y U_{ij} &= \frac{1}{2}(U_{i,j+1} + U_{i,j-1}) \\ \bar{\delta}_x U_{ij} &= \frac{1}{2}(U_{i+1,j} - U_{i-1,j}) & \bar{\delta}_y U_{ij} &= \frac{1}{2}(U_{i,j+1} - U_{i,j-1}) \end{aligned} \quad (17.1.31)$$

$$U_{ij}^{n+1} = \bar{\mu}_x \bar{\mu}_y u_{ij} - \bar{\tau}_x \bar{\mu}_y \bar{\delta}_x^n f_{ij} - \bar{\tau}_y \bar{\mu}_x \bar{\delta}_y^n g_{ij} \quad (17.1.32)$$

From Figure 17.1.3, it is seen that the modified scheme decouples the even- and odd-numbered mesh points. This could generate some oscillations; see Chapter 4 in Volume 1 for a discussion on this problem.

The linearized amplification matrix is (see Problem 17.2)

$$G = \cos \phi_x \cos \phi_y - I \sigma_x \sin \phi_x \cos \phi_y - I \sigma_y \cos \phi_x \sin \phi_y \quad (17.1.33)$$

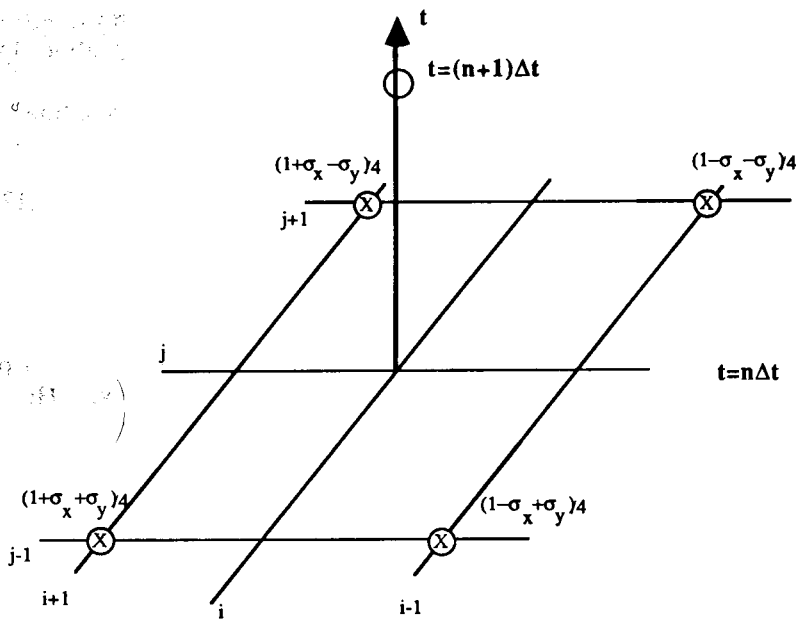


Figure 17.1.3 Computational stencil for the two-dimensional Lax-Friedrichs scheme (17.1.30)

and sufficient stability conditions are given by

$$\sigma_x \leq 1 \quad \text{and} \quad \sigma_y \leq 1 \quad (17.1.34)$$

increasing the stability range with respect to the original scheme (17.1.21).

### 17.1.3 Corrected viscosity scheme

An attempt to improve the accuracy of the Lax-Friedrichs scheme by achieving asymptotically second-order accuracy for steady-state problems has been introduced by McDonald (1971) and further analysed by Couston *et al.* (1975).

In the one-dimensional case, the quantity  $(\beta \Delta x^2 / \Delta t) u_{xx}$  is subtracted from the right-hand side of equation (17.1.7), leading to a scheme

$$u_i^{n+1} = u_i^n - \frac{\tau}{2}(f_{i+1}^n - f_{i-1}^n) + \frac{1}{2}(u_{i+1}^n - 2u_i^n + u_{i-1}^n) - \frac{\beta}{2}(u_{i+1}^l - 2u_i^l + u_{i-1}^l) \quad (17.1.35)$$

where the last term is updated every  $N$  iterations; that is  $l$  is kept constant between two updatings and set equal to  $l = N \cdot \text{mod}(n, N)$ , where  $\text{mod}(n, N)$  is the integer part of  $n/N$ .

When this term is not updated, the scheme has the properties of the original Lax scheme, but the solution is regularly corrected every  $N$  iterations for the accumulated truncation error.

The solution of the difference equation converges to the solution of the corrected equation

$$u_t + f_x = (1 - \beta - \sigma^2) \frac{\Delta x^2}{2\Delta t} u_{xx} \quad (17.1.36)$$

and if the coefficient  $\beta$  is chosen as  $\beta = 1 - \sigma^2 - O(\Delta x)$ , the final accuracy will approach second order. An improvement in accuracy is obtained, however calibrations of  $N$  and  $\beta$  are required. In particular, the corrected scheme is linearly stable only if  $N$  is larger than the maximum number of mesh points on the  $x$  axis. The interested reader will find more details in Van Hove and Arts (1979). Note that the Lax–Friedrichs version of McDonald (1971) is probably the first application of a finite volume method to the Euler equations (see Problem 17.3).

Another scheme based on a first-order discretization with corrected viscosity in order to approach second-order accuracy has been developed by Denton (1975, 1982) and is widely used in the field of internal turbomachinery flows.

## 17.2 THE SPACE-CENTRED EXPLICIT SCHEMES OF SECOND ORDER

The second-order space-centred explicit schemes are all derived from the basic Lax–Wendroff scheme (1960). It has already been shown in Chapter 9 in Volume 1 that this scheme is the unique second-order space-centred discretization on the three-point support  $(i-1, i, i+1)$  for the linear one-dimensional convection equation. Therefore, the numerous variants of the Lax–Wendroff scheme differ in the treatment of the non-linearities and in their multi-dimensional aspects, but reduce to the same linearized, one-dimensional form.

The popularity of these schemes, and in particular the two-step version of MacCormack (1969), is due to their second-order accuracy and simplicity, although their behaviour around discontinuities is not fully satisfactory.

We will review first the one-dimensional, linear and non-linear versions of the Lax–Wendroff schemes (Sections 17.2.1, 17.2.2 and 17.2.3) and then discuss in Sections 17.2.4 and 17.2.5 the two-dimensional extensions.

### 17.2.1 The basic one-dimensional Lax–Wendroff scheme

The idea behind the Lax–Wendroff scheme is to stabilize the unstable central scheme (17.1.1), while obtaining second-order accuracy in space and time. A close look at the origin of the instability of this scheme shows that it is due to the combination of a first-order time difference with a second-order space discretization of the flux term.

Indeed, developing equation (17.1.1) in a Taylor series, gives a truncation error of the form

$$u_t + au_x = -\frac{\Delta t}{2} u_{tt} + O(\Delta x^2, \Delta t^2) \quad (17.2.1)$$

leading to a negative numerical viscosity.

Hence, if the term  $\Delta t u_{tt}/2$  is added to the left-hand side, the truncation error would be of second order in  $\Delta x$  and  $\Delta t$ .

The basic approach is therefore as follows: in the time series development

$$U^{n+1} = U^n + \Delta t U_t + \frac{\Delta t^2}{2} U_{tt} + \frac{\Delta t^3}{6} U_{ttt} \quad (17.2.2)$$

the  $\Delta t^2$  term is maintained and replaced by the space derivative term

$$\frac{\partial^2 U}{\partial t^2} = -\frac{\partial^2 f}{\partial x \partial t} = -\frac{\partial}{\partial x} \left( A \frac{\partial U}{\partial t} \right) = \frac{\partial}{\partial x} \left( A \frac{\partial f}{\partial x} \right) \quad (17.2.3)$$

where the Jacobian  $A = \partial f / \partial U \equiv f_U$  is introduced.

Equation (17.2.2) becomes

$$U^{n+1} = U^n - \Delta t \frac{\partial f}{\partial x} + \frac{\Delta t^2}{2} \frac{\partial}{\partial x} \left( A \frac{\partial f}{\partial x} \right) + O(\Delta t^3) \quad (17.2.4)$$

and is discretized at point  $i$  with second-order central differences, leading to the *one-step* non-linear version of the Lax–Wendroff scheme:

$$U_i^{n+1} = U_i^n - \frac{1}{2}\tau(f_{i+1}^n - f_{i-1}^n) + \frac{1}{2}\tau^2[A_{i+1/2}^n(f_{i+1}^n - f_i^n) - A_{i-1/2}^n(f_i^n - f_{i-1}^n)] \quad (17.2.5a)$$

with

$$A_{i+1/2} = A(U_{i+1/2}) \quad (17.2.5b)$$

or

$$A_{i+1/2} = \frac{1}{2}(A_i + A_{i+1}) \quad (17.2.5c)$$

The linearized form can be written as

$$u_i^{n+1} = u_i^n - \frac{1}{2}\sigma(u_{i+1}^n - u_{i-1}^n) + \frac{1}{2}\sigma^2(u_{i+1}^n - 2u_i^n + u_{i-1}^n) \quad (17.2.6)$$

Equation (17.2.5a) can also be written in conservative form as the difference in numerical fluxes  $f^*$ :

$$U_i^{n+1} - U_i^n = -\tau(f_{i+1/2}^* - f_{i-1/2}^*) \quad (17.2.7)$$

with

$$\begin{aligned} f_{i+1/2}^* &= f_{i+1/2} - \frac{\tau}{2} A_{i+1/2} (f_{i+1} - f_i) \\ f_{i+1/2} &= \frac{f_i + f_{i+1}}{2} \end{aligned} \quad (17.2.8)$$

Introducing the compact difference notations defined in Chapter 4,

$$\begin{aligned}\delta U_i &= U_{i+1/2} - U_{i-1/2} \\ \mu U_i &= \frac{U_{i+1/2} + U_{i-1/2}}{2} \\ \delta^+ U_i &= U_{i+1} - U_i \\ \delta^- U_i &= U_i - U_{i-1}\end{aligned}\quad (17.2.9)$$

the Lax–Wendroff scheme can be rewritten as follows:

$$U_i^{n+1} - U_i^n = -\tau \bar{\delta} f_i^n + \frac{1}{2} \tau^2 \delta^+ (A_{i-1/2} \delta^- f_i^n) \quad (17.2.10)$$

or

$$U_i^{n+1} - U_i^n = -\tau \bar{\delta} f_i^n + \frac{1}{2} \tau^2 \delta (A_i \delta f_i^n) \quad (17.2.11)$$

The stability conditions for the Lax–Wendroff scheme are obtained from a linearized Von Neumann analysis, leading to the amplification matrix

$$G = 1 - I\tau A \sin \phi - \tau^2 A^2 (1 - \cos \phi) \quad (17.2.12)$$

The stability condition on the spectral radius of  $G$  requires the computation of its eigenvalues  $\lambda(G)$ :

$$\rho(G) = \lambda(G)_{\max} = 1 - I\sigma \sin \phi - \sigma^2 (1 - \cos \phi) \quad (17.2.13)$$

defining  $\sigma$  by

$$\sigma = \frac{\Delta t}{\Delta x} \lambda(A)_{\max} \quad (17.2.14)$$

In the complex  $\lambda(G)$  plane, this represents an ellipse centred on the real axis at the abscissa  $(1 - \sigma^2)$  with a semi-axis of  $\sigma^2$  along the real axis and  $\sigma$  along the vertical axis, leading to the CFL condition (see Chapter 8). We recall here that for the Euler equations, the CFL condition is to be applied to the highest eigenvalue ( $u + c$ ). The modulus of the amplification factor is given by

$$|\rho(G)|^2 = 1 - 4\sigma^2(1 - \sigma^2) \sin^2 \frac{\phi}{2} \quad (17.2.15)$$

and the phase  $\Phi$  is defined by

$$\tan \Phi = \frac{\sigma \sin \phi}{1 - 2\sigma^2 \sin \phi / 2} \quad (17.2.16)$$

The relative phase error

$$\varepsilon_\phi = \frac{\Phi}{\sigma \phi} \quad (17.2.17)$$

is mostly lower than one, indicating a dominating lagging phase error. The highest frequencies, corresponding to  $\phi = \pi$ , are damped by a factor  $|G|_\pi = 1 - 2\sigma^2$ , while the phase angle  $\phi$  goes to zero if  $\sigma^2 < \frac{1}{2}$  and tends to  $\pi$  if  $\sigma^2 > \frac{1}{2}$ .

At low CFL values, for  $\sigma^2 < \frac{1}{2}$ , the phase error is the largest at the high frequencies, since  $\varepsilon_\phi = 0$  for  $\phi = \pi$ . Hence, this will tend to accumulate the high-frequency errors generated at a discontinuity and oscillations will appear, for instance for a propagating discontinuity, since the phase error indicates a lagging computed phase.

The truncation error of the Lax–Wendroff scheme is, in the linear case,

$$\begin{aligned}\epsilon_T &= -\frac{\sigma^2}{6}u_{ttt} - \frac{\Delta x^3}{6} \cdot \frac{\sigma}{\Delta t} u_{xxx} = \frac{\Delta x^3}{6}(1 - \sigma^2)u_{xxt} \\ &= \frac{-\Delta x^2 a}{6}(1 - \sigma^2)u_{xxx}\end{aligned}\quad (17.2.18)$$

The equivalent equation has now a dispersive term in the right-hand side. The dissipation of the scheme is of fourth order, since for small  $\phi = k \Delta x$ , one has, from equation (17.2.15),

$$|\rho(G)|^2 \simeq 1 - \frac{\sigma^2}{4}(1 - \sigma^2)\phi^4 \quad (17.2.19)$$

showing that the Lax–Wendroff scheme is dissipative to the fourth order, in the sense of Kreiss, for  $0 < \sigma < 1$ .

### Non-linear variant

The non-linear formulation of the Lax–Wendroff scheme requires the evaluation of the Jacobian  $A_{i+1/2}$ , defined by equation (17.2.5b) or (17.2.5c). However, other definitions are possible, leading to alternative, non-linear variants of the basic scheme (17.2.5a). Instead of evaluating analytically the Jacobian  $A$  and calculating its values at  $U_{i+1/2} = (U_i + U_{i+1})/2$ , one can perform a direct numerical evaluation of  $A_{i+1/2}$  by the following formula (Roe, 1981; Harten, 1983b):

$$A_{i+1/2} = \begin{cases} \frac{f_{i+1} - f_i}{U_{i+1} - U_i} & \text{if } U_{i+1} - U_i \neq 0 \\ A(U_i) & \text{if } U_{i+1} = U_i \end{cases} \quad (17.2.20)$$

for vector equations  
this must be rewritten  
 $A_{i+1/2}(U_{i+1} - U_i) = f_{i+1} - f_i$

With this definition, the Lax–Wendroff scheme takes the form

$$U_i^{n+1} = U_i^n - \frac{\tau}{2}(f_{i+1}^n - f_{i-1}^n) + \frac{1}{2}\tau^2[A_{i+1/2}^2(U_{i+1}^n - U_i^n) - A_{i-1/2}^2(U_i^n - U_{i-1}^n)] \quad (17.2.21)$$

and the associated numerical flux becomes, instead of (17.2.8),

$$f_{i+1/2}^* = f_{i+1/2} - \frac{\tau}{2}A_{i+1/2}^2(U_{i+1} - U_i) \quad (17.2.22)$$

In order to generalize the above definition of  $A_{i+1/2}$  to non-linear systems of equations, one can apply a decomposition in simple waves of the form (16.3.40):

$$\delta U_{i+1/2} = U_{i+1} - U_i = \sum_k \delta w_{i+1/2}^k r_{i+1/2}^k \quad (17.2.23)$$

where  $r^k$  are the right eigenvectors of the Jacobian matrix  $A$  and  $\delta w^k$  are the characteristic variables.

The operator  $A_{i+1/2}^2(U_{i+1} - U_i)$  is decomposed as

$$A_{i+1/2}^2(U_{i+1} - U_i) = \sum_k (a_{i+1/2}^k)^2 \delta w_{i+1/2}^k r_{i+1/2}^k \quad (17.2.24)$$

This can be realized in a most natural way by the linearization introduced by Roe (1981) (see Section 20.5.3), where a Jacobian matrix  $A_{i+1/2}$  is defined which satisfies *exactly* the numerical relation

$$f_{i+1} - f_i = A_{i+1/2}(U_{i+1} - U_i) \quad (17.2.25)$$

with

$$A_{i+1/2} = A_{i+1/2}(U_i, U_{i+1})$$

such that

$$A_{i+1/2}(U_i, U_i) = A(U_i) \quad (17.2.26)$$

## 17.2.2 The two-step Lax–Wendroff schemes in one dimension

The scheme represented by equation (17.2.5a) requires the evaluation of the Jacobian matrices  $A$ , which can be a costly operation in practical computations. Hence a two-step procedure has been introduced by Richtmyer and Morton (1967) that avoids the estimation of the Jacobians. This scheme, known as the *Richtmyer scheme*, is at the basis of many modern two-step predictor–corrector methods which are able to handle non-linearities in a straightforward way.

An intermediate state is introduced which can be considered as the solution at a time  $t = (n + \frac{1}{2})\Delta t$ , followed by a second step which brings the solution to the final time step  $t = (n + 1)\Delta t$ . Richtmyer's scheme is then defined as

$$\begin{aligned} U_{i+1/2}^{n+1/2} &= \frac{1}{2}(U_i^n + U_{i+1}^n) - \frac{\tau}{2}(f_{i+1}^n - f_i^n) \\ U_i^{n+1} &= U_i^n - \tau(f_{i+1/2}^{n+1/2} - f_{i-1/2}^{n+1/2}) \end{aligned} \quad (17.2.27)$$

The first step is identical to the Lax–Friedrichs scheme (LF) applied to the mid-point  $(i + \frac{1}{2})$  between times  $n$  and  $(n + \frac{1}{2})$ , while the second step is a leapfrog scheme, applied at  $(n + \frac{1}{2})$  (see Figure 17.2.1).

This second step is of second-order accuracy at the points  $(i, n + \frac{1}{2})$ , while the first step has first-order accuracy at the points  $(i + \frac{1}{2}, n + \frac{1}{2})$  at fixed Courant number. Globally, the two-step scheme is second order in space and time at  $(i, n + 1)$ . It is easily seen that in the linear case  $f = a \cdot u$ , the two-step scheme becomes identical to the single-step Lax–Wendroff scheme equation (17.2.6).

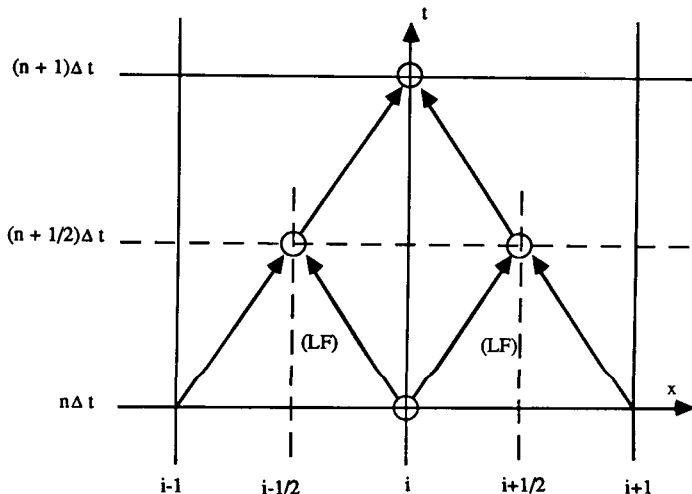


**Figure 17.2.1** Computational stencil for the two-step Richtmyer variant of the Lax–Wendroff scheme

### MacCormack's scheme

The two-step predictor–corrector scheme of MacCormack (1969) is another version of the Lax–Wendroff discretization to which it becomes identical in the linear case. This scheme is probably the most widely applied version of the Lax–Wendroff schemes. Predictor values are defined at  $(n + 1)$  and point  $i$ , followed by a corrector step, where  $\bar{f}_i = f(\bar{U}_i)$ :

$$\begin{aligned}\bar{U}_i &= U_i^n - \tau(f_{i+1}^n - f_i^n) \\ U_i^{n+1} &= \frac{1}{2}(U_i^n + \bar{U}_i) - \frac{\tau}{2}(\bar{f}_i - \bar{f}_{i-1})\end{aligned}\quad (17.2.28)$$

This scheme has been introduced in a linearized version in Chapter 11 in Volume 1.

The first step is a first-order forward discretization in space, which is actually unstable for positive eigenvalues of  $A$ , that is for supersonic velocities.

The second, corrector, step is a backward first-order scheme, which will be unstable for negative characteristic speeds of propagation, that is for subsonic flows. However, the overall combined scheme is stable and of second order due to the cancellations of the truncation errors of each step.

MacCormack's scheme can be written more explicitly in a predictor–corrector sequence where the symmetry between the two steps is more apparent:

$$\bar{U}_i = U_i^n - \tau(f_{i+1}^n - f_i^n) \quad (17.2.29a)$$

$$\bar{\bar{U}}_i = U_i^n - \tau(\bar{f}_i - \bar{f}_{i-1}) \quad (17.2.29b)$$

Updating gives

$$U_i^{n+1} = \frac{1}{2}(\bar{U}_i + \bar{\bar{U}}_i) \quad (17.2.29c)$$

An alternative is to reverse the order of the predictor and the corrector:

$$\text{Predictor: } \bar{U}_i = U_i^n - \tau(f_i^n - f_{i-1}^n) \quad (17.2.30a)$$

$$\text{Corrector: } \bar{\bar{U}}_i = U_i^n - \tau(\bar{f}_{i+1} - \bar{f}_i) \quad (17.2.30b)$$

$$\text{Updating: } U_i^{n+1} = \frac{1}{2}(\bar{U}_i + \bar{\bar{U}}_i) \quad (17.2.30c)$$

Note that, for non-linear problems, the three versions (17.2.27), (17.2.29) and (17.2.30) will lead to different results, although they are identical on linear problems.

Since the predictor of the version (17.2.30) only transmits downwind influences, an error generated at a shock discontinuity, for instance, will tend to propagate downstream. Hence, this version will be better adapted for discontinuities moving from right to left, while the version (17.2.29) might be more suitable in the opposite situation. This is confirmed by Lerat and Peyret (1975), where it is shown that this choice gives the best non-linear dissipation properties. However, this can be strongly dependent on the way the boundary conditions are treated and on the presence of artificial viscosity.

When the boundary conditions are applied at the downstream end of the  $x$  domain the predictor of (17.2.30) will treat the last point in the same way as all the others, while a numerical boundary condition will be imposed in this point at the corrector sequence. Similar situations occur at the other end of the interval with the predictor and corrector roles inversed.

The MacCormack schemes can also be written for the variations  $\Delta U$ , as follows for the version (17.2.29):

$$\overline{\Delta U}_i = -\tau \cdot \delta^+ f_i^n \quad (17.2.31a)$$

$$\overline{\overline{\Delta U}}_i = -\tau \cdot \delta^- \bar{f}_i \quad (17.2.31b)$$

$$\Delta U_i \equiv U_i^{n+1} - U_i^n = \frac{1}{2}(\overline{\Delta U}_i + \overline{\overline{\Delta U}}_i) = -\frac{\tau}{2}[f_{i+1}^n - f_i^n + \bar{f}_i - \bar{f}_{i-1}] \quad (17.2.31c)$$

where  $\overline{\Delta U}$  is the predictor variation ( $\bar{U} - U^n$ ),  $\overline{\overline{\Delta U}}$  is the corrector variation ( $\bar{\bar{U}} - U^n$ ) and  $\Delta U$  the global variation of the solution over one full step.

A similar form is obtained for scheme (17.2.30) by interchanging the forward and backward differences. Equation (17.2.31c) shows that the MacCormack schemes are in the conservation form with the numerical fluxes  $f_{i+1/2}^*$  equal to

$$\begin{aligned} f_{i+1/2}^* &= \frac{1}{2}(\bar{f}_i + f_{i+1}^n) \\ &= \frac{1}{2}[f(U_{i+1}^n) + f^n[U_i - \tau(f_{i+1}^n - f_i^n)]] \\ &= f_{i+1/2} - \frac{\tau}{2} A_{i+1/2}(f_{i+1} - f_i) + O(\Delta t^2) \end{aligned} \quad (17.2.32)$$

It is of importance to notice here that the steady-state solution satisfies the balance of the numerical flux  $f^*$ :

$$f_{i+1/2}^* = f_{i-1/2}^*$$

or from (17.2.32), for scheme (17.2.29),

$$f_{i+1} + f[U_i - \tau(f_{i+1} - f_i)] = f_i + f[U_{i-1} - \tau(f_i - f_{i-1})]$$

The steady-state solution will therefore depend on the time step  $\Delta t$ ,  $\tau = \Delta t / \Delta x$ . This is considered as a drawback, since it introduces a dependence on a non-physical parameter unless the predictor and the corrector converge separately to the steady state. This is, however, not the case generally.

Indeed, if the predictor step would converge to zero residual, that is to  $\bar{U}_i = U_i^n$ , implying  $f_i = f_{i+1}$ , the residual of the corrector step would be proportional to  $(f_{i+1} - f_{i-1})$  and of the order of the truncation error. Hence, the final residual after the two steps is

$$\Delta U_i = U_i^{n+1} - U_i = -\Delta t \cdot R_i^n \equiv -\tau(f_{i+1/2}^* - f_{i-1/2}^*)$$

where  $R^n$  is the difference of the numerical fluxes and will not necessarily converge to machine zero but may remain at the level of the truncation error of the discretization.

Predictor–corrector sequences using the same operator for each step will not be subject to this problem and the residual will be able to converge to machine zero. This in turn will lead to the same steady-state solution, independent of the time step size  $\Delta t$ .

### *Example 17.2.1 MacCormack scheme for the Euler equations with source term*

The quasi-one-dimensional Euler equations for the flow in a nozzle of varying cross-section  $S(x)$  are given by equation (16.4.1). The adaptation of the scheme (17.2.29) to a system with a source term can be done in a straightforward way. Denoting by  $Q$  the source term vector for the system

$$\frac{\partial U}{\partial t} + \frac{\partial f}{\partial x} = Q \quad (\text{E17.2.1})$$

the scheme (17.2.29) is extended as follows:

$$\bar{U}_i = U_i^n - \tau(f_{i+1}^n - f_i^n) + \Delta t Q_i^n \quad (\text{E17.2.2a})$$

$$\bar{\bar{U}}_i = U_i^n - \tau(\bar{f}_i - \bar{f}_{i-1}) + \Delta t \bar{Q}_i \quad (\text{E17.2.2b})$$

Updating gives

$$U_i^{n+1} = \frac{1}{2}(\bar{U}_i + \bar{\bar{U}}_i) \quad (\text{E17.2.2c})$$

In the corrector step the source term is evaluated as  $\bar{Q} = Q(\bar{U})$ . With the numerical flux (17.2.32) the scheme can be written as

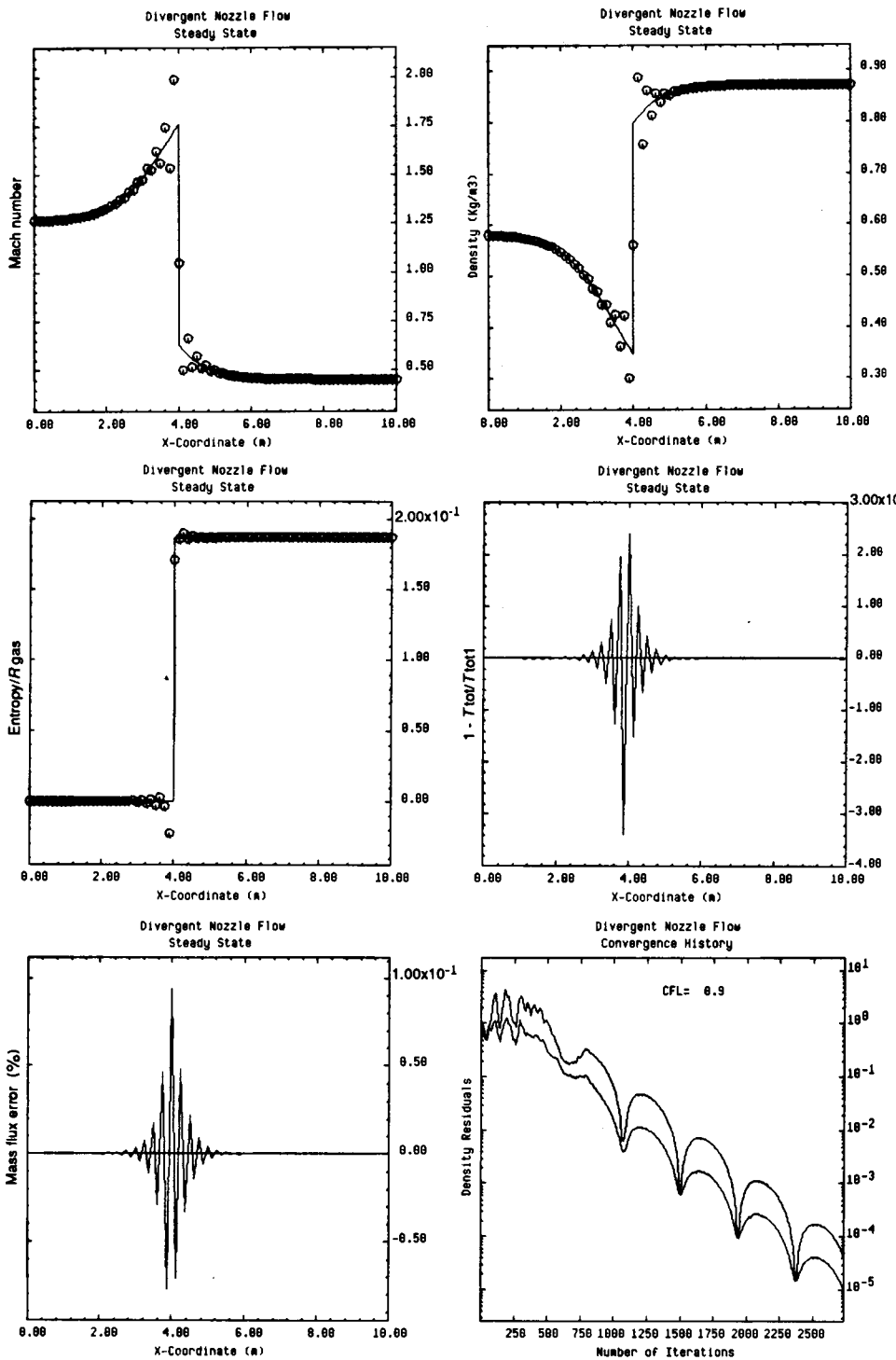


**Figure 17.2.2** Results of MacCormack's scheme applied to the stationary flow in a diverging nozzle with 81 mesh points at CFL = 0.9. Calculated results  $\circ\circ\circ$  Exact solution —

$$\Delta U_i = U_i^{n+1} - U_i^n = -\tau(f_{i+1/2}^* - f_{i-1/2}^*) + \frac{\Delta t}{2}(Q_i^n + \bar{Q}_i) \quad (\text{E17.2.3})$$

See also Problem 17.11 for a formulation of the one-step Lax–Wendroff scheme in the presence of source terms.

Figure 17.2.2 shows a computation of the stationary transonic flow in the diverging nozzle of Problem 16.26 with MacCormack's scheme (17.2.29) at a Courant number of 0.9 with 81 mesh points. Results for Mach number, density, entropy and stagnation temperature variations are plotted as a function of distance, next to the exact solution shown by a continuous line. Figure 17.2.2 also displays the streamwise evolution of the error in mass flux, expressed as a percentage of the exact value  $(\rho u)_{ex}$ . The plotted quantity is  $[(\rho u)/(\rho u)_{ex} - 1]$  as a percentage. The convergence history is also shown via the  $L_2$  and max norms of the density residuals.

As can be observed, excellent accuracy is obtained in the smooth regions, but strong oscillations appear around the shock. The plots of entropy and stagnation temperature are very instructive with regard to the hidden deficiencies or qualities of a scheme, since both are derived quantities. Entropy should remain constant everywhere with the exception of the discontinuity, while stagnation temperature has to remain constant for stationary flows, even over discontinuities. The errors occurring in the shock region are an indication of the way the scheme treats discontinuous variations, and in the present case the behaviour of the mass flux error is an additional indication of the generated high-frequency oscillations.

This is typical of all the central second-order algorithms and requires the introduction of some mechanism to damp the high-frequency errors generated at discontinuities.

Figure 17.2.3 presents a computation of the unsteady shock tube flow with the same version of MacCormack's scheme (17.2.29) at  $\text{CFL} = 0.95$  after 35 time steps.

This test case corresponds to the data of Figure 16.6.8 and shows an expansion shock at the original position ( $x = 5$ ) of the diaphragm, where sonic conditions would occur if the expansion fan would reach this location. The acceleration phase through the expansion fan comes close enough to sonic velocities, as can be seen from the Mach number distribution, to generate the expansion shock. This is due to the lack of dissipation of the scheme at the points where the Courant number goes to zero (see equation (17.2.13)). This equation shows indeed that the eigenvalues of the amplification matrix are equal to one when the eigenvalues of the Jacobian matrix vanish, that is for sonic conditions. Hence there is no mechanism to ensure the increase in entropy required by the second law of thermodynamics. This is confirmed by the entropy diagram in Figure 17.2.3, showing no entropy variation over the expansion shock at  $x = 5$ .

Similar results are obtained in Figure 17.2.4 which displays the computations for the test case of Figure 16.6.9, corresponding to an expansion fan acceleration

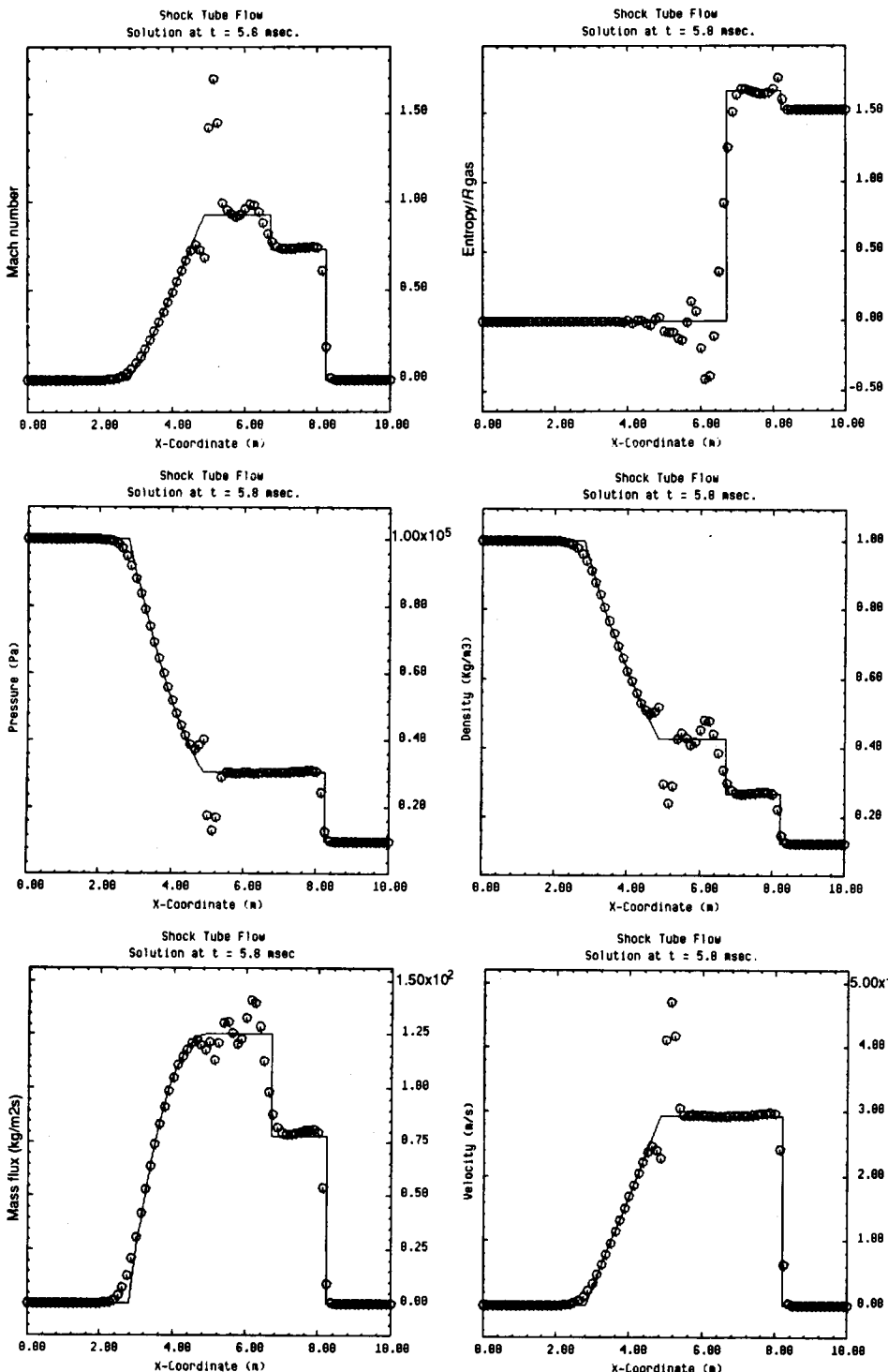
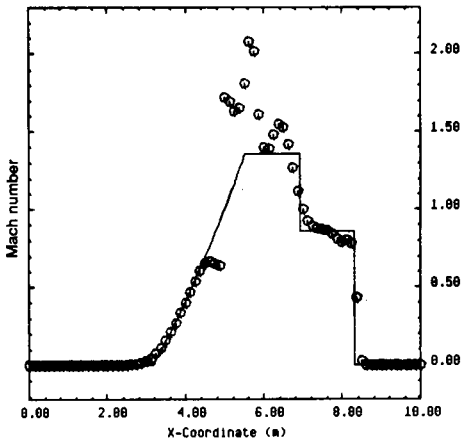
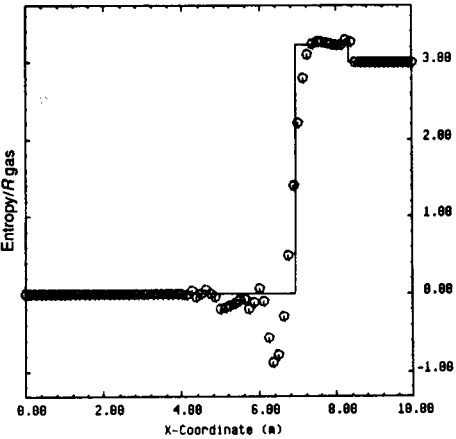


Figure 17.2.3 Results of MacCormack's scheme applied to the shock tube problem of Figure 16.6.8, with 81 mesh points at  $CFL = 0.95$  after 35 time steps. Calculated results  $\circ\circ\circ$  Exact solution —

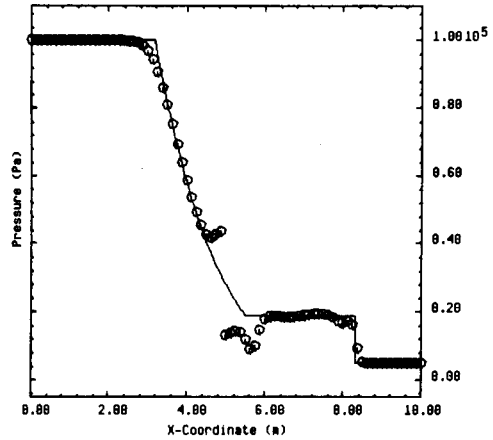
Shock Tube Flow  
Solution at  $t = 4.9$  asec.



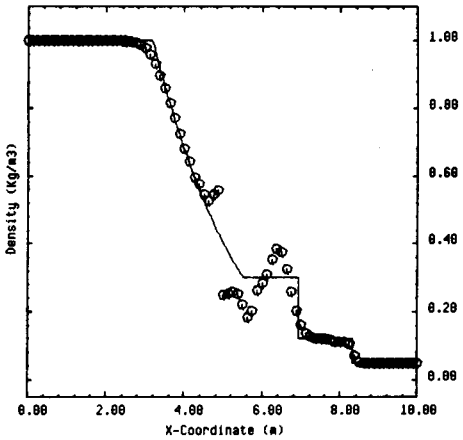
Shock Tube Flow  
Solution at  $t = 4.9$  msec.



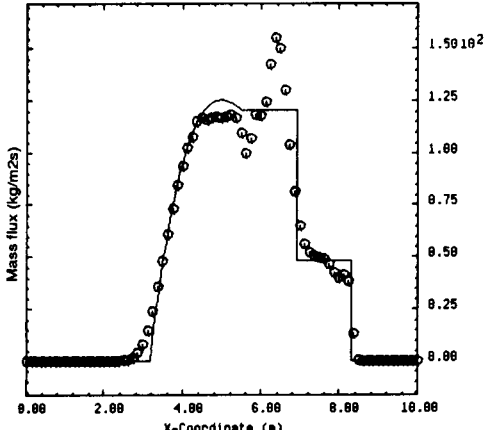
Shock Tube Flow  
Solution at  $t = 4.9$  asec



Shock Tube Flow  
Solution at  $t = 4.9$  msec



Shock Tube Flow  
Solution at  $t = 4.9$  asec



Shock Tube Flow  
Solution at  $t = 4.9$  msec

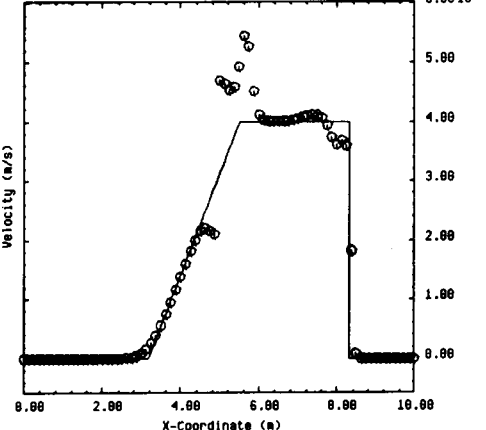


Figure 17.2.4 Results of MacCormack's scheme applied to the shock tube problem of Figure 16.6.9, with 81 mesh points at  $\text{CFL} = 0.95$  after 35 time steps. Calculated results  $\circ\circ\circ$  Exact solution —

to supersonic velocities. The expansion shock at  $x = 5$  is clearly seen. On the other hand, the shock is sharply resolved but the contact discontinuity is smeared. This is a feature common to many schemes.

The cure to the stationary shock oscillations as well as to the expansion shock lies in the introduction of additional dissipative terms proportional to the mesh size and of the same order or higher than the truncation error. This will be discussed in Section 17.3.

### *The semi-explicit variant of Casier, Deconinck and Hirsch (1983)*

From a bidiagonal implicit family of schemes developed by Casier *et al.* (1983), a subclass can be extracted that can be considered as a generalization of MacCormack's schemes. The following represents a quasi-explicit extension of the explicit scheme (17.2.31):

$$(\xi + \frac{1}{2})\overline{\Delta U}_i = -\tau \cdot \delta^+ f_i^n + (\xi - \frac{1}{2})\overline{\Delta U}_{i-1} \quad (17.2.33a)$$

$$(\xi + \frac{1}{2})\overline{\overline{\Delta U}}_i = -\tau \cdot \delta^- \bar{f}_i + (\xi - \frac{1}{2})\overline{\overline{\Delta U}}_{i+1} \quad (17.2.33b)$$

$$\Delta U_i^n = \frac{1}{2}(\overline{\Delta U}_i + \overline{\overline{\Delta U}}_i) \quad (17.2.33c)$$

This scheme is conditionally stable for the CFL condition

$$|\sigma| \leq 2\xi \quad (17.2.34)$$

and reduces to (17.2.31) for  $\xi = \frac{1}{2}$ .

Each step involves only two mesh points and is a bidiagonal system, which is solved by a single sweep through the mesh. Details concerning the properties of the sweeps and the related boundary conditions are given in the original reference.

For steady calculations in particular, computations at high Courant numbers can be performed by appropriate choices of  $\xi$ . Hence the number of iterations to reach steady state can be considerably reduced, as shown in Figure 17.2.5 at similar computational cost per iteration. In addition the parameter  $\xi$  introduces a dissipation at each step level. Figure 17.2.5 shows the results obtained with scheme (17.2.33) at  $\xi = 20$ , CFL = 39 for a supersonic flow in a converging-diverging nozzle. Observe the excellent shock resolution, typical of compact box-type schemes, to be compared with Figure 17.2.2. The comparison of the convergence histories with MacCormack's scheme shows the considerable improvement obtained with the above scheme.

### 17.2.3 Lerat and Peyret's $S_\alpha^\beta$ family of non-linear, two-step Lax-Wendroff schemes

Lerat and Peyret (1974, 1975) made a systematic investigation of all the explicit second-order accurate schemes in space and time, which are centrally differenced

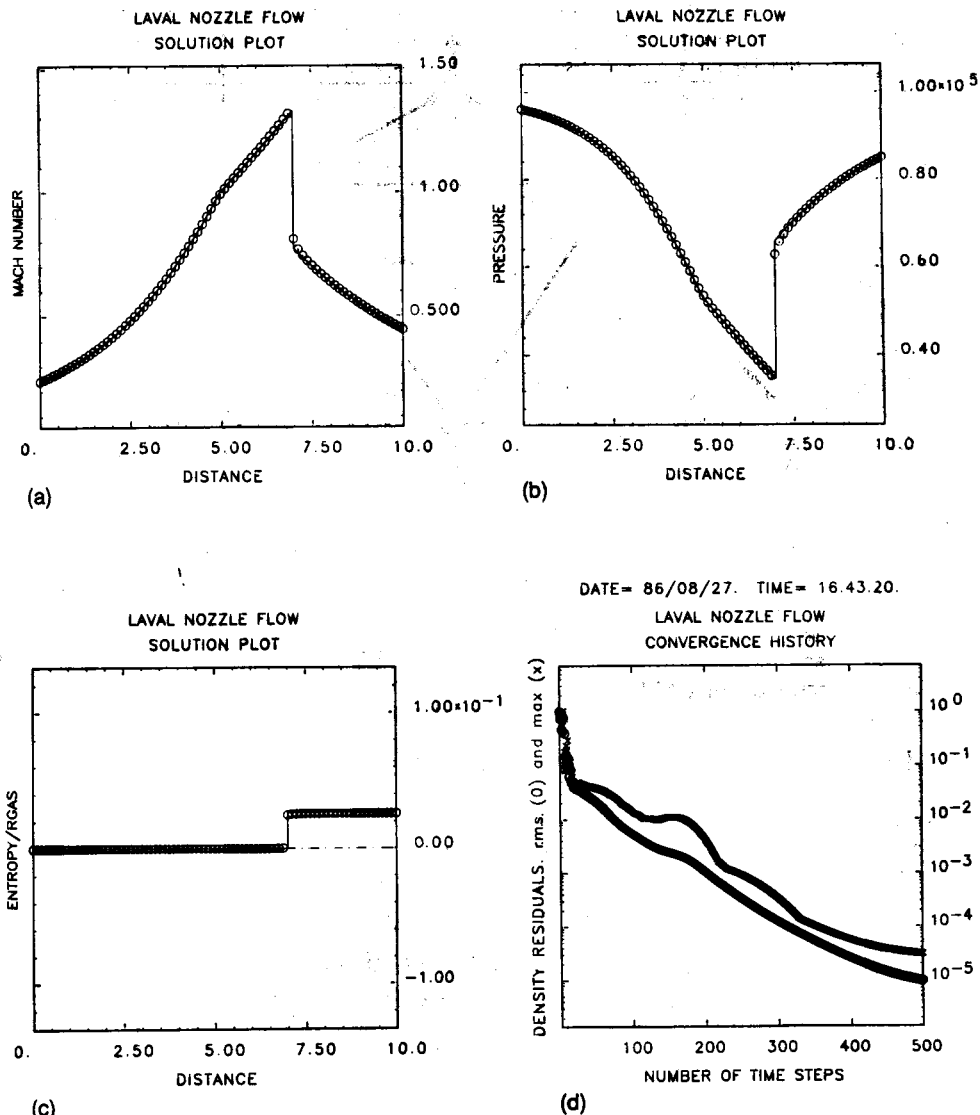
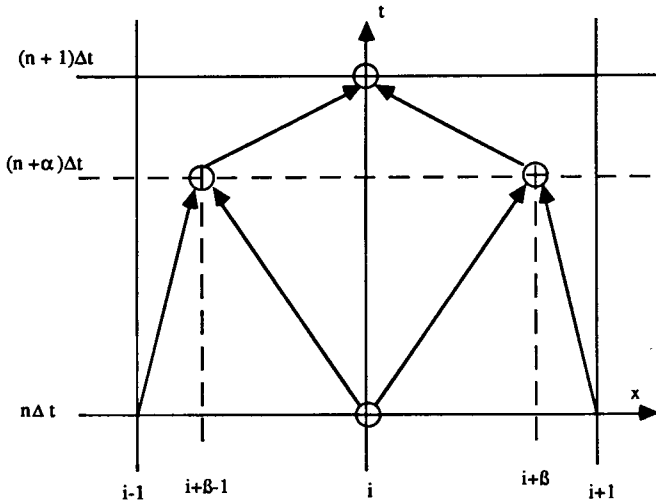


Figure 17.2.5 Results of scheme (17.2.33) with  $CFL = 39$  and  $\xi = 20$  applied to a stationary, transonic nozzle flow

with respect to  $(i-1), i, (i+1)$  and have a predictor–corrector two-step structure between the time levels  $n$  and  $n+1$ .

These schemes correspond to an explicit discretization of the predictor variables in  $(i+\beta)$  at time level  $(n+\alpha)$  (Figure 17.2.6). The predictor step leads to the following equations, for a forward differencing choice, by performing a

Figure 17.2.6 Computational molecule in Lerat and Peyret's  $S_\alpha^\beta$  schemes

Taylor expansion of  $U_{i+\beta}^{n+\alpha}$ :

$$\begin{aligned}
 U_{i+\beta}^{n+\alpha} &= U_{i+\beta}^n + \alpha \Delta t (U_i)_{i+\beta} + \frac{\alpha^2 \Delta t^2}{2} (U_{tt})_{i+\beta} + \dots \\
 &= U_i^n + \beta \Delta x (U_x)_i^n + \alpha \Delta t (U_t)_i^n + \alpha \beta \Delta t \Delta x U_{tx} + \frac{\beta^2 \Delta x^2}{2} U_{xx} + \frac{\alpha^2 \Delta t^2}{2} U_{tt}
 \end{aligned} \tag{17.2.35}$$

The last three terms are the truncation error of the predictor step at  $(n, i)$ . Applying forward difference formulas for the space derivatives after replacing  $U_t$  by  $-f_x$  leads to

$$U_{i+\beta}^{n+\alpha} \equiv \bar{U}_i = U_i^n + \beta(U_{i+1}^n - U_i^n) - \alpha\tau(f_{i+1}^n - f_i^n) \tag{17.2.36}$$

The corrector step is defined as to obtain overall second-order accuracy and can be written as

$$U_i^{n+1} = U_i^n - \frac{\tau}{2\alpha}(\bar{f}_i - \bar{f}_{i-1}) - \frac{\tau}{2\alpha}[(\alpha - \beta)f_{i+1}^n + (2\beta - 1)f_i^n + (1 - \alpha - \beta)f_{i-1}^n] \tag{17.2.37}$$

This family of schemes for arbitrary  $(\alpha, \beta)$  are designated as the  $S_\alpha^\beta$  schemes by Lerat and Peyret. They can be written in the alternative way by introducing the predictor and corrector variations  $\overline{\Delta U}, \underline{\Delta U}$  with the same definitions as for

MacCormack's scheme (17.2.29), namely

$$\overline{\Delta U}_i = -\tau(f_{i+1}^n - f_i^n) \quad (17.2.38a)$$

$$\overline{\overline{\Delta U}}_i = -\tau(\bar{f}_i - \bar{f}_{i-1}) \quad (17.2.38b)$$

where

$$\bar{f}_i = f(\bar{U}_i) \equiv f(U_{i+\beta}^{n+\alpha}) \quad (17.2.38c)$$

The  $S_\alpha^\beta$  schemes take the following form:

$$\bar{U}_i = U_i^n + \beta(U_{i+1}^n - U_i^n) + \alpha \overline{\Delta U}_i \quad (17.2.39a)$$

$$\Delta U_i \equiv U_i^{n+1} - U_i^n = \frac{1}{2\alpha} [(\alpha - \beta)\overline{\Delta U}_i + (\alpha + \beta - 1)\overline{\Delta U}_{i-1} + \overline{\overline{\Delta U}}_i] \quad (17.2.39b)$$

The interpretation of the predictor variation  $(\bar{U}_i - U_i^n)$  is clear from the Taylor expansion (17.2.35). It represents the flux contribution to the solution at the predictor level at point  $(i + \beta), (n + \alpha)$ . The corrector variation  $\overline{\Delta U}$  is also to be considered as a flux contribution at level  $(n + \alpha)$  to the final correction  $\Delta U = U^{n+1} - U^n$ , which can be written as

$$\Delta U_i = \frac{1}{2}(\overline{\Delta U}_i + \overline{\Delta U}_{i-1}) - \frac{1}{2\alpha} [\beta \overline{\Delta U}_i + (1 - \beta) \overline{\Delta U}_{i-1} + \overline{\overline{\Delta U}}_i] \quad (17.2.40)$$

With regard to the conservative form of the equations, the numerical flux of the  $S_\alpha^\beta$  scheme is

$$\begin{aligned} f_{i+1/2}^* &= \frac{1}{2\alpha} [(\alpha - \beta)f_{i+1} + (\alpha + \beta - 1)f_i + \bar{f}_i] \\ &= \frac{1}{2}(f_{i+1} + f_i) - \frac{1}{2\alpha} [\beta f_{i+1} + (1 - \beta)f_i] + \frac{1}{2\alpha} \bar{f}_i \end{aligned} \quad (17.2.41)$$

For  $\alpha = \beta = \frac{1}{2}$  one obtains exactly the Richtmyer two-step version of the Lax-Wendroff scheme, while  $\alpha = 1, \beta = 0$  gives MacCormack's scheme (17.2.29) and  $\alpha = 1, \beta = 1$  gives the variant (17.2.30). The family of schemes  $\alpha, \beta = \frac{1}{2}, S_\alpha^{1/2}$ , has been considered by McGuire and Morris (1973), while the particular case  $\alpha = 1, \beta = \frac{1}{2}$  has been proposed by Rubin and Burstein (1967). Another family  $\alpha, \beta = 0, S_\alpha^0$ , or  $\beta = 1, S_\alpha^1$ , has also been investigated independently by Warming *et al.* (1973).

All the  $S_\alpha^\beta$  schemes reduce to the Lax-Wendroff scheme in the linear case  $f = a \cdot u$  and have therefore identical linear properties. Hence, they represent a family of non-linear splittings of the Lax-Wendroff scheme into two steps. Lerat and Peyret (1975) made an investigation of the optimal properties for non-linear problems, in particular for Burgers equation, which allows a detailed analysis of the truncation errors, with the aim of reducing the oscillations around shock waves generated by the insufficient dissipation of three-point, explicit, central, second-order schemes.

Computing the truncation error of the  $S_\alpha^\beta$  schemes in the general non-linear case up to the highest order (see Section 9.4, equations (9.4.21) to (9.4.24) in Volume 1) leads to the equivalent differential equation of the scheme

$$U_t + f_x = \varepsilon_T \quad (17.2.42)$$

where  $\varepsilon_T$  is the truncation error.

From the definition of the numerical flux  $f_{i+1/2}^*$ , the contribution to the truncation error arising from the non-linearity contains a term proportional to the mixed derivative of  $f^*$  with respect to  $U_i$  and  $U_{i+1}$ . This is the term  $g_{12}$  in equations (9.4.21) to (9.4.25), where

$$g_{12} = \frac{\partial^2 f_{i+1/2}^*}{\partial U_i \partial U_{i+1}} = \frac{1}{2\alpha} A_U (1 - \beta + \alpha\tau A)_i (\beta - \alpha\tau A)_i \quad (17.2.43)$$

Hence, the truncation error becomes, with  $\sigma = \tau A$ ,

$$\varepsilon_T = \frac{\Delta x^2}{6} \frac{\partial}{\partial x} \left[ (\sigma^2 - 1) f_{xx} + \frac{3}{2\alpha} A_U (\beta - \alpha\sigma)(1 - \beta + \alpha\sigma) U_x^2 + 2\sigma^2 A_U U_x^2 \right] \quad (17.2.44)$$

By applying the relation  $A U_x = f_x$ , an alternative expression for the truncation error is

$$\varepsilon_T = \frac{\Delta x^2}{6} \frac{\partial}{\partial x} \left\{ (\tau^2 A^2 - 1) f_{xx} + \frac{3}{2\alpha} A_U (\beta U - \alpha\tau f)_x [(1 - \beta)U + \alpha\tau f]_x + 2\tau^2 A_U f_x^2 \right\} \quad (17.2.45)$$

where the subscripts indicate derivatives, in particular  $A_U$  is the derivative of the Jacobian with respect to  $U$ ,  $A_{UU} = f_{UU}$ .

The first term is the only one in the linear case  $A_U = 0$ , and is of a dispersive nature as discussed earlier. The second term is proportional to the second derivative  $f_{uu}$  and, hence, if the coefficient is appropriately chosen, could allow a non-linear dissipation to be introduced in order to damp the oscillations created at shock or contact discontinuities. However, since the coefficient of this term is proportional to  $f_x$ , the scheme can be made dissipative for compression shocks but would then be antidissipative for expansion waves. A detailed analysis, based on Burgers equation, shows that the choice

$$\begin{aligned} \alpha &= 1 + \sqrt{\frac{5}{2}} \\ \beta &= \frac{1}{2} \end{aligned} \quad (17.2.46)$$

gives a maximum dissipation with compression shocks and keeps the antidissipation to a minimum with rarefaction waves (Lerat and Peyret, 1975).

It is to be noted that the effect of the antidissipative term is partly counterbalanced by a higher-order term proportional to  $\Delta x^4 (\partial^4 f / \partial x^4)$  with a negative coefficient. The optimum values above are confirmed by numerical experiments on Euler equations, to minimize the non-linear oscillations at discontinuities.

### 17.2.4 One-step Lax-Wendroff schemes in two dimensions

The one-step Lax-Wendroff scheme for the multi-dimensional Euler equations is obtained from equation (17.2.2), following the same procedure as in one dimension. In two dimensions, the equation  $U_t + f_x + g_y = 0$  leads to the following estimation of  $U_u$ :

$$\begin{aligned} U_u &= \frac{\partial}{\partial t}(-f_x - g_y) \\ &= -\frac{\partial}{\partial x}\left(A \frac{\partial U}{\partial t}\right) - \frac{\partial}{\partial y}\left(B \frac{\partial U}{\partial t}\right) \\ &= \frac{\partial}{\partial x}[A(f_x + g_y)] + \frac{\partial}{\partial y}[B(f_x + g_y)] \\ &= \frac{\partial}{\partial x}\left(A \frac{\partial f}{\partial x}\right) + \frac{\partial}{\partial y}\left(B \frac{\partial g}{\partial y}\right) + \frac{\partial}{\partial x}\left(A \frac{\partial g}{\partial y}\right) + \frac{\partial}{\partial y}\left(B \frac{\partial f}{\partial x}\right) \quad (17.2.47) \end{aligned}$$

The mixed derivatives that appear in the last two terms are somewhat cumbersome, so much so that  $A$  and  $B$  do not commute.

The direct generalization of equation (17.2.11), with central symmetric difference formulas for the mixed derivatives, leads to the following scheme, written in difference operators notation:

$$\begin{aligned} U_{ij}^{n+1} &= U_{ij}^n - \tau_x \bar{\delta}_x f_{ij}^n - \tau_y \bar{\delta}_y g_{ij}^n + \frac{\tau_x^2}{2} \delta_x (A_{ij} \delta_x f_{ij}) + \frac{\tau_y^2}{2} \delta_y (B_{ij} \delta_y g_{ij}) \\ &\quad + \frac{\tau_x \tau_y}{2} [\bar{\delta}_x (A_{ij} \bar{\delta}_y g_{ij}) + \bar{\delta}_y (B_{ij} \bar{\delta}_x f_{ij})] \quad (17.2.48) \end{aligned}$$

where

$$\tau_x = \frac{\Delta t}{\Delta x} \quad \tau_y = \frac{\Delta t}{\Delta y} \quad (17.2.49)$$

and the central difference operators  $\bar{\delta}_x$  and  $\bar{\delta}_y$  are defined by equation (17.1.31), while  $\delta_x, \delta_y$  are the operators in the  $x$  and  $y$  directions defined as in equation (17.2.9).

This scheme uses all of the nine points surrounding  $(ij)$ , and various other variants can be defined by treating the mixed derivative terms differently (see Problem 17.4).

The stability of the two-dimensional Lax-Wendroff scheme (17.2.48) is analysed by the Von Neumann method. The following amplification matrix is obtained for constant Jacobians  $A, B$  and linearized fluxes  $f = Au, g = Bu$ :

$$\begin{aligned} G &= 1 - I(\tau_x A \sin \phi_x + \tau_y B \sin \phi_y) - \tau_x^2 A^2 (1 - \cos \phi_x) - \tau_y^2 B^2 (1 - \cos \phi_y) \\ &\quad - \frac{\tau_x \tau_y}{2} (AB + BA) \sin \phi_x \sin \phi_y \quad (17.2.50) \end{aligned}$$

For real, symmetric and commuting matrices  $A, B$ , Turkel (1977) has shown that the following condition is necessary and sufficient for the Von Neumann stability:

$$|\tau_x \rho(A)|^{2/3} + |\tau_y \rho(B)|^{2/3} \leq 1 \quad (17.2.51)$$

Since the matrices  $A$  and  $B$  do not commute, this condition is only sufficient (Turkel, 1977). Weaker conditions had been given originally by Lax and Wendroff (1964) as

$$\tau_x \rho(A) \leq \frac{1}{\sqrt{8}} \quad \text{and} \quad \tau_y \rho(B) \leq \frac{1}{\sqrt{8}} \quad (17.2.52)$$

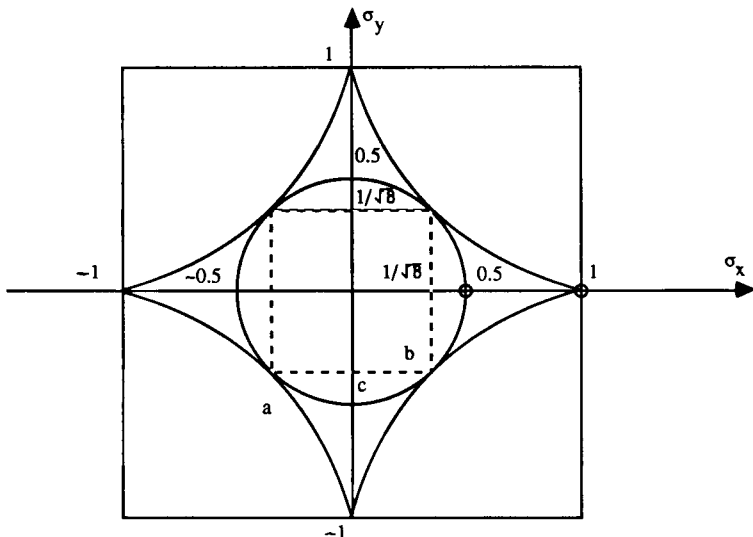
and an improvement found by Tadmor is reported by Turkel (1977) as

$$[\tau_x \rho(A)]^2 + [\tau_y \rho(B)]^2 \leq \frac{1}{4} \quad (17.2.53)$$

All of the above sufficient relations are valid for real, symmetric matrices  $A$  and  $B$  are compared in Figure 17.2.7, in a diagram  $(\sigma_x, \sigma_y)$

$$\sigma_x = \tau_x \rho(A) \quad \sigma_y = \tau_y \rho(B) \quad (17.2.54)$$

It is worth mentioning that for a scalar equation with  $\Delta x = \Delta y$ , a numerical study of the amplification factor (17.2.50) performed by Burstein (1967) has led



a - condition (17.2.51)

b - condition (17.2.52)

c - condition (17.2.53)

Figure 17.2.7 Comparison of different sufficient stability conditions for the one-step Lax-Wendroff scheme in two dimensions

to the stability condition

$$\tau(|\vec{v}| + c) < 0.5406$$

which is close to the condition (17.2.53).

Although interesting conceptually, the one-step Lax-Wendroff schemes are rarely applied since they require many Jacobian matrices evaluations; therefore one favours, in practice, extensions of the two-step methods.

#### *Reinterpretation of the one-step Lax-Wendroff scheme*

The one-step Lax-Wendroff schemes have recently gained a renewed interest for practical computations in the framework of multi-grid schemes (Ni, 1982; Hall, 1985; see also Koeck, 1985). Ni (1982) reformulated the Taylor expansion in time (17.2.2) as a ‘distribution’ formula for the finite variation  $\Delta U = U^{n+1} - U^n$  at a mesh point.

The guiding idea is obtained from rewriting the Lax-Wendroff algorithm in the form (17.2.7), (17.2.8) as a two-step procedure:

$$\overline{\Delta U}_{i+1/2} = -\tau(f_{i+1}^n - f_i^n) \quad (17.2.55)$$

$$f_{i+1/2}^* = f_{i+1/2} + \frac{1}{2} A_{i+1/2}^n \overline{\Delta U}_{i+1/2} \quad (17.2.56)$$

$$\Delta U^n = -\tau(f_{i+1/2}^* - f_{i-1/2}^*) \quad (17.2.57)$$

The variation  $\Delta U_i^n = U_i^{n+1} - U_i^n$  from time  $n$  to time level  $n+1$  is considered to result from contributions of the flux imbalance over the cells  $(i+1, i)$  and  $(i, i-1)$  (Figure 17.2.8). The flux imbalance over cell  $(i+1/2)$  is  $(f_{i+1} - f_i)$  and contributes to the overall variation  $\Delta U_i^n$  by an amount

$$\overline{\Delta U}_{i+1/2} \equiv -\tau(f_{i+1}^n - f_i^n) = -\tau \delta f_{i+1/2}^n \quad (17.2.58)$$

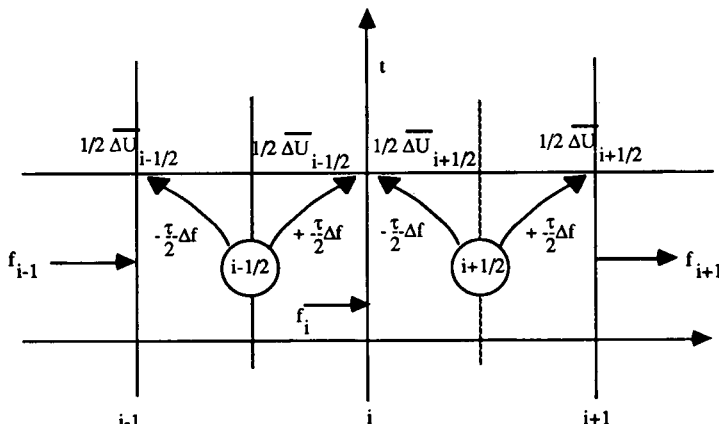


Figure 17.2.8 Distribution of flux imbalances in the distribution interpretation of the one-step Lax-Wendroff scheme

Similarly, the cell  $(i - 1/2)$  contributes with

$$\overline{\Delta U}_{i-1/2} \equiv -\tau(f_i^n - f_{i-1}^n) = -\tau\delta f_{i-1/2}^n \quad (17.2.59)$$

If no other contributions to  $\Delta U_i$  are taken into account, the formula

$$\Delta U_i^n = \frac{1}{2}(\overline{\Delta U}_{i+1/2} + \overline{\Delta U}_{i-1/2}) = -\frac{\tau}{2}(f_{i+1}^n - f_{i-1}^n) \quad (17.2.60)$$

is the unstable central difference scheme.

The contributions from the second time derivative  $U_{tt}$  stabilizes the central scheme while maintaining second-order accuracy. As seen from equation (17.2.5), the stabilizing terms can be viewed as arising from a contribution

$$\overline{\Delta f}_{i-1/2} \equiv A_{i-1/2} \cdot \overline{\Delta U}_{i-1/2} = \left( \frac{\partial f}{\partial U} \right)_{i-1/2} \cdot \overline{\Delta U}_{i-1/2} \quad (17.2.61)$$

from cell  $(i - 1/2)$  and

$$\Delta f_{i+1/2} \equiv A_{i+1/2} \cdot \overline{\Delta U}_{i+1/2} = \left( \frac{\partial f}{\partial U} \right)_{i+1/2} \cdot \overline{\Delta U}_{i+1/2} \quad (17.2.62)$$

from cell  $(i + 1/2)$ .

The total contribution from cell  $(i - 1/2)$  to  $U_i^{n+1}$  is defined in the Lax-Wendroff scheme as

$$\Delta U_{i-1/2}^+ \equiv \frac{1}{2}(\overline{\Delta U}_{i-1/2} + \tau \overline{\Delta f}_{i-1/2}) \quad (17.2.63)$$

and the contribution from the downstream cell  $(i + 1/2)$  is

$$\Delta U_{i+1/2}^- \equiv \frac{1}{2}(\overline{\Delta U}_{i+1/2} - \tau \overline{\Delta f}_{i+1/2}) \quad (17.2.64)$$

The Lax-Wendroff scheme can then be written as

$$\Delta U_i \equiv U_i^{n+1} - U_i^n = (\Delta U_{i+1/2}^- + \Delta U_{i-1/2}^+) \quad (17.2.65)$$

Within each cell, for instance cell  $(i + 1/2)$ , the first variation  $\overline{\Delta U}_{i+1/2}$  is equally distributed to the points  $i$  and  $i + 1$ , while the second contribution  $\overline{\Delta f}_{i+1/2}$  is added to the downstream point and subtracted from the upstream point; that is one has

$$\Delta U_{i+1/2}^+ = \frac{1}{2}(\overline{\Delta U}_{i+1/2} + \tau \overline{\Delta f}_{i+1/2}) \quad (17.2.66)$$

such that

$$\Delta U_{i+1/2}^- + \Delta U_{i+1/2}^+ = \overline{\Delta U}_{i+1/2} \quad (17.2.67)$$

Although the resultant scheme is central, each separate contribution has an upwind character. This can best be seen for a scalar (characteristic) equation where  $A$  or its eigenvalue  $a$  is taken as positive.

In this case, with  $\sigma = \tau a > 0$ ,

$$\Delta U_{i-1/2}^+ = \frac{1}{2}(1 + \sigma) \overline{\Delta U}_{i-1/2} \quad (17.2.68)$$

and

$$\Delta U_{i+1/2}^- = \frac{1}{2}(1-\sigma)\overline{\Delta U}_{i+1/2} \quad (17.2.69)$$

showing that the upstream cell provides a larger correction to  $\Delta U_i$  than the downstream cell. This is in agreement with the physical properties of wave propagations. The central properties of the Lax-Wendroff scheme result from the equal distribution of  $\Delta f$  contained in equation (17.2.65).

The interpretation of Lax-Wendroff scheme as distribution formulas of corrections is used by Ni (1982) and Hall (1985) in order to define multi-grid strategies, whereby the above formulas are applied on a succession of coarser meshes.

It is interesting to observe at this point that MacCormack's scheme (17.2.29) can be interpreted as a distribution scheme whereby

$$\Delta U_{i+1/2}^+ = \frac{1}{2}\overline{\Delta U}_{i+1/2} \quad (17.2.70)$$

and

$$\Delta U_{i-1/2}^- = \frac{1}{2}\tilde{\Delta}\tilde{U}_{i-1/2} \quad (17.2.71)$$

where the tilde indicates that the variation in the upstream cell ( $i - 1/2$ ) is considered to have been already affected by the downstream cell variation; that is

$$\Delta U_{i-1/2}^- = \frac{1}{2}\overline{\Delta U}_{i-1/2}(U_i^n + \Delta U_{i+1/2}^+, U_{i-1}^n + \Delta U_{i-1/2}^+) \equiv \frac{1}{2}\tilde{\Delta}\tilde{U}_{i+1/2} \quad (17.2.72)$$

with

$$\Delta U_{i-1/2}^+ = \frac{1}{2}\overline{\Delta U}_{i-1/2}(U_i^n, U_{i-1}^n) \quad (17.2.73)$$

The alternative version (17.2.30) is obtained by considering the downstream cell variations to be affected by the prior, upstream corrections.

Various ways can be defined for the computation of the flux corrections  $\Delta f_{i\pm 1/2}$ . A straightforward way, avoiding the calculation of the Jacobian matrices, consists in the following equations:

$$\Delta f = \Delta \begin{vmatrix} \rho u \\ \rho u^2 + p \\ \rho u + 1 \end{vmatrix} = \begin{vmatrix} \Delta(\rho u) \\ u \Delta(\rho u) + \rho u \Delta u + \Delta p \\ H \Delta(\rho u) + \rho u \Delta H \end{vmatrix} \quad (17.2.74)$$

where  $\Delta$  represents the appropriate finite difference and

$$\Delta U = \begin{vmatrix} \Delta \rho \\ \Delta(\rho u) \\ \Delta(\rho E) \end{vmatrix} \quad (17.2.75)$$

is used to derive the values of  $\Delta p$ ,  $\Delta u$  and  $\Delta H$  from their relations to the conservative variables seen in Chapter 16.

### *Two-dimensional distribution formulas*

The extension of the above interpretation to two dimensions has the additional advantage that the mixed derivative terms of equation (17.2.48) do not appear

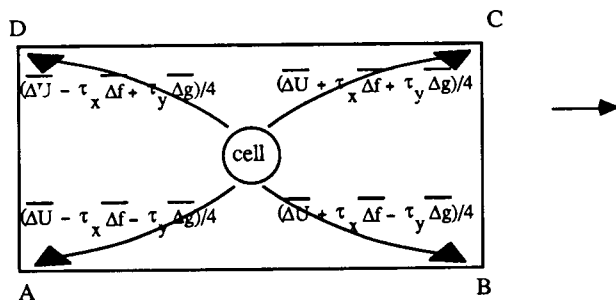
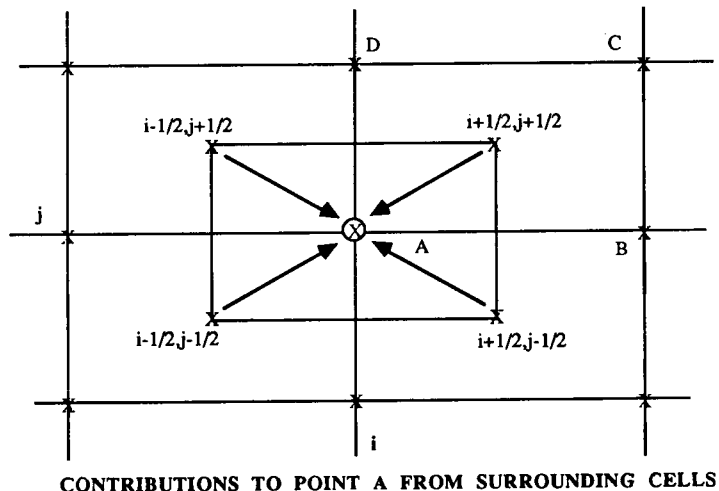


Figure 17.2.9 Two-dimensional distribution interpretation of the Lax-Wendroff one-step schemes

explicitly in the calculation. Indeed, referring to Figure 17.2.9, four cells will contribute to the variation  $\Delta U_{ij}^n = U_{ij}^{n+1} - U_{ij}^n$ .

Considering cell  $(i + 1/2, j + 1/2)$ , the variations associated to the first derivative terms of equation (17.2.48) lead to a contribution

$$\overline{\Delta U}_{i+1/2,j+1/2} = -\tau_x(f_{i+1,j+1/2} - f_{i,j+1/2}) - \tau_y(g_{i+1/2,j+1} - g_{i+1/2,j}) \quad (17.2.76)$$

where

$$f_{i,j+1/2} = \frac{1}{2}(f_{i,j} + f_{i,j+1}) \quad (17.2.77)$$

and similar formulas for the other flux components at mid-side points.

For an arbitrary mesh, the contribution  $\Delta U_{i+1/2,j+1/2}$  will be defined by a finite volume discretization with a control volume ABCD having the mesh

points at its corners:

$$\overline{\Delta U}_{i+1/2,j+1/2} = -\frac{\Delta t}{S_{i+1/2,j+1/2}} \sum_{ABCD} (f \Delta y - g \Delta x) \quad (17.2.78)$$

where  $S_{i+1/2,j+1/2}$  is the area of ABCD and the summation extends to the four sides of the cell.

This variation is distributed equally to the four corners of the cell with a weight coefficient of  $\frac{1}{4}$  and when these contributions from the four cells common to point  $(i,j)$  are added to form  $\Delta U_{ij}^n$ , one obtains again the central unstable scheme.

The stabilizing terms arising from the  $U_n$  contributions are evaluated from the second line of equation (17.2.47). With

$$\begin{aligned} \overline{\Delta f}_{i+1/2,j+1/2} &= A_{i+1/2,j+1/2} \overline{\Delta U}_{i+1/2,j+1/2} \\ \overline{\Delta g}_{i+1/2,j+1/2} &= B_{i+1/2,j+1/2} \overline{\Delta U}_{i+1/2,j+1/2} \end{aligned} \quad (17.2.79)$$

the following distributions occur within the cell  $(i+1/2,j+1/2)$  towards the four corners:

$$\Delta U_{i+1/2,j+1/2}^{\pm\pm} = \frac{1}{4}(\overline{\Delta U} \pm \tau_x \overline{\Delta f} \pm \tau_y \overline{\Delta g})_{i+1/2,j+1/2} \quad (17.2.80)$$

with obvious definitions of the four combinations of signs. For instance

$$\begin{aligned} \Delta U_{i+1/2,j+1/2}^{(C)} &= \Delta U_{i+1/2,j+1/2}^{++} \\ \Delta U_{i+1/2,j+1/2}^{(B)} &= \Delta U_{i+1/2,j+1/2}^{+-} \end{aligned} \quad (17.2.81)$$

Finally, the distribution form of the Lax-Wendroff scheme can be written as

$$\begin{aligned} \Delta U_{ij} &= U_{ij}^{n+1} - U_{ij}^n = \Delta U_{i+1/2,j+1/2}^{--} + \Delta U_{i+1/2,j-1/2}^{--} \\ &\quad + \Delta U_{i-1/2,j-1/2}^{++} + \Delta U_{i-1/2,j+1/2}^{+-} \end{aligned} \quad (17.2.82)$$

For unequal mesh sizes, the above formula can be replaced by volume-weighted averages.

For more details on the multi-grid application we refer the reader to the above-mentioned references for two-dimensional applications and to the extension to three dimensions developed by Koeck (1985).

Figure 17.2.10, from Ni (1982), is an example of a transonic flow in a channel with a circular arc obstacle on the lower wall. The height of the channel is equal to the chord of the circular arc, and its thickness to chord ratio is 10 per cent.

For an incident Mach number of  $M_\infty = 0.675$ , a supersonic region terminated by a normal shock is obtained. Behind the non-uniform shock, the flow is known to become rotational, and this can be seen from the way the iso-mach lines intersect the flat surfaces. Upstream of the circular arc, the flow is irrotational and the iso-mach lines are perpendicular to the surface, which is not the case any-longer in the downstream part (see Problem 17.12).

The stagnation pressure contours (Figure 17.2.10(c)) show the generated

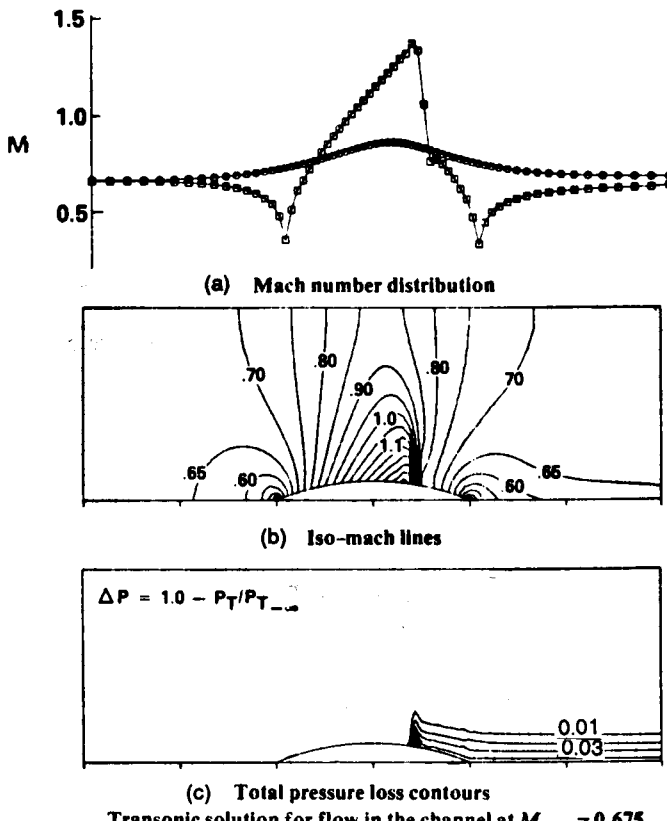


Figure 17.2.10 Transonic flow in a channel with a circular arc obstacle on the lower wall. (From Ni, 1982)

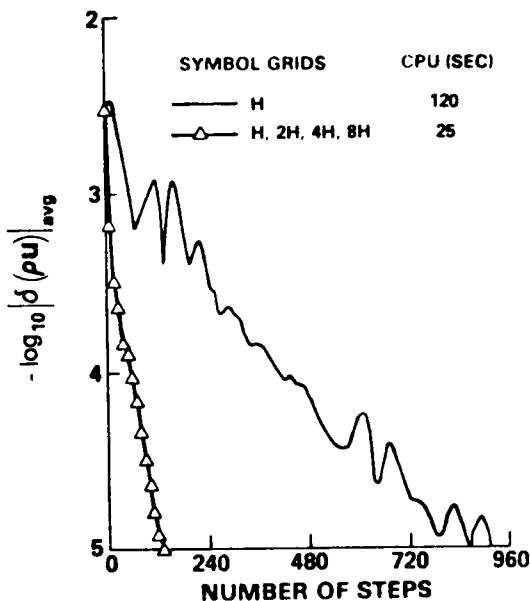
entropy at the shock being convected further downstream. The convergence history in Figure 17.2.11 shows the improvement achieved by the multi-grid strategy using four successive grids.

### 17.2.5 Two-step Lax-Wendroff schemes in two dimensions

As with one-dimensional problems, the one-step Lax-Wendroff schemes also suffer from the difficulty of requiring calculations of Jacobian matrices. This can be avoided by the two-step versions, such as the Richtmyer and MacCormack schemes, which are generalized by the two-dimensional versions of the  $S_{\alpha}^{\beta}$  schemes of Lerat and Peyret.

#### *The two-step Richtmyer scheme*

Equation (17.2.27) can be generalized to two (or three) dimensions in a straightforward way by applying a first-step Lax-Friedrichs scheme (17.1.21), followed



Convergence history for transonic flow in the channel.

Figure 17.2.11 Convergence history for the transonic channel flow of Figure 17.2.10. (From Ni, 1982)

by a leapfrog step. One obtains, in two dimensions,

$$\begin{aligned} U_{ij}^{n+1/2} &= \frac{1}{4}(U_{i+1,j}^n + U_{i-1,j}^n + U_{i,j+1}^n + U_{i,j-1}^n) \\ &\quad - \frac{\tau_x}{2}(f_{i+1,j}^n - f_{i-1,j}^n) - \frac{\tau_y}{2}(g_{i,j+1}^n - g_{i,j-1}^n) \\ U_{ij}^{n+1} &= U_{ij}^n - \tau_x(f_{i+1,j}^{n+1/2} - f_{i-1,j}^{n+1/2}) - \tau_y(g_{i,j+1}^{n+1/2} - g_{i,j-1}^{n+1/2}) \end{aligned} \quad (17.2.83)$$

This scheme involves the points  $(i \pm 1, j)$  and  $(i, j \pm 1)$  at two different time levels, since the first step is written at integer mesh points.

The more direct generalization of equation (17.2.27) has also been considered as follows (Zwas, 1973):

$$\begin{aligned} U_{i+1/2,j+1/2}^{n+1/2} &= \frac{1}{4}(U_{i+1,j+1}^n + U_{i+1,j}^n + U_{i,j+1}^n + U_{i,j}^n) - \frac{\tau_x}{2}(f_{i+1,j+1/2}^n - f_{i,j+1/2}^n) \\ &\quad - \frac{\tau_y}{2}(g_{i+1/2,j+1}^n - g_{i+1/2,j}^n) \\ U_{ij}^{n+1} &= U_{ij}^n - \tau_x(f_{i+1/2,j}^{n+1/2} - f_{i-1/2,j}^{n+1/2}) - \tau_y(g_{i,j+1/2}^{n+1/2} - g_{i,j-1/2}^{n+1/2}) \end{aligned} \quad (17.2.84)$$

These two versions are equivalent but not identical. In the version (17.2.84), the half-integer mesh point values can be estimated as

$$\begin{aligned} f_{i+1,j+1/2}^n &= f\left(\frac{U_{i+1,j+1}^n + U_{i+1,j}^n}{2}\right) \\ f_{i+1/2,j}^{n+1/2} &= f\left(\frac{U_{i+1/2,j+1/2}^{n+1/2} + U_{i+1/2,j-1/2}^{n+1/2}}{2}\right) \end{aligned} \quad (17.2.85)$$

The alternative option

$$\begin{aligned} f_{i+1/2,j}^{n+1/2} - f_{i-1/2,j}^{n+1/2} &= \frac{1}{2}(f_{i+1/2,j+1/2}^{n+1/2} + f_{i+1/2,j-1/2}^{n+1/2}) \\ &\quad - \frac{1}{2}(f_{i-1/2,j+1/2}^{n+1/2} + f_{i-1/2,j-1/2}^{n+1/2}) \end{aligned} \quad (17.2.86)$$

is a third-order estimation.

The stability conditions of these two versions are also different. Applying a Von Neumann analysis, scheme (17.2.83) gives, in the linearized case,

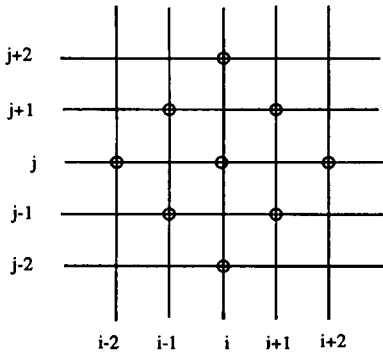
$$G = 1 - I(\tau_x A \sin \phi_x + \tau_y B \sin \phi_y)(\cos \phi_x + \cos \phi_y) - 2(\tau_x A \sin \phi_x + \tau_y B \sin \phi_y)^2 \quad (17.2.87)$$

When the scheme (17.2.83) is reduced to a single equation, it involves points  $(i \pm 2, j)$  and  $(i, j \pm 2)$  shown in Figure 17.2.12.

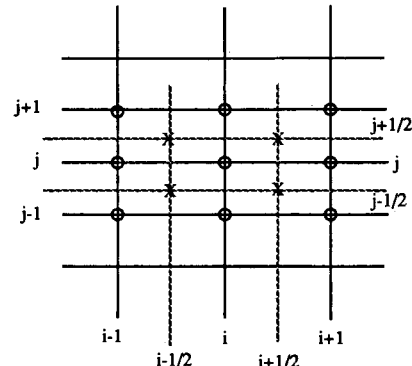
The necessary and sufficient stability property can be found in this case (Richtmyer and Morton, 1967), and for  $\Delta x = \Delta y$  can be written as

$$\frac{\Delta t}{\Delta x}(|\vec{v}| + c) \leq \frac{1}{\sqrt{2}} \quad (17.2.88)$$

which is a CFL condition with the limit  $1/\sqrt{2}$ .



(a) Computational stencil  
for scheme (17.2.83)



(b) Computational stencil  
for scheme (17.2.84)

Figure 17.2.12 Computational molecules for schemes (17.2.83) and (17.2.84)

The variant (17.2.84) is more compact and involves the nine points indicated in Figure 17.2.12(b), leading to the amplification matrix

$$G = 1 - \frac{I}{2} [\tau_x A \sin \phi_x (1 + \cos \phi_y) + \tau_y B \sin \phi_y (1 + \cos \phi_x)] - \left( \tau_x A \sin \frac{\phi_x}{2} \cos \frac{\phi_y}{2} + \tau_y B \cos \frac{\phi_x}{2} \sin \frac{\phi_y}{2} \right)^2 \quad (17.2.89)$$

Here, also, a necessary and sufficient condition for stability can be found (Zwas, 1973; Turkel, 1977), for  $\Delta x = \Delta y$ :

$$\frac{\Delta t}{\Delta x} (|\vec{v}| + c) \leq 1 \quad (17.2.90)$$

which is a CFL condition limited by one. Hence this version of the Richtmyer scheme allows a maximum time step larger by a factor  $\sqrt{2}$  compared to the scheme (17.2.83).

### *The two-step MacCormack scheme*

This scheme is the most popular two-step variant of the explicit Lax–Wendroff family as it involves only seven points instead of nine.

Since MacCormack's scheme combines forward and backward differences in separate predictor and corrector steps, four different schemes can be defined in two dimensions, through various combinations of the one-sided differences on the flux components  $f$  and  $g$ . For instance, in the line of scheme (17.2.29), one would write the following version of MacCormack's scheme:

$$\begin{aligned} \bar{U}_{ij} &= U_{ij}^n - \tau_x (f_{i+1,j}^n - f_{ij}^n) - \tau_y (g_{i,j+1}^n - g_{ij}^n) \\ \bar{\bar{U}}_{ij} &= U_{ij}^n - \tau_x (\bar{f}_{ij} - \bar{f}_{i-1,j}) - \tau_y (\bar{g}_{ij} - \bar{g}_{i,j-1}) \\ U_{ij}^{n+1} &= \frac{1}{2} (\bar{U}_{ij} + \bar{\bar{U}}_{ij}) \end{aligned} \quad (17.2.91)$$

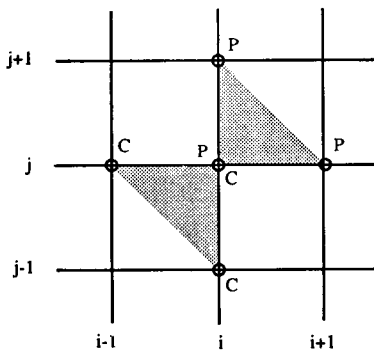
Figure 17.2.13 shows the computational molecule associated to scheme (17.2.91) where the points marked P indicate the values used at the predictor level.

The amplification matrix of the two-dimensional MacCormack scheme can be derived for the version (17.2.91) by defining  $\bar{G}$  as  $\bar{U} = \bar{G}U^n$ ,  $\bar{\bar{G}}$  as  $\bar{\bar{U}} = \bar{\bar{G}}U^n$  and  $G = (\bar{G} + \bar{\bar{G}})/2$ , leading to

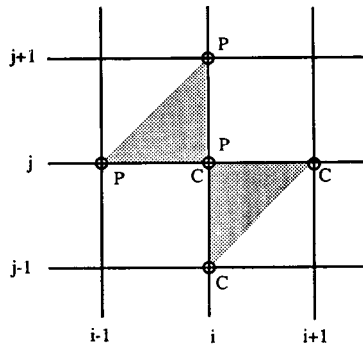
$$\begin{aligned} \bar{G} &= 1 - \tau_x A (e^{I\phi_x} - 1) \tau_y B (e^{I\phi_y} - 1) \\ \bar{\bar{G}} &= 1 - \bar{G} [\tau_x A (1 - e^{-I\phi_x}) + \tau_y B (1 - e^{-I\phi_y})] \\ G &= 1 - I (\tau_x A \sin \phi_x + \tau_y B \sin \phi_y) \\ &\quad - \left[ (\tau_x^2 A^2 (1 - \cos \phi_x) + \tau_y^2 B^2 (1 - \cos \phi_y) \right. \\ &\quad \left. + 4 \tau_x \tau_y A B \sin \frac{\phi_x}{2} \cdot \sin \frac{\phi_y}{2} \cos \frac{\phi_x - \phi_y}{2} \right] \end{aligned} \quad (17.2.92)$$

written for commuting matrices  $A, B$ .

Forward-forward version



Forward-backward version



P : Predictor points

C : Corrector points

Figure 17.2.13 Computational molecule for MacCormack's scheme

This expression is quite complicated and no analytically derived stability condition is known. An experimentally derived necessary condition for stability is obtained by MacCormack and Paullay (1972) as a CFL condition, indicating that the physical domain of dependence should be contained in the numerical one:

$$(\tau_x |\lambda(A)|_{\max} + \tau_y |\lambda(B)|_{\max}) \leq 1 \quad (17.2.93)$$

or

$$\Delta t \leq \left[ \frac{|\lambda(A)|_{\max}}{\Delta x} + \frac{|\lambda(B)|_{\max}}{\Delta y} \right]^{-1}$$

This condition is obtained from the stability condition  $\rho(G) \leq 1$  for  $\phi_x = \phi_y = \pi$ . See also Tong (1987) for an independent confirmation through a numerical evaluation of the amplification factor  $G$ . In Cartesian coordinates,  $|\lambda(A)|_{\max} = |u| + c$  and  $|\lambda(B)|_{\max} = |v| + c$ , where  $u$  and  $v$  are the  $x$  and  $y$  components of the velocity vector  $\vec{v}$ . Hence, one obtains for the Euler equations

$$\Delta t \leq \frac{1}{(|u| + c)/\Delta x + (|v| + c)/\Delta y} < \frac{\Delta x \Delta y}{|u| \Delta y + |v| \Delta x + c \sqrt{\Delta x^2 + \Delta y^2}} \quad (17.2.94)$$

where the right-hand side is the current form, as generally found in the literature.

A backward-backward predictor version is described by the scheme

$$\begin{aligned} \bar{U}_{ij} &= U_{ij}^n - \tau_x(f_{ij}^n - f_{i-1,j}^n) - \tau_y(g_{ij}^n - g_{i,j-1}^n) \\ \bar{\bar{U}}_{ij} &= U_{ij}^n - \tau_x(\bar{f}_{i+1,j} - \bar{f}_{ij}) - \tau_y(\bar{g}_{i,j+1} - \bar{g}_{ij}) \\ U_{ij}^{n+1} &= \frac{1}{2}(\bar{U}_{ij} + \bar{\bar{U}}_{ij}) \end{aligned} \quad (17.2.95)$$

A comparative study of the four variants has led Lerat and Sides (1977) to the conclusion that the best results are obtained in steady flows when the corrector step is upwind with regard to the flow direction, in concordance with the one-dimensional observations. A dynamic switch between the four variants as a function of the flow direction is applied by Lerat and Sides (1977), but most of the applications use a fixed version. In this case, it is recommended to cycle between the four possibilities during a computation, in order to avoid a bias provided by an eventual accumulation of errors.

#### *Finite volume formulation of MacCormack's scheme*

Due to its importance, we present here a finite volume formulation of MacCormack's scheme on an arbitrary mesh, which was actually one of the first applications of the finite volume method (see Chapter 6 in Volume 1).

The current approach consists of a discretization of both predictor and corrector steps on the same control volume ABCD with mesh points  $(i, j)$  at its centre (Figure 17.2.14). The two steps are distinguished by the way the fluxes are estimated. In the predictor forward-forward version, for instance, the flux along the downstream side BC is defined as being equal to the flux value at point Q  $(i + 1, j)$  and along the side CD to the value at point R  $(i, j + S)$ . In the corrector step, the upstream flux values are selected.

Designating the cell side normals by  $\vec{S}_{i \pm 1/2}$  and  $\vec{S}_{j \pm 1/2}$ , the predictor step is defined by

$$\bar{U}_{ij} = U_{ij}^n - \frac{\Delta t}{\Omega_{ij}} (\vec{F}_{i+1,j} \cdot \vec{S}_{i+1/2} + \vec{F}_{i,j+1} \cdot \vec{S}_{j+1/2} + \vec{F}_{ij} \cdot \vec{S}_{i-1/2} + \vec{F}_{ij} \cdot \vec{S}_{j-1/2}) \quad (17.2.96)$$

where  $\Omega_{ij}$  is the area of the cell.

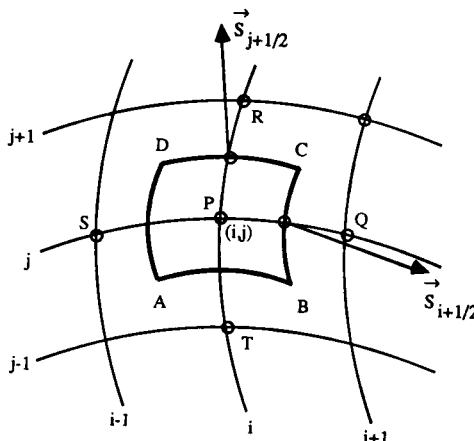


Figure 17.2.14 Control volume ABCD for finite volume discretization of MacCormack's scheme

The corrector step is

$$\bar{U}_{ij} = U_{ij}^n - \frac{\Delta t}{\Omega_{ij}} (\vec{F}_{ij} \cdot \vec{S}_{i+1/2} + \vec{F}_{ij} \cdot \vec{S}_{j+1/2} + \vec{F}_{i-1} \cdot \vec{S}_{i-1/2} + \vec{F}_{j-1} \cdot \vec{S}_{j-1/2}) \quad (17.2.97)$$

and

$$U_{ij}^{n+1} = \frac{1}{2}(\bar{U}_{ij} + \bar{U}_{ij}) \quad (17.2.98)$$

The flux contributions are evaluated, for instance, as follows:

$$\begin{aligned} \vec{S}_{i+1/2} &= (y_{i+1/2,j+1/2} - y_{i+1/2,j-1/2}) \vec{1}_x \\ &\quad - (x_{i+1/2,j+1/2} - x_{i+1/2,j-1/2}) \vec{1}_y \\ &\equiv \Delta y_{i+1/2} \vec{1}_x - \Delta x_{i+1/2} \vec{1}_y \\ \vec{F}_{i+1,j} \vec{S}_{i+1/2} &= f_{i+1,j} \Delta y_{i+1/2} - g_{i+1,j} \Delta x_{i+1/2} \end{aligned} \quad (17.2.99)$$

*Computational note* With the definitions of the flux components  $f$  and  $g$  in conservative variables, the above contributions can be calculated as follows, where  $U$  is the vector of the conservative variables:

$$\vec{F} \cdot \vec{S} = \begin{vmatrix} \rho(u \Delta y - v \Delta x) \\ \rho u(u \Delta y - v \Delta x) + p \Delta y \\ \rho v(u \Delta y - v \Delta x) - p \Delta x \\ \rho H(u \Delta y - v \Delta x) \end{vmatrix} = U(u \Delta y - v \Delta x) + p \begin{vmatrix} 0 \\ \Delta x \\ -\Delta x \\ 0 \end{vmatrix} \quad (17.2.100)$$

The scalar quantity

$$q \equiv u \Delta y - v \Delta x = \vec{v} \cdot \vec{S} \quad (17.2.101)$$

is the volume flow rate through the cell side  $\vec{S}$ . Hence, it is computationally advantageous and recommended to follow this approach, defining

$$\vec{F}_{i+1,j} \vec{S}_{i+1/2} = U_{i+1,j} q_{i+1,j} + p_{i+1,j} \begin{vmatrix} 0 \\ \Delta y \\ -\Delta x \\ 0 \end{vmatrix} \quad (17.2.102)$$

Other variants can be defined by selecting different control volumes for predictor and corrector steps and defining the points at which the fluxes are estimated in an appropriate way; see, for instance, Thompkins *et al.* (1983) and Problem 17.24.

A three-dimensional finite volume formulation can be found in Rizzi and Inouye (1973).

A necessary CFL condition for stability is expressed by the condition that the numerical domain of dependence should contain all of the physical one.

This can be expressed by the general form

$$\Delta t \leq \min_{(ij)} \left( \frac{\Omega_{ij}}{|\vec{v}_{ij} \vec{S}_{i-1/2}| + |\vec{v}_{ij} \vec{S}_{j-1/2}| + c_{ij} \sqrt{|\vec{S}_{i+1/2}|^2 + |\vec{S}_{j+1/2}|^2}} \right) \quad (17.2.103)$$

### *The operator splitting approach to multi-dimensional explicit schemes*

An alternative to the multi-dimensional schemes of the previous section consists in splitting the discretized space operators into products of one-dimensional operators. This is also known as the fractional step method, advocated by Yanenko (1971).

A similar, but not identical, concept has been introduced for the resolution of multi-dimensional implicit schemes in Chapter 11 in Volume 1, known as ADI factorization. In the present context, the operator splitting has to be handled with more care than the ADI factorization, since the splitting acts directly on the order of accuracy of the scheme.

As a result it is expected that the split formulation will lead to improved stability properties or to reduced computational work. For instance, the two-dimensional Lax–Wendroff scheme could be replaced by a product of one-dimensional schemes as follows. Defining the Lax–Wendroff discretization operator for a one-dimensional equation, following equation (17.2.10),

$$\begin{aligned} U_{ij}^{n+1} &= L_x^{(LW)} U_{ij}^n = U_{ij}^n - \tau_x \bar{\delta}_x f_{ij} + \frac{\tau_x^2}{2} \delta_x^+ (A_{i-1/2,j} \delta_x^- f_{ij}^n) \\ &= \left[ 1 - \tau_x A_{ij} \bar{\delta}_x + \frac{\tau_x^2}{2} \delta_x^+ (A_{ij}^2 \delta_x^-) \right] U_{ij}^n \end{aligned} \quad (17.2.104)$$

one can define a two-dimensional Lax–Wendroff scheme as

$$U_{ij}^{n+1} = L_x^{(LW)} L_y^{(LW)} U_{ij}^n \quad (17.2.105)$$

The Von Neumann stability analysis for linear equations is readily obtained as the product of the one-dimensional amplification matrices (17.2.12):

$$G = G_x G_y \quad (17.2.106)$$

where  $G_x$  and  $G_y$  are the expressions (17.2.12) for the  $x$  and  $y$  variables respectively. Hence, the stability conditions will be

$$|\sigma_x| \leq 1 \quad \text{and} \quad |\sigma_y| \leq 1 \quad (17.2.107)$$

These conditions are more favourable than those represented in Figure 17.2.7.

Working out the product  $L_x^{(LW)} L_y^{(LW)}$ , it is seen that third- and fourth-order terms in  $\tau^3$  and  $\tau^4$  appear in the development that are not present in the original two-dimensional form (17.2.48) (see Problem 17.15). If the matrices  $A, B$  do not commute, all the terms of (17.2.48) cannot be obtained by the product  $L_x L_y$ , and the second-order accuracy might be lost. Therefore, the symmetric splitting

$$U_{ij}^{n+1} = \frac{1}{2} (L_x L_y + L_y L_x) U_{ij}^n \quad (17.2.108)$$

will reproduce all the  $\tau_x \tau_y$  terms, plus additional terms, but the resulting scheme will remain second order in  $\Delta t$  and  $\Delta x$ .

### *Split MacCormack scheme*

The two-dimensional MacCormack scheme can be formulated in split form by products of one-dimensional operators. The operator  $L_x^{(M)}(\Delta t/2)$  is defined by the scheme (17.2.29) as

$$U_{ij}^{n+1/2} \equiv L_x^{(M)}\left(\frac{\Delta t}{2}\right) U_{ij}^n \quad (17.2.109)$$

where  $L_x^{(M)}$  results from the predictor corrector sequence

$$\bar{U}_{ij} = U_{ij}^n - \tau_x(f_{i+1,j}^n - f_{ij}^n) \quad (17.2.110)$$

$$U_{ij}^{n+1/2} = \frac{1}{2}(U_{ij}^n + \bar{U}_{ij}) - \frac{\tau_x}{2}(\bar{f}_{ij} - \bar{f}_{i-1,j}) \quad (17.2.111)$$

The operator  $L_y^{(M)}(\Delta t)$  is defined in a similar way by interchanging the roles of  $i$  and  $j$  as well as  $f$  and  $g$ . Hence, the scheme

$$U_{ij}^{n+1} = L_x^{(M)}\left(\frac{\Delta t}{2}\right) L_y^{(M)}\left(\frac{\Delta t}{2}\right) U_{ij}^n \quad (17.2.112)$$

is an alternative to MacCormack's scheme (17.2.91). The linear stability analysis is identical to the one just described, since each factor  $L_x^{(M)}, L_y^{(M)}$  has the amplification matrix of the corresponding one-dimensional Lax–Wendroff scheme. Hence, one also obtains the conditions (17.2.107).

Here, again, it is seen by developing the operator product  $L_x^{(M)} \cdot L_y^{(M)}$  that an order of accuracy is lost when the Jacobian matrices  $A, B$  do not commute.

In order to maintain the second order of accuracy, it is necessary to define symmetric sequences of split operators (see Strang, 1976). The following alternatives are valid:

- (1) Alternate the sequences  $L_x^{(M)} L_y^{(M)}$  and  $L_y^{(M)} L_x^{(M)}$ ; a  $2\Delta t$  cycle is defined whereby

$$\begin{aligned} U_{ij}^{n+1} &= L_x^{(M)}\left(\frac{\Delta t}{2}\right) L_y^{(M)}\left(\frac{\Delta t}{2}\right) U_{ij}^n \\ U_{ij}^{n+2} &= L_y^{(M)}\left(\frac{\Delta t}{2}\right) L_x^{(M)}\left(\frac{\Delta t}{2}\right) U_{ij}^{n+1} \\ &= L_y^{(M)}\left(\frac{\Delta t}{2}\right) L_x^{(M)}\left(\frac{\Delta t}{2}\right) L_x^{(M)}\left(\frac{\Delta t}{2}\right) L_y^{(M)}\left(\frac{\Delta t}{2}\right) U_{ij}^n \end{aligned} \quad (17.2.113)$$

- (2) Distribute the time interval in fractions through the scheme

$$U_{ij}^{n+2} = L_y^{(M)}\left(\frac{\Delta t}{2}\right) L_x^{(M)}(\Delta t) L_y^{(M)}\left(\frac{\Delta t}{2}\right) U_{ij}^n \quad (17.2.114)$$

or

$$U_{ij}^{n+2} = L_x^{(M)} \left( \frac{\Delta t}{2} \right) L_y^{(M)}(\Delta t) L_x^{(M)} \left( \frac{\Delta t}{2} \right) U_{ij}^n \quad (17.2.115)$$

advancing the solution by two time steps  $2\Delta t$ .

(3) A still more general splitting sequence is

$$U_{ij}^{n+2} = \left[ L_y^{(M)} \left( \frac{\Delta t}{2N} \right) \right]^N L_x^{(M)} \left[ L_y^{(M)} \left( \frac{\Delta t}{2N} \right) \right]^N U_{ij}^n \quad (17.2.116)$$

In these sequences the one-dimensional operators have different time steps. For unequal mesh sizes  $\Delta x \neq \Delta y$ , larger time steps can be chosen for the direction with the larger mesh size. If  $\Delta y > \Delta x$ , one can allow  $L_y(\Delta t_y)$  with the CFL limitation  $\Delta t_y \leq \Delta y / \rho(B)$  and combine in a symmetric set with  $L_x(\Delta t_x)$  operators, such that the sum of all  $\Delta t$  equals the interval  $\Delta T$  over which the solution is advanced in time.

### *The two-dimensional version of the $S_\alpha^\beta$ schemes*

The extension of the  $S_\alpha^\beta$  schemes to two-dimensional problems has been investigated by Lerat (1981) in a systematic analysis of predictor–corrector schemes, which reduce in the linear case to the two-dimensional Lax–Wendroff schemes (see also Lerat and Sides, 1982).

A first extension with one predictor in unsplit form did not appear to be satisfactory. Consequently, Lerat considered schemes with two predictors and a single corrector, in an approach which resembles the operator splitting concept. However, the predictors are not pure one-dimensional operators.

Requiring the schemes to be restricted to nine points around  $(i, j)$  to be second-order accurate in space and time leads to a family with four parameters  $\alpha_1, \alpha_2, \beta_1, \beta_2$ , which can be extracted from the original 67 parameters and defined as follows:

$$\begin{aligned} \bar{U}_{ij} &= U_{ij}^n + \beta_1(U_{i+1,j}^n - U_{ij}^n) - \alpha_1 \tau_x(f_{i+1,j}^n - f_{ij}^n) \\ &\quad - \alpha_1 \frac{\tau_y}{4}(g_{i+1,j+1}^n + g_{i,j+1}^n - g_{i+1,j-1}^n - g_{i,j-1}^n) \end{aligned} \quad (17.2.117)$$

$$\begin{aligned} \bar{\bar{U}}_{ij} &= U_{ij}^n + \beta_2(U_{i,j+1}^n - U_{ij}^n) - \alpha_2 \tau_y(g_{i,j+1}^n - g_{ij}^n) \\ &\quad - \alpha_2 \frac{\tau_x}{4}(f_{i+1,j+1}^n + f_{i+1,j}^n - f_{i-1,j+1}^n - f_{i-1,j}^n) \end{aligned} \quad (17.2.118)$$

$$U_{ij}^{n+1} = U_{ij}^n - \tau_x(f_{i+1/2,j}^* - f_{i-1/2,j}^*) - \tau_y(g_{i,j+1/2}^* - g_{i,j-1/2}^*) \quad (17.2.119)$$

$$\begin{aligned} f_{i+1/2,j}^* &= \frac{1}{2\alpha_1} [(\alpha_1 - \beta_1)f_{i+1,j}^n + (\alpha_1 + \beta_1 - 1)f_{ij}^n + \bar{f}_{ij}] \\ g_{i,j+1/2}^* &= \frac{1}{2\alpha_2} [(\alpha_2 - \beta_2)g_{i,j+1}^n + (\alpha_2 + \beta_2 - 1)g_{ij}^n + \bar{g}_{ij}] \end{aligned} \quad (17.2.120)$$

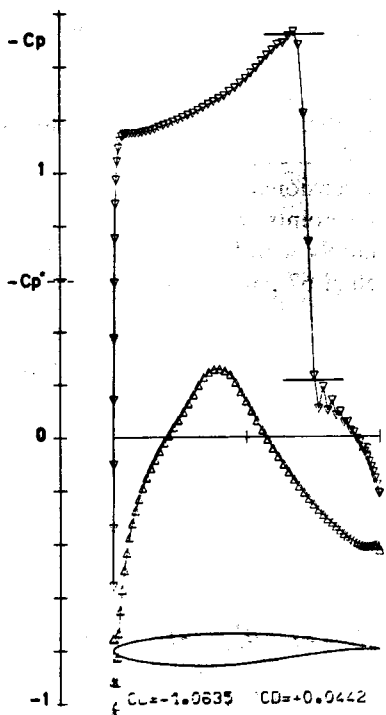
The numerical flux  $f_{i+1/2,j}^*$  is defined as in equation (17.2.41) with  $\alpha = \alpha_1$  and  $\beta = \beta_1$  while  $g_{i,j+1/2}^*$  is obtained from a similar expression with  $j$  taking the role of  $i$ , with  $\alpha = \alpha_2$ ,  $\beta = \beta_2$  and  $f$  replaced by  $g$ . In addition,  $\bar{f}_{ij}$  is defined by  $f(\bar{U}_{ij})$  in  $f_{i+1/2,j}^*$  and by  $\bar{g}_{ij} = g(\bar{U}_{ij})$  in  $g_{i,j+1/2}^*$ .

It can be observed that the predictor steps are close to the one-dimensional predictors (17.2.38), except for the last terms, which represent a two-dimensional contribution. Hence these schemes are a straightforward extension of the one-dimensional  $S_\alpha^\beta$  schemes.

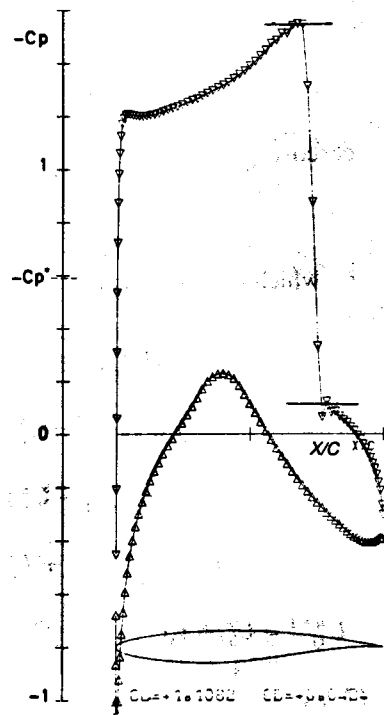
This family of predictor–corrector schemes contains several known schemes as a particular case. For  $\alpha_1 = \alpha_2 = \beta_1 = \beta_2 = \frac{1}{2}$  one obtains a scheme proposed earlier by Thommen (1966) for the Navier–Stokes equations and applied by Singleton (1968) and Magnus and Yoshihara (1975) to the Euler equations.

The choice  $\alpha_1 = \alpha_2 = 1$ ,  $\beta_1 = \beta_2 = \frac{1}{2}$  corresponds to a scheme proposed by Palumbo and Rubin (1972).

It is to be noticed, however, that the two-dimensional MacCormack schemes are not included in the above four-parameter family, in contrast to the one-dimensional case where the choice  $\alpha = 1$ ,  $\beta = 0$  or  $\alpha = 1$ ,  $\beta = 1$  reduce to



(a) MacCormack scheme



(b) Optimal  $S(\alpha, \beta)$  scheme

Figure 17.2.15 Pressure distribution on an RAE 2822 airfoil at  $M_\infty = 0.75$  and  $3^\circ$  incidence.  
(From Lerat and Sides, 1982)

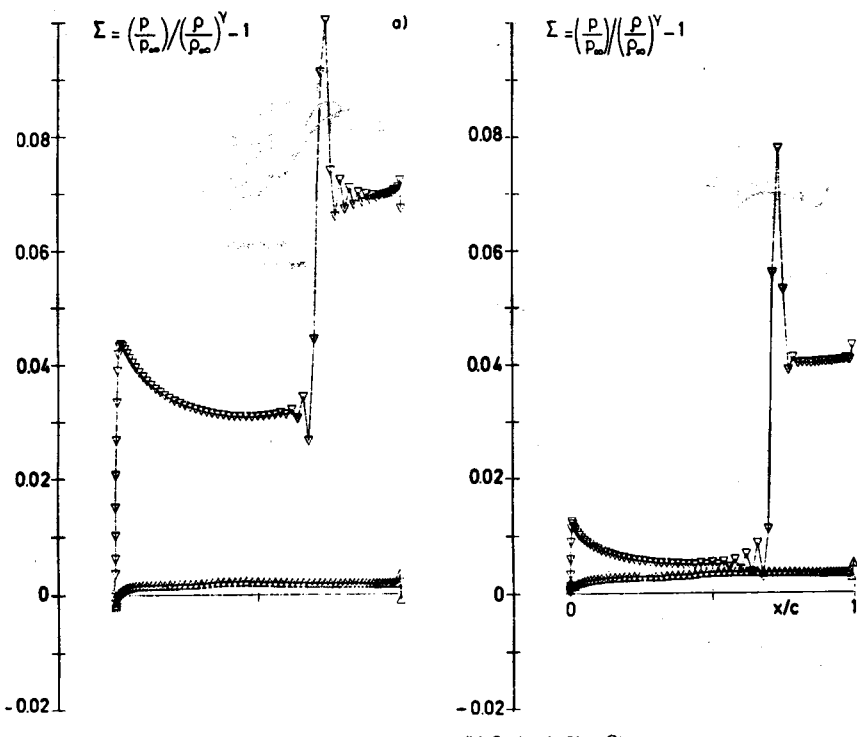
the MacCormack schemes. Observe also that for  $\beta_1 = \beta_2 = \frac{1}{2}$ , the schemes are symmetric around  $i + \frac{1}{2}$  and  $j + \frac{1}{2}$ .

All the schemes reduce to the Lax-Wendroff form (17.2.48) for constant matrices  $A$  and  $B$ , independently of the  $\alpha_1, \alpha_2, \beta_1, \beta_2$  coefficients. They represent therefore a family of non-linear multi-step variants of the Lax-Wendroff scheme.

In calculating the equivalent differential equations, the coefficients of  $\Delta x^2$  and  $\Delta y^2$  are identical to the corresponding one-dimensional terms (17.2.45) and hence an optimal scheme selection can be made, which would, as in the one-dimensional  $S_\alpha^\beta$  schemes, have an optimal dissipation for the compression waves due to the non-linear contributions in the truncation error, while keeping to a minimum the antidissipation of the expansion waves. This can then be obtained for the same set of values; that is

$$\alpha_1 = \alpha_2 = 1 + \sqrt{\frac{5}{2}} \quad \beta_1 = \beta_2 = \frac{1}{2}$$

Figure 17.2.15 shows a comparison between MacCormack's scheme and the above optimal scheme for a transonic airfoil computation, from Lerat and Sides (1982). Both calculations have been performed on the same mesh of  $224 \times 29$



(a) MacCormack scheme

(b) Optimal  $S(\alpha, \beta)$  scheme

Figure 17.2.16 Entropy distribution on an RAE 2822 airfoil at  $M_\infty = 0.75$  and  $3^\circ$  incidence.  
(From Lerat and Sides, 1982)

cells, with the same boundary conditions and additional artificial viscosity (see Section 17.3 for more details on this last aspect).

The calculations performed on an RAE 2822 airfoil at  $M_\infty = 0.75$  and  $3^\circ$  incidence show the postshock oscillations with MacCormack's method on the pressure distributions (Figure 17.2.15(a)), compared to the results of the optimal scheme (Figure 17.2.15(b)). The horizontal bars indicate the Rankine–Hugoniot jump, which appears somewhat inaccurate with the MacCormack computation. The plot of the surface entropy distribution on Figure 17.2.16 gives a better view of the difference in behaviour of the two schemes.

It can be seen that the strong expansion at the leading edge produces a large entropy rise with the MacCormack scheme—about four times as large as with the optimal scheme.

The plotted quantity  $\Sigma = (\rho/\rho^\gamma)(p_0/\rho_0^\gamma) - 1$  is a measure of the entropy errors, since the entropy should remain zero in this isentropic flow, except at the shock,

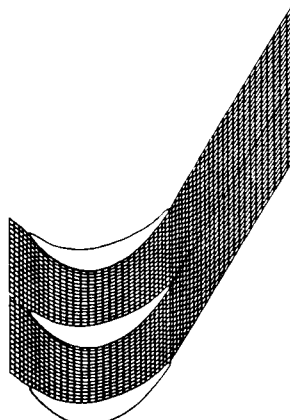
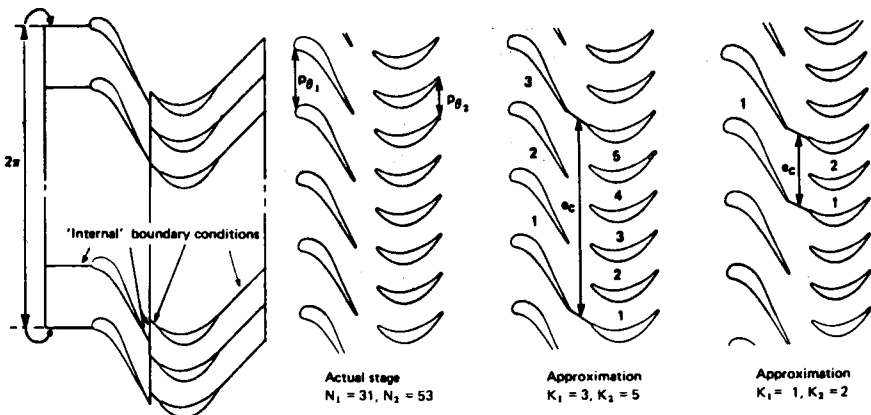
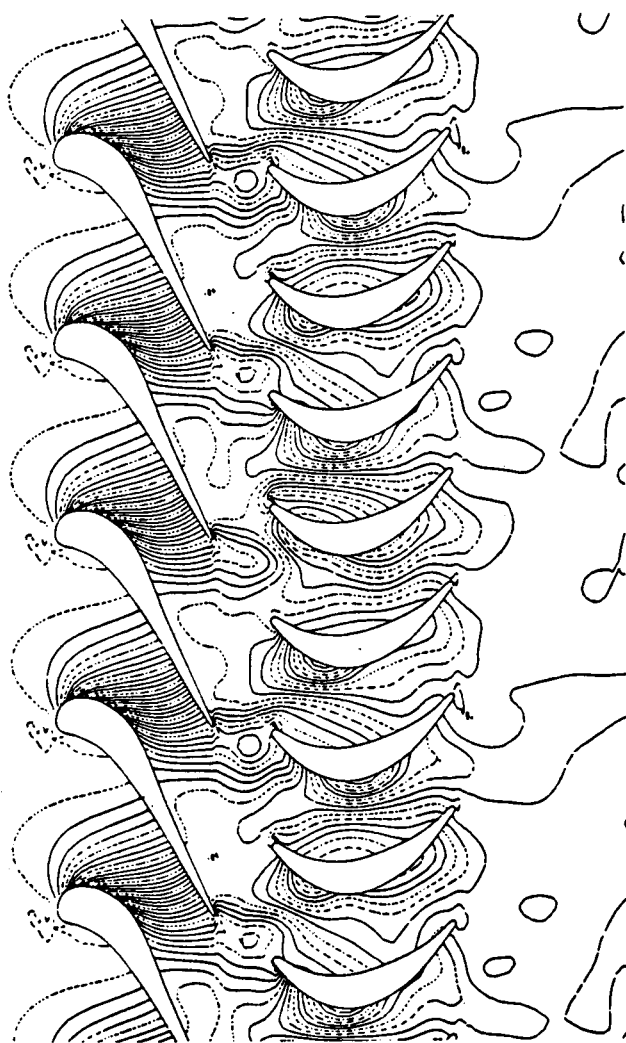


Figure 17.2.17 Geometry and mesh for the stator–rotor interaction in the two-dimensional section of a turbine stage. (From Fourmaux and Le Meur, 1987)

where the Rankine-Hugoniot conservation laws impose an entropy discontinuity. Hence any deviation from this behaviour indicates a generation of numerical (unwanted) viscosity.

Observe also that the entropy has a maximum inside the numerical shock structure. A similar property is actually obtained when physical shock structures are analysed on the basis of the Navier-Stokes equations; see, for example, Zeldovich and Rainer (1967).



**Figure 17.2.18** Instantaneous pressure field for the stator-rotor interaction in the two-dimensional section of a turbine stage. (From Fourmaux and Le Meur, 1987)

*Example 17.2.2 Unsteady flow in a two-dimensional section of a turbine stage*

The interaction between the rotor and stator in turbomachines creates an unsteady flow component which can have a non-negligible effect on performance. Calculations of this interaction on a domain composed of three stator and five rotor blades have been performed at ONERA with MacCormack's scheme (Fourmaux and Le Meur, 1987). Figure 17.2.17 displays the mesh between two consecutive blades and several of the full-stage arrangements considered. The total mesh contains 40 000 points and characteristic relations are applied as boundary conditions. A typical instantaneous pressure field is shown in Figure 17.2.18 for steady inflow conditions in front of the stator demonstrating the unsteady flow pattern.

### 17.3 THE CONCEPT OF ARTIFICIAL DISSIPATION OR ARTIFICIAL VISCOSITY

All the second-order, three-point central schemes of the Lax–Wendroff family generate oscillations around sharp discontinuities, as shown in Figures 17.2.2 to 17.2.4. Similar effects were also observed with the linear convection equation in Chapters 8 and 9 in Volume 1.

First-order schemes, on the other hand, have truncation errors proportional to a second derivative which acts as an added numerical viscosity (see equation (17.1.7)). Therefore, these schemes will damp the high-frequency components and smooth out strong gradients.

An alternative explanation for the oscillatory behaviour of the shock transition with Lax–Wendroff schemes is given by Lax and Wendroff (1960) in their original paper. This remarkable paper contains many basic ideas and considerations which are still highly up to date and we strongly recommend a careful reading of this work.

A stationary solution, in particular a stationary discontinuity, will satisfy the asymptotic part of the scheme (17.2.6), that is the steady state  $\bar{u}_i$  will satisfy in the linearized case

$$-\frac{\sigma}{2}(\bar{u}_{i+1} - \bar{u}_{i-1}) + \frac{1}{2}\sigma^2(\bar{u}_{i+1} - 2\bar{u}_i + \bar{u}_{i-1}) = 0 \quad (17.3.1)$$

When this solution is approached, for  $u_i^{n+1} = u_i^n$ , the spatial error  $\varepsilon_i = u_i^n - \bar{u}_i$  satisfies the same equation

$$-\frac{\sigma}{2}(\varepsilon_{i+1} - \varepsilon_{i-1}) + \frac{1}{2}\sigma^2(\varepsilon_{i+1} - 2\varepsilon_i + \varepsilon_{i-1}) = 0 \quad (17.3.2)$$

Following the normal mode analysis of Section 10.5 in Volume 1, an exact solution of the form  $\varepsilon_i = \kappa^i$  can be found, leading to

$$\kappa = \frac{1 + \sigma}{\sigma - 1} \quad (17.3.3)$$

Since the stability limit is  $|\sigma| < 1$ ,  $\kappa$  will always be negative. Hence at consecutive points  $i$ ,  $i+1$ , the error  $\varepsilon_i = \kappa^i$  will change sign, leading to an oscillatory behaviour of the numerical solution. This behaviour represents an ‘odd–even’ point error of wavelength  $2\Delta x$ , that is of high frequency. Since  $G(\pi) = 1 - 2\sigma^2$ , these oscillations will not be damped when  $\sigma \approx 0$ , that is when a sonic point is encountered.

For the Lax–Friedrichs first-order scheme,  $\kappa$  is always positive, since  $\kappa = (1 + \sigma)/(1 - \sigma)$  in this case.

In order to remove the unavoidable high-frequency oscillations around discontinuities in second-order central schemes, Von Neumann and Richtmyer (1950) introduced the concept of *artificial viscosity* or *artificial dissipation*. These additional terms should simulate the effects of the physical viscosity, *on the scale of the mesh*, locally around the discontinuities and be negligible, that is of an order equal or higher than the truncation error, in smooth regions. Additional dissipation is also required to avoid the appearance of expansion shocks, as seen in Figures 17.2.3 and 17.2.4, by providing enough dissipation when the intrinsic dissipation of the scheme vanishes at sonic transitions.

### 17.3.1 General form of artificial dissipation terms

Lax and Wendroff (1960) made a general analysis on the conditions to be fulfilled by an additional dissipative term added to a difference scheme of second-order accuracy.

The numerical fluxes  $f_{i+1/2}^*$  given by equations (17.2.8), (17.2.32) or (17.2.41) for the different versions of the non-linear Lax–Wendroff schemes do all have the same structure and are members of a general family, which can be written according to Lax and Wendroff (1960) as

$$f_{i+1/2}^* = \frac{f_{i+1} + f_i}{2} - \frac{1}{2}\tau A_{i+1/2}(f_{i+1} - f_i) - D(U_i, U_{i+1}) \cdot (U_{i+1} - U_i) \quad (17.3.4)$$

where  $D$  is any positive function of  $(U_{i+1} - U_i)$  which goes to zero at least linearly with  $(U_{i+1} - U_i)$ .

All the numerical fluxes of the form (17.3.4) satisfy the requirement derived in Section 9.4 for second-order accuracy (equation (9.4.22)), written here as

$$\left( \frac{\partial f^*}{\partial U_{i+1}} - \frac{\partial f^*}{\partial U_i} \right)_{U_i} = -\tau A_i^2 \quad (17.3.5)$$

The freedom in the choice of the function  $D$  can be used to generate additional dissipation in the scheme in order to control the high-frequency oscillations generated around discontinuities.

The function  $D$  must have the dimensions of  $A$ , that is the dimension of a velocity, and therefore  $D\Delta x$  has the dimensions of a viscosity if  $u$  represents a velocity component; Lax and Wendroff call  $D$  the *artificial viscosity*. Introducing (17.3.4) into the general form of the conservative scheme (17.2.7) leads to the

Lax–Wendroff scheme (17.2.5) with an additional contribution from  $D$ :

$$U_i^{n+1} - U_i^n = -\tau(f_{i+1/2}^* - f_{i-1/2}^*)_{\text{LW}} + \tau[D_{i+1/2}(U_{i+1} - U_i) - D_{i-1/2}(U_i - U_{i-1})] \quad (17.3.6)$$

where the artificial viscosity term can be considered as a discretization of  $\Delta x(\partial/\partial x)(D(\partial U/\partial x))$ . Hence, the addition of an artificial viscosity (AV) term can be considered as a modification of the numerical flux  $f^*$  which is replaced by

$$f^{(\text{AV})*} = f^* - \Delta x D \frac{\partial U}{\partial x} \quad (17.3.7a)$$

and in discretized form

$$f_{i+1/2}^{(\text{AV})*} = f_{i+1/2}^{(\text{LW})*} - D_{i+1/2}(U_{i+1} - U_i) \quad (17.3.7b)$$

where  $D$  is at least proportional to  $\Delta x$  in order to maintain the second-order accuracy. Note the similarity of equation (17.3.7a) with the viscous flux terms of the Navier–Stokes equations, where  $D \Delta x$  plays the role of the viscosity.

The additional terms will have a non-negligible influence at points where the solution undergoes strong variations, but will be negligible in smooth regions where they are at least of the order of the truncation error.

In order for  $D_{i+1/2}$  to have a stabilizing influence, it has to be positive.

However, one can also define  $D$  as a polynomial function of  $(U_{i+1} - U_i)$ , which is often done in practical implementations of artificial viscosity terms.

### 17.3.2 Von Neumann–Richtmyer artificial viscosity

The original method applied by Von Neumann and Richtmyer (1950) can be written for a one-dimensional flow in the above form, when the conservative variable  $U$  is replaced by the velocity  $u$  for the momentum and energy equations and is not considered with the continuity equation. The origin of the method is based on the consideration of an additional pressure term, which is added only to the momentum and energy equations, under the following form, for a one-dimensional case:

$$D \frac{\partial u}{\partial x} = \alpha \Delta x \rho \begin{vmatrix} 0 \\ 1 \\ u \end{vmatrix} \begin{vmatrix} \frac{\partial u}{\partial x} \\ \frac{\partial u}{\partial x} \end{vmatrix} \quad (17.3.8)$$

The discretized form of the associated dissipation terms is

$$D_{i+1/2}(u_{i+1} - u_i) = \alpha \rho_{i+1/2} \begin{vmatrix} 0 \\ 1 \\ u \end{vmatrix}_{i+1/2} |u_{i+1} - u_i|(u_{i+1} - u_i) \quad (17.3.9a)$$

or as alternative

$$D_{i+1/2}(u_{i+1} - u_i) = \alpha \rho_i \begin{vmatrix} 0 \\ 1 \\ u \end{vmatrix}_i |u_{i+1} - u_i|(u_{i+1} - u_i) \quad (17.3.9b)$$

The coefficient  $\alpha$  is of the order of unity and has to be adjusted empirically.

In multi-dimensional problems, similar terms are added to each flux component separately.

The Von Neumann and Richtmyer artificial viscosity can be generalized to the following form:

$$f^{(\text{AV})*} = f^* - \varepsilon \cdot \Delta x^2 \psi \left| \frac{\partial U}{\partial x} \right| \frac{\partial U}{\partial x} \quad (17.3.10)$$

where  $\psi$  are positive coefficients, which could depend on the mesh point  $i$ , such that  $\psi \cdot U$  has the dimension of a velocity. Equation (17.3.10) is not to be interpreted as matrix products, but is to be read componentwise.

The artificial dissipation of Von Neumann and Richtmyer is non-linear and proportional to  $\Delta x^2$ . Lower-order expressions have been attempted, for instance of the form

$$D = \alpha \Delta x (|u| + c) \quad (17.3.11)$$

but this gives generally too much dissipation in smooth flow regions and is not sufficiently selective in regions of sharp discontinuities.

### *Example 17.3.1 MacCormack scheme with artificial dissipation*

In MacCormack's scheme the dissipation terms are generally added both at the predictor and corrector levels. In this case the scheme can be written as follows:

$$\overline{\Delta U}_i = -\tau(f_{i+1} - f_i)^n + \Delta t Q_i^n + \tau D_{i+1/2}^n (U_{i+1} - U_i)^n - \tau D_{i-1/2}^n (U_i - U_{i-1})^n \quad (\text{E17.3.1})$$

$$\overline{\Delta \bar{U}}_i = -\tau(\bar{f}_i - \bar{f}_{i-1}) + \Delta t \bar{Q}_i + \tau \bar{D}_{i+1/2} (\bar{U}_{i+1} - \bar{U}_i) - \tau \bar{D}_{i-1/2} (\bar{U}_i - \bar{U}_{i-1}) \quad (\text{E17.3.2})$$

The modified numerical flux of the explicit MacCormack scheme with the addition of artificial viscosity becomes

$$f_{i+1/2}^{(\text{AV})*} = \frac{1}{2}(f_{i+1} + \bar{f}_i) - \frac{1}{2}[D_{i+1/2} (U_{i+1} - U_i) + \bar{D}_{i+1/2} (\bar{U}_{i+1} - \bar{U}_i)] \quad (\text{E17.3.3})$$

Figure 17.3.1 shows the result of the application of MacCormack's scheme to the stationary nozzle flow of Figure 17.2.2 under the same conditions but with the addition of the Von Neumann–Richtmyer artificial viscosity. As can be seen, the oscillations at the shock have been damped and the mass flux error is reduced in amplitude from a maximum of 10 per cent to 0.4 per cent, but remains still spread over a large part of the flow region.

Figures 17.3.2 and 17.3.3 show the effects of the same dissipation terms on the shock tube flows of Figures 17.2.3 and 17.2.4. The artificial dissipation has prevented the appearance of the expansion shocks at the sonic transition. Observe also the smearing of the contact discontinuity and the good resolution of the shock. However, the results are not totally satisfactory, since some oscillations can still be observed.

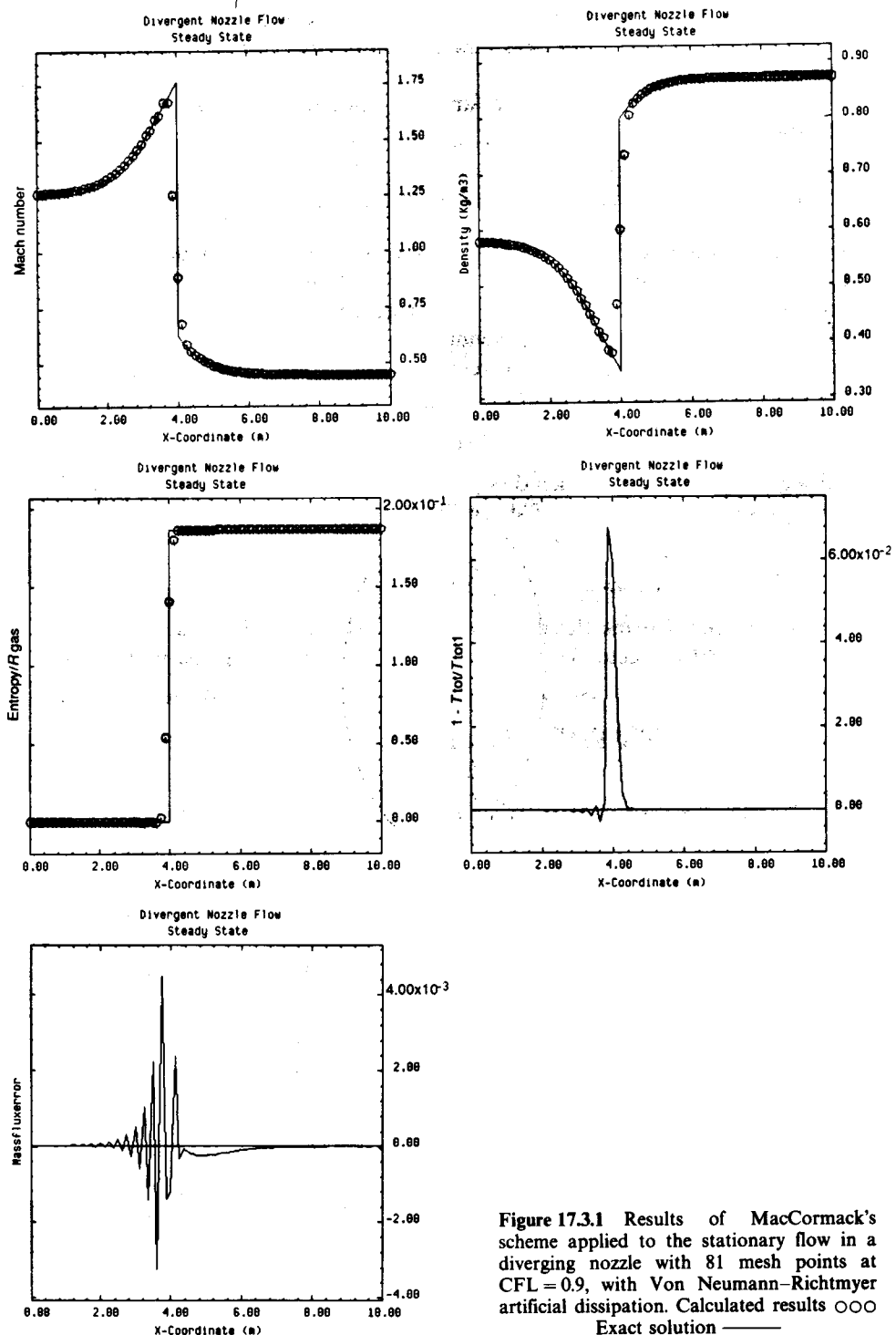
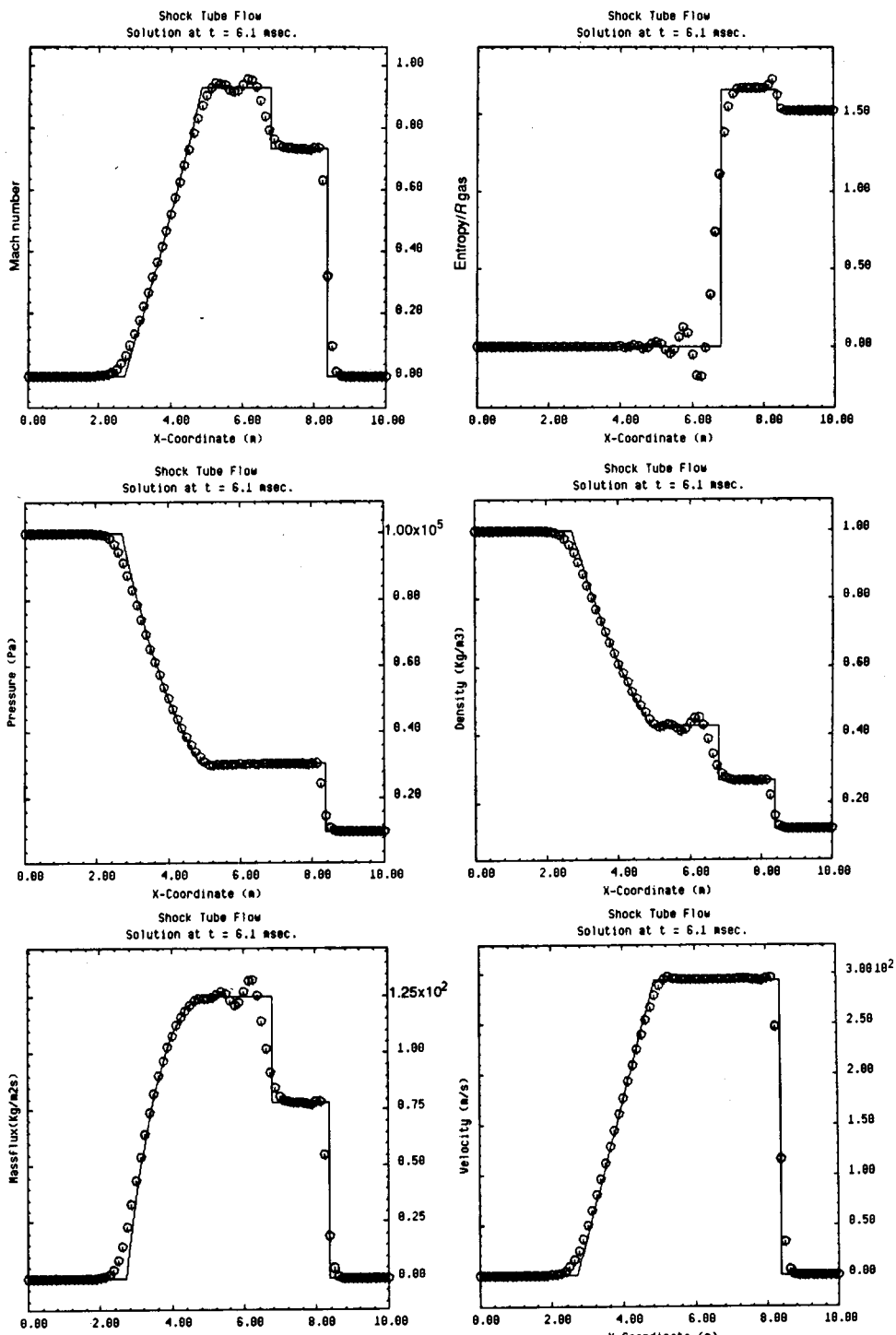


Figure 17.3.1 Results of MacCormack's scheme applied to the stationary flow in a diverging nozzle with 81 mesh points at  $CFL = 0.9$ , with Von Neumann-Richtmyer artificial dissipation. Calculated results  $\circ\circ\circ$   
Exact solution —



**Figure 17.3.2** Results of MacCormack's scheme applied to the shock tube problem of Figure 16.6.8, with 81 mesh points at  $\text{CFL} = 0.95$ , after 35 time steps, with Von Neumann–Richtmyer artificial dissipation. Calculated results  $\circ\circ\circ$  Exact solution —

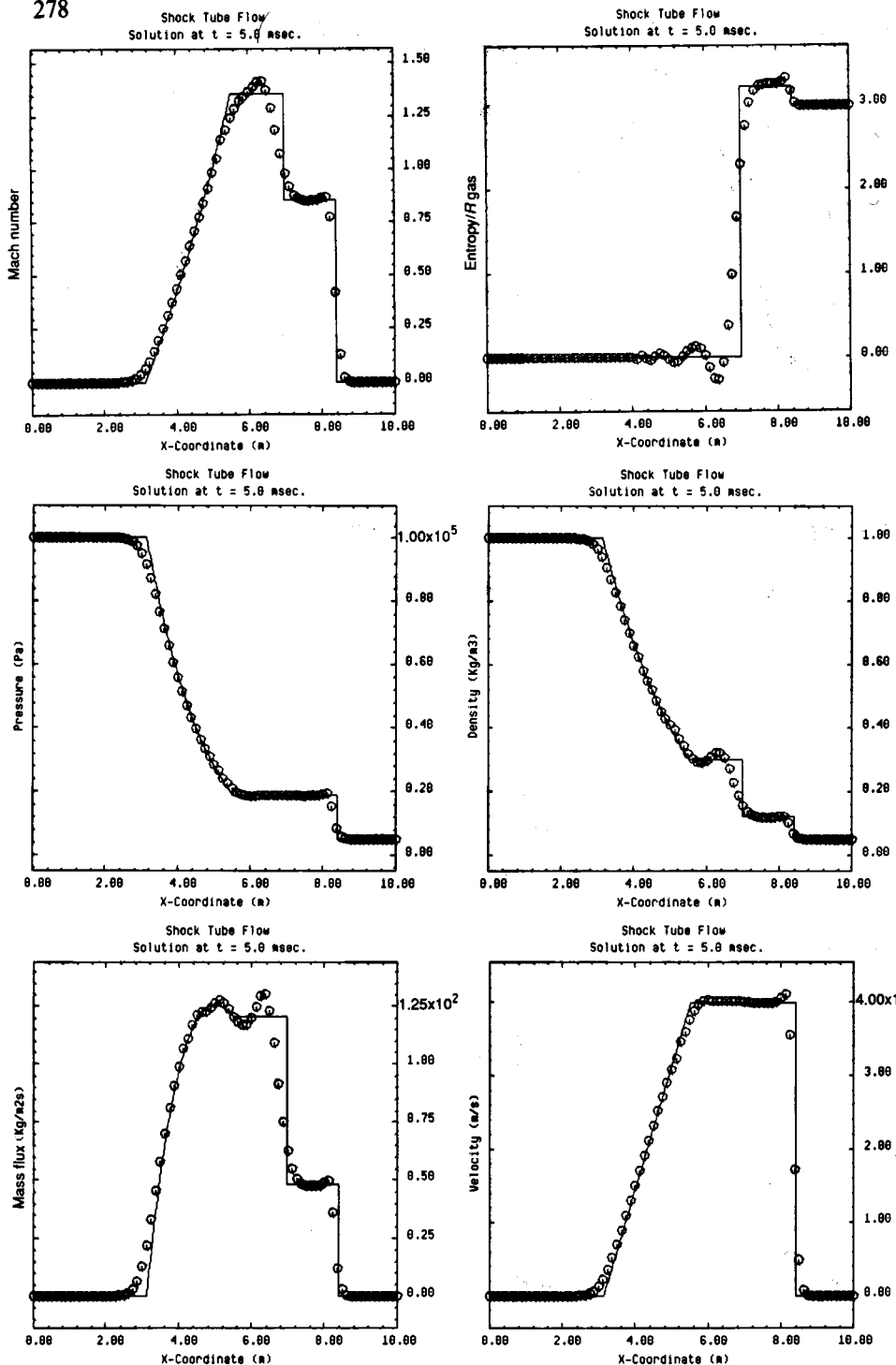


Figure 17.3.3 Results of MacCormack's scheme applied to the shock tube problem of Figure 16.6.9, with 81 mesh points at  $\text{CFL} = 0.95$ , after 35 time steps, with Von Neumann–Richtmyer artificial dissipation. Calculated results  $\circ\circ\circ$  Exact solution —

### 17.3.3 Higher-order artificial viscosities

A third-order artificial viscosity has been applied by MacCormack and Baldwin (1975), whereby  $D$  is made proportional to a second derivative of the pressure field in order to enhance the effect of the dissipation in the presence of strong pressure gradients and to reduce it in the smooth flow regions.

The  $D$  factor is defined as follows:

$$D = \varepsilon \Delta x^2 \frac{|u| + c}{p} \left| \frac{\partial^2 p}{\partial x^2} \right| \quad (17.3.12)$$

and the modified numerical flux becomes

$$f^{(\text{AV})*} = f^* - \varepsilon \Delta x^3 \frac{|u| + c}{p} \left| \frac{\partial^2 p}{\partial x^2} \right| \cdot \frac{\partial U}{\partial x} \quad (17.3.13)$$

It is generally computed as follows:

$$f_{i+1/2}^{(\text{AV})*} = f_{i+1/2}^{(\text{LW})*} - \varepsilon(|u| + c)_{i+1/2} \frac{|p_{i+1} - 2p_i + p_{i-1}|}{p_{i+1} + 2p_i + p_{i-1}} (U_{i+1} - U_i) \quad (17.3.14)$$

Another form of artificial viscosity is based on the addition of higher-order derivatives. It cannot be written as (17.3.7) but takes the form, with  $a = |u| + c$  as the scaling velocity,

$$f^{(\text{AV})*} = f^* + \varepsilon \Delta x^3 (|u| + c) \frac{\partial^3 U}{\partial x^3} \quad (17.3.15)$$

and represents a dissipation proportional to a fourth difference, linear in  $U$ .

This last expression has been introduced by Steger (1978) in the Beam and Warming schemes to be discussed in the following chapter.

#### *Jameson's artificial dissipation*

Jameson and others (Jameson *et al.*, 1981; Jameson, 1982) apply a blend of the expressions (17.3.14) and (17.3.15) with excellent shock-capturing properties. In this approach the third derivative term is switched off when the quantity (17.3.12) dominates. The same formulation has also been applied by Pulliam (1984) and Pulliam and Steger (1985) into the Beam and Warming codes with excellent results.

The corrected numerical flux is defined by

$$f_{i+1/2}^{(\text{AV})*} = f_{i+1/2}^* - d_{i+1/2} \quad (17.3.16)$$

where  $d$  combines the MacCormack–Baldwin artificial dissipation with the linear fourth-order dissipation (17.3.15) in the following way:

$$d_{i+1/2} = \varepsilon_{i+1/2}^{(2)} (U_{i+1} - U_i) - \varepsilon_{i+1/2}^{(4)} (U_{i+2} - 3U_{i+1} + 3U_i - U_{i-1}) \quad (17.3.17)$$

where  $\varepsilon^{(2)}$  is defined according to equation (17.3.14) and  $\varepsilon^{(4)}$  according to equation (17.3.15).

The non-linear coefficient  $\varepsilon^{(2)}$  is evaluated by

$$\varepsilon_{i+1/2}^{(2)} = \frac{1}{2}(\varepsilon_i^{(2)} + \varepsilon_{i+1}^{(2)}) \quad (17.3.18)$$

or

$$\varepsilon_{i+1/2}^{(2)} = \max(\varepsilon_i^{(2)}, \varepsilon_{i+1}^{(2)}) \quad (17.3.19)$$

where

$$\varepsilon_i^{(2)} = \alpha^{(2)}(|u| + c)_i \frac{|p_{i+1} - 2p_i + p_{i-1}|}{p_{i+1} + 2p_i + p_{i-1}} \quad (17.3.20)$$

The pressure term in  $\varepsilon^{(2)}$  is generally of second order, except in regions of strong pressure gradients, where it reduces to first order or becomes of the order of one. Hence, around shocks, the  $\varepsilon^{(2)}$  term is dominating.

This did not appear to be sufficient to avoid completely some small oscillations, of the order of 1 per cent in density variation, preventing the complete convergence to the steady state. They are noticeable mostly near regions with sharp gradients, such as airfoil trailing edges.

These oscillations were removed by the introduction of the third derivative term (17.3.15), providing some background dissipation through the domain, but led to the reappearance of overshoots around the shockwaves. Hence, the background dissipation is turned off when  $\varepsilon^{(2)}$  is large and one defines

$$\varepsilon_{i+1/2}^{(4)} = \max[0, (\alpha^{(4)} - \varepsilon_{i+1/2}^{(2)} / (u + c)_{i+1/2})] \quad (17.3.21)$$

where  $\alpha^{(4)}$  is an adjustable constant.

Typical values of  $\alpha^{(2)}$  and  $\alpha^{(4)}$  are

$$\alpha^{(2)} \approx \frac{1}{4} \quad \alpha^{(4)} \approx \frac{1}{256} \quad (17.3.22)$$

The dissipation terms are added to the four equations, but in the energy equation the fourth component of  $U$ , namely  $\rho E$ , is replaced by  $\rho H$  in equation (17.3.17). This ensures that the steady state satisfies  $H = H_\infty = \text{constant}$ . Details of implementation and considerations of boundary treatment of these dissipation terms can be found in Pulliam (1985) and Swanson and Turkel (1987).

Many other forms of artificial viscosity can be found in the literature, and although the introduction of artificial viscosity may appear somewhat arbitrary it is by far not as 'artificial' as a first impression might lead us to think.

It will be shown indeed in Chapter 20 that any upwind scheme can be written as a central scheme plus dissipation terms. This fact has already been introduced in Chapter 15 when dealing with the calculation of transonic potential flows.

It shows that the dissipation terms introduce an upwind correction to the central schemes, such as to remove non-physical effects arising from the central discretization of wave propagation phenomena. These effects arise mainly around discontinuities, where a sudden change in the propagation direction of certain waves occurs. Due to its nature, the central discretization is not able to

handle this discontinuous change and generates oscillations. On the other hand, the upwind schemes are on the contrary defined as a function of the signs of the propagation velocities. Some form of equivalence is obtained in this way between upwind schemes, on one hand, and central schemes with artificial viscosity, on the other hand. It will even be shown in Chapter 21 that the introduction of upwind, second-order non-linear algorithms, controlling and preventing the appearance of unwanted oscillations, called TVD (total variation diminishing) schemes, allow the definition of artificial viscosity terms for Lax–Wendroff schemes, rendering them equivalent to upwind TVD schemes. This approach leads to artificial viscosity forms, without adjustable and empirical constants.

In the following we will refer to various forms of artificial viscosity and we encourage the reader to experiment with various forms on simple test cases.

Figure 17.3.4 shows the same test case as Figure 17.3.1 with the MacCormack–Baldwin dissipation (17.3.12) and  $\varepsilon = 0.625$ . Comparing to Figure 17.3.1 one notices the sharper shock, which is resolved over two mesh cells. The mass flux error is also extremely narrow and concentrated over the shock only. This indicates that the filter provided by the pressure derivatives in the dissipation terms is indeed very effective. Note, however, that the maximum mass flux error remains here at the level reached without artificial dissipation.

When applied to the shock tube problems of Figures 17.3.2 and 17.3.3, similar observations can be made with regard to the shock definition, namely that the shock is sharper with the MacCormack–Baldwin dissipation.

### *Remark*

Some ambiguity is found in the literature with regard to the definition of numerical and artificial viscosities.

Lax and Wendroff call the function  $D$  in equation (17.3.4) the *artificial viscosity* defined as the contribution in the numerical flux *above* the Lax–Wendroff term  $\frac{1}{2}\tau A_{i+1/2}(f_{i+1} - f_i)$  or, according to (17.2.22),  $(\tau/2)A_{i+1/2}^2(U_{i+1} - U_i)$ .

More recent trends write the numerical flux as

$$f_{i+1/2}^* = \frac{f_{i+1} + f_i}{2} - \frac{1}{2}\bar{D}_{i+1/2}(U_{i+1} - U_i) \quad (17.3.23)$$

and call the function  $\bar{D}_{i+1/2} = \bar{D}(A_{i+1/2})$  the coefficient of numerical viscosity.

The significance of these denominations should be related to the numerical dissipation as obtained from the truncation errors. A first observation should be kept in mind, namely that the truncation error will have the structure of an effective viscosity or dissipation only if the scheme is first order. In this case, the truncation error has a term proportional to  $U_{xx}$ .

For instance, in the Lax–Friedrichs scheme, equation (17.1.19) shows that  $\bar{D}(A_{i+1/2}) = 1/\tau$ , but from the truncation error one has an expression of the form of equation (17.1.7), where  $\alpha = (\Delta x^2/2\Delta t)(1 - \tau^2 A^2)$  plays the role of an effective numerical dissipation coefficient.

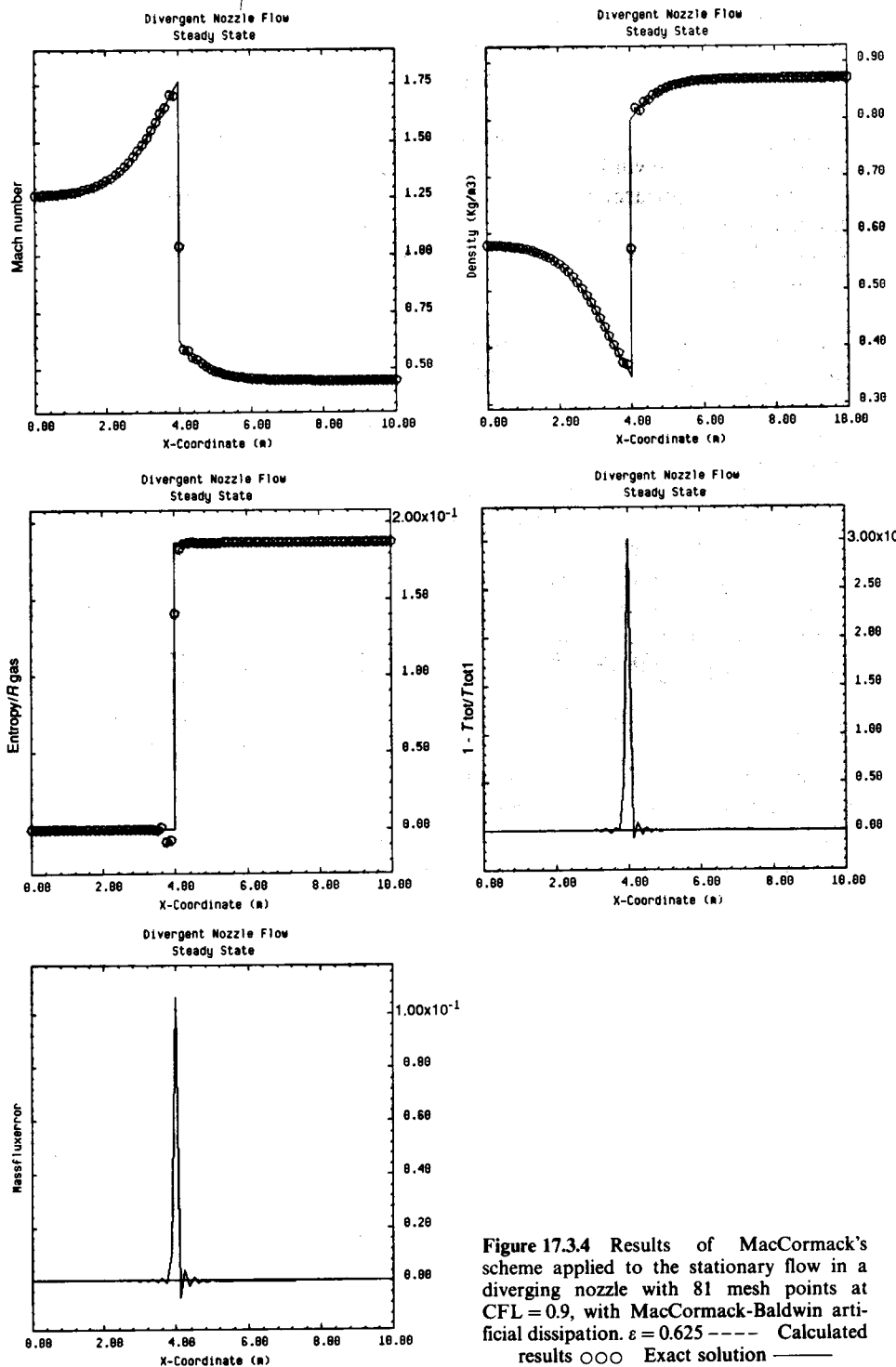


Figure 17.3.4 Results of MacCormack's scheme applied to the stationary flow in a diverging nozzle with 81 mesh points at  $\text{CFL} = 0.9$ , with MacCormack-Baldwin artificial dissipation.  $\varepsilon = 0.625$  — Calculated results  $\circ\circ\circ$  Exact solution —

More generally, the first-order truncation term of a scheme in conservative form with a numerical flux  $f^*$  is given by equation (9.4.21), Chapter 9 in Volume 1. Applied to the above equation (17.3.16), the coefficient of the  $U_{xx}$  term can be written as

$$\frac{\partial f^*}{\partial U_{i+1}} - \frac{\partial f^*}{\partial U_i} + \tau A^2 = -\bar{D} + \tau A^2 \quad (17.3.24)$$

and the effective numerical dissipation coefficient, to be compared to the physical viscosity, is

$$\alpha = \frac{\Delta x}{2} (\bar{D} - \tau A^2) \quad (17.3.25)$$

The Lax–Wendroff scheme corresponds to  $\bar{D} = \tau A^2$  and equation (17.3.4) corresponds to  $\bar{D} = \tau A^2 + 2D$ , where  $D$  goes to zero with  $(U_{i+1} - U_i)$ . Hence  $D$  is proportional to  $\Delta x$  and does not contribute to the  $U_{xx}$  truncation error.

For second-order schemes, the lowest-order truncation error is a dispersive error of the form  $\beta \Delta x^2 U_{xxx}$ . Hence, the dominating effect is not of a dissipative nature and care has to be exercised in the interpretation of terms like  $\bar{D}$  and  $D$  as ‘viscosity’ coefficients in a strict sense.

## 17.4 LERAT'S IMPLICIT SCHEMES OF LAX–WENDROFF TYPE

The schemes of the Lax–Wendroff family presented in the previous sections are explicit as an outcome of the initial derivation by a Taylor expansion in time, followed by a central space discretization. When compared to the straightforward central space discretization of the flux terms,  $f_x = (f_{i+1} - f_{i-1})/2\Delta x$ , which is unstable with an explicit forward difference in time, the Lax–Wendroff approach can be considered as a means to introduce some dissipation in the scheme through the time derivative terms. This dissipation is proportional to the time step and is sufficient to stabilize the central flux difference, although additional dissipation has to be introduced in order to resolve the shock oscillations.

A similar line of development can be adopted to generate implicit schemes, in the line of the Lax–Wendroff ‘methodology’, by combining time and space discretizations in order to achieve certain desirable properties. This approach has been applied by Lerat (1979, 1985) to generate a family of implicit, central, second-order schemes depending on three parameters that are unconditionally stable and have dissipative properties, resulting in an implicit extension of the Lax–Wendroff schemes.

The reason behind the development of implicit schemes is to be found in the severe limitation on the permissible time step of explicit schemes as a consequence of the CFL-condition. If  $a_{\max}$  is the maximum speed of propagation of a one-dimensional problem  $a_{\max} = (|u| + c)_{\max}$ , the time step  $\Delta t$  is limited by

$$\Delta t < \text{CFL} \frac{\Delta x_{\min}}{a_{\max}} = \frac{\Delta x_{\min}}{(|u| + c)_{\max}} \text{CFL}$$

where CFL is the maximum Courant number. The maximum allowable time step  $\Delta t$  can become very small, particularly with fine meshes.

With steady-state problems, where the stationary solution is sought and convergence is reached when the variations  $\Delta U = U^{n+1} - U^n$  come below an imposed limit, explicit schemes will require a large number of time steps, of the order of several thousands. Although this concern becomes less severe with the development of new generations of vector and parallel processors and with the introduction of multi-grid techniques, it is still important to be able to reach the computed steady-state flow in a minimum of time steps.

When time accuracy is not required for stationary flows solved with a time-dependent method, one can apply a simple convergence acceleration technique by using *local time steps* which differ from one point to the other as a function of the local propagation speeds and corresponding local CFL condition. Hence, one will allow the solution to progress in time towards the steady-state conditions, at a different pace in each point.

The local time step at point  $i$  will be defined by

$$\text{CFL} \frac{\Delta x_{\min}}{(|u| + c)_{\max}} < \Delta t_i < \frac{\Delta x_{\min}}{(|u| + c)_i} \text{CFL}$$

The time evolution of the solution loses its physical significance since the time-dependent problem which is solved in this way corresponds to the pseudo time-dependent equation  $U_{,t^*} + f_x = 0$ , where  $t^* = t \cdot (|u| + c)_{\max}/(|u| + c)$ . An alternative for strongly varying mesh sizes is to select

$$t^* = t \frac{(|u| + c)_{\max}}{(|u| + c)} \cdot \frac{\Delta x}{\Delta x_{\min}}$$

leading to a local permissible time step

$$\Delta t_i = \text{CFL} \frac{\Delta x_i}{(|u| + c)_i} \quad (17.4.1)$$

This leads to significant improvements of convergence rates but remains limited since the overall convergence rate will still depend on the slowest progressing zones.

Implicit schemes can also be important for time-dependent problems when the time scale of the unsteady phenomena is much larger than the time step allowed by the CFL condition. Although time-accurate solutions are required in this case, the possibility of allowing larger time steps than the CFL limit leads to a welcome gain in computational efficiency.

Therefore an alternative to the explicit schemes lies in the development of implicit methods that allow, as a consequence of their unconditional stability, higher time steps, limited only by accuracy requirements and eventual non-linear stability problems or boundary condition treatment.

We will present the developments of Lerat in some detail in this section, not only because of the interest and importance of the resulting schemes but also

because of the considerable didactic value of the rigorous and systematic analysis at the basis of these developments. As we will see from the following, all the properties of numerical schemes will be called upon in order to specify conditions on the parameters of the scheme. The truncation error analysis will lead to conditions on the order of accuracy and the development of the equivalent differential equation will provide guidelines for optimization of the dispersion and diffusion errors. The Von Neumann analysis will lead to conditions for the stability of the scheme and also to conditions for the solvability of the implicit operators (non-vanishing of the implicit operator). Furthermore, the error analysis will allow conditions to be set for maximal dissipation of high-frequency errors; in particular it can be requested that the Kreiss dissipative condition be satisfied for the parameters of the schemes. The available degrees of freedom also allow the imposition of an additional condition on the implicit operator, namely strict diagonal dominance.

Finally, the resulting three-parameter family of schemes can be tuned to optimize certain desirable properties: for instance, maximize convergence rates for stationary problems, or minimize dissipation and dispersion errors for unsteady flows, or fix the order of accuracy of the first, explicit, step, opening a wide range of Lax–Wendroff variants for this step.

#### 17.4.1 Analysis for linear systems in one dimension

The starting point is the following, most general, implicit scheme with two time levels and three-point support for the linear system  $U_t + AU_x = 0$ , which generalizes the explicit form (9.2.10) in Volume 1:

$$c_{-1}U_{i-1}^{n+1} + c_0U_i^{n+1} + c_1U_{i+1}^{n+1} = b_{-1}U_{i-1}^n + b_0U_i^n + b_1U_{i+1}^n \quad (17.4.2)$$

The coefficients  $b_j$  and  $c_j$  are general functions of  $\tau = \Delta t/\Delta x$  and  $A$ . The following considerations are an extension of the procedures developed in Section 9.2 in Volume 1, to which the reader is referred for the details of the calculations concerning the truncation errors and the consistency conditions.

A first consistency condition, expressing that a constant  $U$  should be a possible solution, is

$$\sum_{j=-1}^{+1} b_j = \sum_{j=-1}^{+1} c_j = 1 \quad (17.4.3)$$

Performing a Taylor expansion in the same way as in Section 9.2.1, the  $(p+1)$  conditions for the scheme (17.4.2) to be accurate of order  $p$  in space and time for fixed ratios  $\tau = \Delta t/\Delta x$  are obtained as

$$\sum_j j^m b_j = \sum_j c_j(j - \sigma)^m \quad \text{for } m = 0, 1, 2, \dots, p \quad (17.4.4)$$

where  $\sigma$  is defined by

$$\sigma = \tau A \quad (17.4.5)$$

For a scalar equation,  $A = a$  and  $\sigma$  is the Courant number. For a system of equations,  $\sigma$  is a matrix whose maximum eigenvalue will represent the Courant number of the scheme, following equation (17.2.14).

It can be seen that equation (17.4.4) is a direct generalization of equation (9.2.23) and that the coefficients  $b_j$  and  $c_j$  are only dependent on  $\sigma$ .

Eliminating  $b_0$  and  $c_0$  via equation (17.4.3), four coefficients are left, and defining

$$\begin{aligned} b_+ &= b_1 + b_{-1} & b_- &= b_1 - b_{-1} \\ c_+ &= c_1 + c_{-1} & c_- &= c_1 - c_{-1} \end{aligned} \quad (17.4.6)$$

the schemes (17.4.2) can be written as follows (see problem 17.31):

$$U_i^{n+1} + c_- \bar{\delta} U_i^{n+1} + \frac{1}{2} c_+ \delta^2 U_i^{n+1} = U_i^n + b_- \bar{\delta} U_i^n + \frac{1}{2} b_+ \delta^2 U_i^n \quad (17.4.7)$$

The difference operators have been defined earlier (equation (14.1.2)) and  $\delta^2$  is the central second difference  $\delta^2 U_i = U_{i+1} - 2U_i + U_{i-1}$ . In  $\Delta$  form, equation (17.4.7) can be written as

$$[1 + c_- \bar{\delta} + \frac{1}{2} c_+ \delta^2] \Delta U_i^n = (b_- - c_-) \bar{\delta} U_i^n + \frac{1}{2} (b_+ - c_+) \delta^2 U_i^n \quad (17.4.8)$$

Note that it is assumed for the moment that  $A$  is a constant matrix and therefore the coefficients  $b$  and  $c$  are also independent of the mesh point index  $i$ .

Obviously we require that the schemes be at least first-order accurate and the first consistency condition (17.4.4) for  $m = 1$ ,

$$b_- - c_- = -\sigma \quad (17.4.9)$$

imposes the condition that the coefficient of the first difference in the right-hand side of equation (17.4.8) be equal to  $-\sigma$ . This merely shows that this term should be an approximation to the space derivative  $A \partial U / \partial x$ .

Equation (17.4.8) becomes

$$[1 + c_- \bar{\delta} + \frac{1}{2} c_+ \delta^2] \Delta U_i^n = -\sigma \bar{\delta} U_i^n + \frac{1}{2} (b_+ - c_+) \delta^2 U_i^n \quad (17.4.10)$$

The choice  $b_+ = c_+ = 0$  and  $c_- = \theta\sigma$  reproduces the Beam and Warming schemes (18.1.10) with  $\xi = 0$  to be introduced in the following chapter (see also Problem 17.30).

In addition, if the coefficient of the second difference term in the right-hand side is set equal to  $\gamma$ , the explicit scheme obtained by  $c_\pm = 0$  reproduces the family of first-order schemes (9.3.3).

If we look for, at least, *second-order schemes in space and time*, the relations (17.4.4) for  $m = 2$ , expressed as a function of the  $b_\pm$  and  $c_\pm$  coefficients, become

$$b_+ - c_+ = -2\sigma c_- + \sigma^2 \quad (17.4.11)$$

and equation (17.4.10) can be expressed as a function of the parameters  $c_\pm$  defining the *implicit part* of the algorithm as

$$[1 + c_- \bar{\delta} + \frac{1}{2} c_+ \delta^2] \Delta U_i^n = -\sigma \bar{\delta} U_i^n + \frac{1}{2} (\sigma - 2c_-) \sigma \delta^2 U_i^n \quad (17.4.12)$$

The explicit scheme, obtained by setting the  $c_{\pm}$  coefficients to zero, is the unique second-order space-centred scheme on the three-point support, namely the Lax–Wendroff scheme (17.2.6). For *any* other choice of the  $c_{\pm}$  coefficients, an implicit scheme is obtained, which maintains the second-order accuracy on the same three-point support.

The Beam and Warming schemes to be discussed in the following chapter are defined by the central discretization of the flux terms in the right-hand side of the  $\Delta$  formulation. This implies the absence of any second difference term in the right-hand side residuals, hence,  $c_- = \sigma/2$ , leading to the trapezoidal scheme  $\theta = \frac{1}{2}$ , when  $c_+ = 0$ .

For third-order accuracy, the additional condition

$$c_+ = \sigma c_- + \frac{1 - \sigma^2}{3} \quad (17.4.13)$$

has to be satisfied, while the unique fourth-order accurate scheme will satisfy, in addition, the condition

$$c_- = \frac{\sigma}{2} \quad (17.4.14)$$

#### *Von Neumann analysis: stability and solvability*

A classical Von Neumann stability analysis is applied to the general scheme (17.4.7), leading to the amplification matrix  $G$  defined by

$$[1 + Ic_- \sin \phi - c_+(1 - \cos \phi)]G = 1 + Ib_- \sin \phi - b_+(1 - \cos \phi) \quad (17.4.15)$$

A first condition to be imposed on the implicit operator is that the factor multiplying  $G$  (which is equal to one for an explicit scheme) should not vanish in the range  $\phi \in [-\pi, \pi]$ . This ensures that the scheme will always be *solvable*.

Hence this will be the case if

$$c_+ < \frac{1}{2} \quad (17.4.16)$$

The stability of the scheme can be analysed following Section 8.6.1 in Volume 1, where the conditions (8.6.7) can be directly applied. The following necessary and sufficient conditions are obtained in this linear case:

$$b_-^2 - c_-^2 \leq b_+ - c_+ \quad (17.4.17a)$$

$$b_+^2 - c_+^2 \leq b_+ - c_+ \quad (17.4.17b)$$

For an explicit scheme, where  $c_+ = c_- = 0$ , the stability conditions reduce to

$$b_-^2 \leq b_+ \leq 1 \quad (17.4.18)$$

For the Lax–Wendroff scheme, with  $b_- = \sigma$  and  $b_+ = \sigma^2$ , one obtains the CFL condition  $|\sigma| \leq 1$ .

#### *Dissipative properties*

The schemes (17.4.7) will be dissipative in the sense of Kreiss (see

equation (8.5.13)) if the spectral radius of  $G$  satisfies the condition

$$\rho(G) \leq 1 - K\phi^{2r} \quad \text{for } K > 0 \quad \text{and} \quad \phi[-\pi, \pi] \quad (17.4.19)$$

From an analysis of the amplification matrix in the limit as  $\phi \rightarrow 0$  and in the region  $\phi = \pi$ , it can be shown (Lerat, 1981) that the schemes considered are dissipative in the sense of Kreiss if the stability conditions (17.4.17) are satisfied with a strict inequality in (17.4.17b). This implies, next to stability, that

$$b_+ \neq c_+ \quad \text{and} \quad b_+ \neq 1 - c_+ \quad (17.4.20)$$

for all eigenvalues of  $A$ .

For an explicit scheme, these conditions reduce to

$$b_+ \neq 0 \quad \text{and} \quad b_+ \neq 1 \quad (17.4.21)$$

When the schemes are dissipative, the order of dissipation is four, with the exception of the first-order schemes which are dissipative of order two only.

For the Lax-Wendroff schemes,  $b_+ = \sigma^2$  and the scheme is dissipative when the Jacobian matrix  $A$  does not have zero eigenvalues.

### *Diagonal dominance*

A property on the implicit operator that guarantees the convenient resolution of the algebraic system of the unknowns  $U^{n+1}$  either by direct or by iterative methods, is the condition of strict diagonal dominance. For the system (17.4.2) applied to a scalar equation, this is expressed by

$$|c_0| > |c_1| + |c_{-1}| \quad (17.4.22)$$

or in function of the  $c_{\pm}$  coefficients as

$$|1 - c_+| > |c_+ + c_-| + |c_+ - c_-| \quad (17.4.23)$$

By simple inspection it is seen that the condition of strict diagonal dominance is satisfied if

$$c_+ < \frac{1}{2} \quad \text{and} \quad c_+ + |c_-| < 1 \quad (17.4.24)$$

Observe that the conditions (17.4.24) are more severe than the solvability condition (17.4.16).

### 17.4.2 Construction of the family of schemes

The above-derived properties have to be satisfied by the coefficients  $b_{\pm}$  and  $c_{\pm}$ , considered as arbitrary functions of  $\sigma = A \Delta t / \Delta x$ .

Realistic algorithms will be obtained if the schemes are restricted to coefficients that are polynomials of  $\sigma$ . Although one could define more complex schemes, they do not appear to be of general interest.

In addition, at least second-order accuracy in space and time is requested and the schemes with the lowest number of free parameters are obtained for

polynomials with degree lower or equal to two, as can be seen from equations (17.4.9) and (17.4.11).

Equation (17.4.11) shows that  $c_-$  may not be of degree higher than one and the most general form is then

$$\begin{aligned} c_- &= \alpha\sigma + \mu \\ c_+ &= \beta\sigma^2 + v\sigma + \gamma \end{aligned} \quad (17.4.25)$$

where  $\alpha, \beta, \gamma, \mu, v$  are real numbers.

If the condition (17.4.13) for third-order accuracy is introduced the coefficients have to be restricted to  $\beta = \alpha - \frac{1}{3}$ ,  $\gamma = \frac{1}{3}$ ,  $\mu = v$ , with  $\alpha \neq \frac{1}{2}$ . For  $\alpha < \frac{1}{2}$ , the third-order schemes are solvable and stable for  $\sigma \leq 1$ , and if the CFL number  $\sigma$  is restricted to  $\sigma < 1$ , the scheme is also dissipative and strictly diagonal dominant. A simple choice is  $\alpha = 0$ ,  $\beta = \frac{1}{3}$  and  $\gamma = \frac{1}{3}$ . The unique fourth-order scheme,  $\alpha = \frac{1}{2}$ ,  $\beta = \frac{1}{6}$ ,  $\gamma = \frac{1}{3}$ ,  $\mu = v = 0$  is solvable only if  $\sigma^2 < 1$  but in this case the scheme is not dissipative. It has been analysed in some detail by Harten and Tal-Ezer (1981).

Family of schemes are now constructed which are implicit and space centred, second-order accurate in space and time, unconditionally stable, dissipative, solvable and satisfying the scalar condition for strict diagonal dominance.

The requirement of space-centred schemes implies that the scheme remains invariant when  $(i-1)$  is changed into  $(i+1)$  while  $A$  changes into  $-A$ . Hence, from the formulation (17.4.7), it is seen that one should have

$$\begin{aligned} c_-(-\sigma) &= -c_-(\sigma) & \text{and} & \quad c_+(-\sigma) = c_+(\sigma) \\ b_-(-\sigma) &= -b_-(\sigma) & \text{and} & \quad b_+(-\sigma) = b_+(\sigma) \end{aligned} \quad (17.4.26)$$

With the choice (17.4.25) these conditions will be satisfied when  $\mu = v = 0$  and one obtains

$$\begin{aligned} c_- &= \alpha\sigma & b_- &= (\alpha - 1)\sigma \\ c_+ &= \beta\sigma^2 + \gamma & b_+ &= (1 - 2\alpha + \beta)\sigma^2 + \gamma \end{aligned} \quad (17.4.27)$$

The schemes (17.4.12) then take the following form:

$$[1 + \alpha\sigma\bar{\delta} + \frac{1}{2}(\beta\sigma^2 + \gamma)\delta^2] \Delta U_i^n = -\sigma\bar{\delta}U_i^n + \frac{1}{2}(1 - 2\alpha)\sigma^2\delta^2U_i^n \quad (17.4.28)$$

Some of the schemes to be discussed in the next chapter belong to the family (17.4.28). The choice  $\alpha = \frac{1}{2}$ ,  $\beta = \gamma = 0$  is the trapezoidal Beam and Warming scheme corresponding to  $\theta = \frac{1}{2}$ ,  $\xi = 0$ . The choice  $\alpha = \frac{1}{2}$ ,  $\beta = 0$ ,  $\gamma = \frac{1}{3}$  reproduces the scheme (18.1.14) for  $\theta = \frac{1}{2}$ ,  $\xi = 0$ , which has fourth-order spatial accuracy but is only second order in time.

More insight is obtained when the algorithm (17.4.28) is written as a two-step scheme, whereby the explicit part is separated from the implicit operations. Defining an intermediate variation  $\bar{\Delta}U$  by

$$\bar{\Delta}U_i = -\sigma\bar{\delta}U_i^n + (\frac{1}{2} - \alpha)\sigma^2\delta^2U_i^n \quad (17.4.29a)$$

$$[1 + \alpha\sigma\bar{\delta} + \frac{1}{2}(\beta\sigma^2 + \gamma)\delta^2] \Delta U_i^n = \bar{\Delta}U_i \quad (17.4.29b)$$

The first step, (17.4.29a), is an explicit operation that defines  $\overline{\Delta U_i}$  by a Lax-Wendroff-type scheme. For  $\alpha = 0$ , this step is identical to the Lax-Wendroff scheme and has the same CFL limitations on the maximum time step for stability. However, the second step introduces an implicit correction on  $\overline{\Delta U_i}$ , which extends the admissible maximum Courant number and provides additional dissipation through the parameters  $\alpha, \beta$  and  $\gamma$ .

When  $\alpha = \beta = \gamma = 0$ , the scheme is identical to the explicit Lax-Wendroff scheme. However, for  $\alpha \neq 0$ , the explicit step is only first-order accurate and the implicit step provides a correction on the truncation error of the first step, such that the overall solution  $U^{n+1} = U^n + \Delta U^n$  is second-order accurate.

The above general requirements can now be translated into conditions on the coefficients  $\alpha, \beta, \gamma$ . The solvability condition (17.4.16) has to be valid for all values of  $\sigma$ , and from

$$\beta\sigma^2 + \gamma < \frac{1}{2} \quad (17.4.30)$$

we deduce

$$\beta \leq 0 \quad \text{and} \quad \gamma < \frac{1}{2} \quad (17.4.31)$$

Adding the conditions for unconditional linear stability requires

$$\beta \leq \alpha - \frac{1}{2}, \quad \gamma < \frac{1}{2}, \quad \alpha \leq \frac{1}{2} \quad (17.4.32)$$

In order to ensure a dissipative scheme, the conditions (17.4.20) have to be satisfied, that is

$$(1 - 2\alpha)\sigma^2 \neq 0 \quad (17.4.33)$$

When the eigenvalues of  $A$  are different from zero, the parameter  $\alpha$  may not take the value  $\frac{1}{2}$ . Hence the last condition in (17.4.32) is to be replaced by

$$\alpha < \frac{1}{2} \quad (17.4.34)$$

It is to be observed at this point that the schemes will not be dissipative when the eigenvalues of the Jacobian matrix go through zero, that is at sonic and stagnation points. Therefore, these schemes might still need some artificial dissipation to damp oscillations that would occur at shock discontinuities (Sides, 1985). However, further extensions by Lerat and Sides (1986) indicate that with an appropriate treatment of the explicit step and the addition of implicit boundary conditions, excellent shock-capturing properties are obtained without any artificial viscosity.

Finally, the conditions (17.4.24) for diagonal dominance are satisfied for all values of  $\sigma$  if

$$\beta < -\frac{\alpha^2}{4(1-\gamma)} \quad \text{or} \quad \alpha = \beta = 0 \quad (17.4.35)$$

and

$$\gamma < \frac{1}{2}$$

Hence all the properties will be satisfied for all values of the CFL number  $\sigma$  if

$$\beta \leq \alpha - \frac{1}{2}, \quad \gamma < \frac{1}{2}, \quad \alpha < \frac{1}{2} \quad \text{and} \quad \beta < -\frac{\alpha^2}{4(1-\gamma)} \quad (17.4.36)$$

This still leaves a large number of possible schemes, and additional conditions can be imposed in order to satisfy certain properties, such as the maximum convergence rate or minimal error generation.

### *Selection of parameters*

The parameter  $\gamma$  does not seem to play an important role in the definition of the properties of the second-order schemes (17.4.29). This can be seen, for instance, on the expression of the amplification matrix  $G$  (equation (17.4.15)), which takes on the following form when the definitions (17.4.27) are introduced:

$$G - 1 = \frac{-I\sigma \sin \phi - (1 - 2\alpha)\sigma^2(1 - \cos \phi)}{1 + I\alpha\sigma \sin \phi - (\beta\sigma^2 + \gamma)(1 - \cos \phi)} \quad (17.4.37)$$

As in the implicit step (17.4.29b), the parameter  $\gamma$  appears always in the combination  $(\beta\sigma^2 + \gamma)$  and its influence can be overtaken by the parameter  $\beta$ . Hence, setting  $\gamma = 0$  will not affect the generality of the schemes, nor limit the influence of the remaining parameters  $\alpha$  and  $\beta$ .

Analysing further the amplification matrix, it is seen that for  $\alpha = \frac{1}{2}$ , the scheme does not damp the high-frequency errors, since in this case  $G = 1$  for  $\phi = \pi$ . Hence the scheme is not dissipative in the sense of Kreiss when  $\alpha = \frac{1}{2}$ . For other values of  $\alpha$ , the parameter  $(1 - 2\alpha)$  controls the dissipation of the high-frequency errors, since

$$G(\phi = \pi) = 1 - \frac{2\sigma^2(1 - 2\alpha)}{1 - 2(\beta\sigma^2 + \gamma)} \quad (17.4.38)$$

On the other hand, the parameter  $\beta$  controls the behaviour of the scheme at high Courant numbers, that is for very large time steps. This is particularly interesting for steady-state computations, where it is expected to reach the stationary conditions as fast as possible.

### *Steady-state computations*

For increasing  $\sigma$ , the amplification matrix tends to the limits

$$G \underset{\sigma \rightarrow \infty}{\approx} 1 + \frac{1 - 2\alpha}{\beta} \quad (17.4.39)$$

and the maximum convergence rate is achieved for

$$\beta = 2\alpha - 1 \quad (17.4.40)$$

since  $G \rightarrow 0$  in this case.

The behaviour at the low-frequency end of the error spectrum is obtained

from an expansion of the amplification matrix in powers of  $\phi$  or, alternatively, from the first terms of the truncation error.

Applying the Taylor expansion technique to the scheme (17.4.29), following the approach outlined in Section 9.2 in Volume 1 leads to the following equivalent differential equation of scheme (17.4.29) (see Problem 17.33):

$$\begin{aligned} U_t + AU_x &= -\frac{\Delta x^2}{6} A[(1-3\gamma) + \sigma^2(3\alpha - 3\beta - 1)]U_{xxx} \\ &\quad - \frac{\Delta x^3}{8} \sigma A(1-2\alpha)[(1-2\gamma) + \sigma^2(2\alpha - 2\beta - 1)]U_{xxxx} \end{aligned} \quad (17.4.41)$$

From the conditions (17.4.36) it is seen that the coefficient of the  $U_{xxx}$  term describing the dispersion error never vanishes, which is to be expected from a second-order scheme. Observe that the conditions  $\gamma = \frac{1}{3}$ ,  $\beta = \alpha - \frac{1}{3}$ , which make the dispersion error vanish, are precisely the conditions for third-order accuracy of the scheme.

### *Unsteady flow computations*

Many unsteady flows have time scales much larger than the time scale of the propagation of the acoustic waves. In this case, the Courant number limitation of an explicit Lax–Wendroff-type method will lead to allowable time steps that are much smaller than the time steps requested by an accurate simulation of the physical phenomena. In these circumstances, occurring for instance for the flow along an oscillating airfoil, there is much to be gained by the use of implicit methods, where one can adapt the time steps to the desired accuracy without being limited by CFL conditions of explicit methods.

One would like, in such a situation, to minimize the dispersion and diffusion errors during computation. This can be achieved by looking at the dominant contributions to these errors from the right-hand side of equation (17.4.41) for large values of the Courant number  $\sigma$ , namely the coefficients of the  $\sigma^2$  terms.

From the conditions (17.4.36), it is seen that the coefficient of  $\sigma^2$  in the dispersion error never vanishes and reaches its lowest value for the choice

$$\beta = \alpha - \frac{1}{2} \quad (17.4.42)$$

which is also the value for which the  $\sigma^2$  term vanishes in the dissipation error term. Observe also that the coefficient of the  $U_{xxxx}$  term is always negative, as it should be for stability, as seen in Section 9.2 in Volume 1.

### 17.4.3 Extension to non-linear systems in conservation form

The derived family of implicit schemes (17.4.29) can be extended in a straightforward way to the non-linear system in conservation form

$$\frac{\partial U}{\partial t} + \frac{\partial f}{\partial x} = 0 \quad (17.4.43)$$

as follows:

$$\overline{\Delta U}_i = -\tau \bar{\delta} f_i^n + (\frac{1}{2} - \alpha) \tau^2 \delta (A_i^n \delta f_i^n) \quad (17.4.44a)$$

$$\left[ 1 + \alpha \tau \bar{\delta} A_i^n + \frac{\beta}{2} \tau^2 \delta (A_i^2 \delta) + \frac{\gamma}{2} \delta^2 \right] \Delta U_i = \overline{\Delta U}_i \quad (17.4.44b)$$

The scheme (17.4.44) can be considered as constituted of an explicit step of the Lax-Wendroff type, to which it reduces exactly for  $\alpha = 0$  (see equation (17.2.5)), followed by an implicit operator defined by equation (17.4.44b).

Introducing the numerical flux of the scheme

$$f_{i+1/2}^* = \frac{f_i + f_{i+1}}{2} - (1 - 2\alpha) \frac{\tau}{2} A_{i+1/2} (f_{i+1} - f_i) \quad (17.4.45)$$

equation (17.4.44) becomes

$$\left[ 1 + \alpha \tau \bar{\delta} A_i + \frac{\beta}{2} \tau^2 \delta (A_i^2 \delta) + \frac{\gamma}{2} \delta^2 \right]^n \Delta U_i = -\tau \delta f_i^* \quad (17.4.46)$$

The choice  $\alpha = 0$  is of particular interest since the explicit step becomes of second-order accuracy and is then identical to the Lax-Wendroff scheme. In addition the  $\beta$  term in the implicit operator,

$$\beta \tau^2 \delta (A^2 \delta \Delta U) \sim \beta \Delta t^3 A^2 U_{txx} \sim \beta \Delta t^3 U_{ttt} \quad (17.4.47)$$

is of the same order as the truncation error of the Lax-Wendroff scheme.

The implicit step can therefore be considered as an implementation of a correction to the explicit truncation error without affecting the overall accuracy of the scheme.

Note that in the non-linear case, the maximum order of accuracy cannot exceed two, since the non-linear fluxes introduce truncation terms proportional to  $\Delta x^2$ , as seen in Section 9.4 in Volume 1.

A similar idea of increasing the accuracy of a scheme by solving a modified equation, obtained after subtracting a fraction of the leading non-linear truncation error, has also been analysed and exploited by Klopfer and McRae (1983).

With the choice  $\gamma = 0$ , the simplified schemes with  $\alpha = 0$  become

$$\overline{\Delta U}_i = -\tau \bar{\delta} f_i^n + \frac{1}{2} \tau^2 \delta (A_i^n \delta f_i^n) \quad (17.4.48a)$$

$$\left[ 1 + \frac{\beta}{2} \tau^2 \delta (A_i^2 \delta) \right] \Delta U_i = \overline{\Delta U}_i \quad (17.4.48b)$$

The choice  $\alpha = 0$  allows the substitution of the explicit step by any other scheme which is linearly equivalent to the Lax-Wendroff schemes. Therefore, any of the methods discussed in Section 17.2 can be used. Lerat (1981) and Lerat *et al.*, (1982, 1985) have applied various versions of the  $S_\alpha^\beta$  scheme, in particular the optimal choice  $(1 + \sqrt{5}/2, 0)$  for the explicit step.

For steady-state calculations, optimal convergence rates will be obtained with

the choice (17.4.40), that is  $\beta = -1$ , while unsteady calculations will be optimized by selecting  $\beta = -\frac{1}{2}$ , following (17.4.42).

Since the first, explicit, step has the full second-order accuracy of the scheme, the intermediate value  $\bar{\Delta}U$  can be considered as equal to  $\Delta t \cdot R^n$ , where  $R^n$  is the residual of the space balance of the fluxes.

The implicit step can therefore be viewed as a way of redistributing the residuals, producing a new value  $\Delta U$  from the explicit initial approximation  $\bar{\Delta}U$ . In particular, considering  $A^2$  as a constant in the implicit step is identical to the residual smoothing step applied by Jameson, as will be seen in next chapter, equation (18.3.10).

For steady-state computations, the *physical* solution corresponds to  $\bar{\Delta}U = 0$ , that is to the right-hand side of the first, explicit, step equal to zero. The second, implicit, step improves the convergence rate by allowing large time steps through the unconditional stability and provides additional dissipation to damp undesirable high-frequency errors. However, it has no effect on the final converged solution which is completely defined by the first, explicit, step. Hence, the second step can be viewed, for steady-state problems, as a *mathematical or numerical step*.

### *Simplification of the schemes*

The block tridiagonal system in (17.4.48b) can be replaced by scalar tridiagonal inversions if  $A_i$  is approximated by its maximum eigenvalue  $a_{\max} = |u| + c_{\max}$ . The system (17.4.48b) becomes, with  $\rho(A)$  representing the spectral radius of the matrix  $A$ ,

$$\left[ 1 + \frac{\beta}{2} \tau^2 \delta (\rho^2(A_i) \delta) \right] \Delta U_i = \bar{\Delta}U_i \quad (17.4.49)$$

The implicit operator is simplified to scalar tridiagonal operations instead of the block tridiagonal. This reduces the computational cost of the scheme but slows down the convergence rate, as can be seen from the amplification matrix, which becomes, instead of (17.4.37),

$$G - 1 = \frac{-\sigma I \sin \phi + \sigma^2 (\cos \phi - 1)}{1 + \beta \sigma_{\max}^2 (\cos \phi - 1)} \quad (17.4.50)$$

In the large time step limit

$$G \underset{\sigma \rightarrow \infty}{\approx} 1 - \frac{\sigma^2}{\beta \sigma_{\max}^2} \quad (17.4.51)$$

Hence, the asymptotic value  $G \rightarrow_{\Delta t \rightarrow \infty} 0$  cannot be reached and slower convergence rates are to be expected. This is confirmed by computations in a diverging nozzle by Lerat *et al.* (1985), as shown in Figure 17.4.1. The results shown in Figure 17.4.1 have been obtained with the simplified schemes (17.4.48) and (17.4.49).

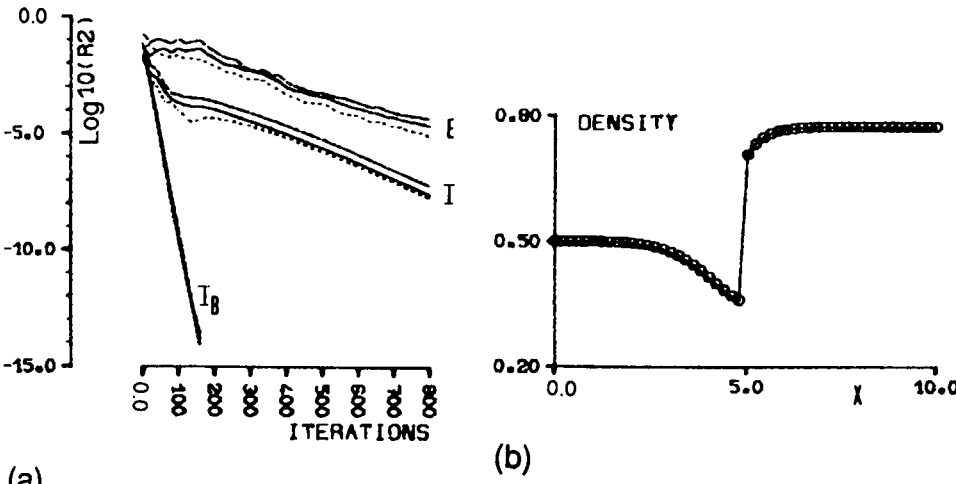


Figure 17.4.1 (a) Convergence history for a one-dimensional nozzle flow with Lerat's implicit (Lax-Wendroff) schemes.  
E Explicit Lax-Wendroff scheme, (CFL = 1)  
I Implicit diagonalized version (17.4.49),  $\beta = -1$ , CFL = 20  
I<sub>B</sub> Implicit block tridiagonal version (17.4.48),  $\beta = -1$ , CFL = 20  
(b) Computed density variation with run I<sub>B</sub>. (From Lerat *et al.*, 1985)

Figure 17.4.1(a) shows a comparison at a CFL number of 20 of the convergence rates for the implicit steps with block tridiagonal inversions (17.4.48b) and with the scalar inversion (17.4.49).

The rate of convergence of the Lax-Wendroff explicit step (E) is also shown at CFL = 1. The converged density distribution is shown in Figure 17.4.1(b), illustrating the good shock-capturing properties of the scheme. The simplification introduced by equation (17.4.49) will therefore only be interesting at low CFL numbers.

#### Boundary conditions

A detailed analysis of the impact of the boundary conditions on stability of the implicit schemes (17.4.48) and (17.4.49) has been performed by Daru (1983) and Daru and Lerat (1985) for the one-dimensional nozzle flows. The results of the analysis can be summarized as follows, referring to Chapter 19 for more details on the various options and to the original references for the detailed derivations:

- (1) At supersonic inlet  $\Delta U = 0$  may be taken at the boundaries.
- (2) At a supersonic outlet section, the unknowns can be obtained by zero-order extrapolation in a stable way.
- (3) At a subsonic outlet, zero-order extrapolation is always stable. Linear extrapolation is also always stable with the exception of the case  $\beta = -1$  for the scheme (17.4.48) for which the stability is conditional and restricted to  $CFL < 5$ . Quadratic extrapolation is always unstable.

#### 17.4.4 Extension to multi-dimensional flows

The family of schemes with  $\alpha = \gamma = 0$  has an explicit step which is identical to the Lax–Wendroff scheme and therefore the extension to two-dimensional flows can be obtained by taking any of the two-dimensional versions of Section 17.2 as the first, explicit, step.

If  $\overline{\Delta U}_{ij}$  is the explicit variation at mesh point  $(i,j)$ , the generalization of the implicit step can be defined as

$$\left[ 1 + \frac{\beta}{2} \tau_x^2 \delta_x (A_{ij}^2 \delta_x) + \frac{\beta}{2} \tau_y^2 \delta_y (B_{ij}^2 \delta_y) \right] \Delta U_{ij} = \overline{\Delta U}_{ij} \quad (17.4.52)$$

In order to avoid block pentadiagonal systems, an ADI factorization is applied, reducing the implicit part of the algorithm to a two-step procedure

$$\begin{aligned} \left[ 1 + \frac{\beta}{2} \tau_x^2 \delta_x (A_{ij}^2 \delta_x) \right] \Delta U_{ij}^* &= \overline{\Delta U}_{ij} \\ \left[ 1 + \frac{\beta}{2} \tau_y^2 (B_{ij}^2 \delta_y) \right] \Delta U_{ij} &= \Delta U_{ij}^* \end{aligned} \quad (17.4.53)$$

For steady-state problems, the value  $\beta = -1$  is recommended.

A further simplification can be considered, losing, however, the optimal convergence rates for high CFL numbers, by replacing the Jacobians  $A$  and  $B$  by their spectral radius. This leads to implicit systems that are scalar tridiagonal, as in equation (17.4.49), and the implicit steps (17.4.53) reduce to

$$\begin{aligned} \left[ 1 + \frac{\beta}{2} \tau_x^2 \delta_x (\rho^2 (A_{ij}) \delta_x) \right] \Delta U_{ij}^* &= \overline{\Delta U}_{ij} \\ \left[ 1 + \frac{\beta}{2} \tau_y^2 \delta_y (\rho^2 (B_{ij}) \delta_y) \right] \Delta U_{ij} &= \Delta U_{ij}^* \end{aligned} \quad (17.4.54)$$

Applications of this approach to steady and unsteady two-dimensional inviscid flows can be found in Sides (1985), Lerat *et al.* (1982, 1985) and Lerat and Sides (1986), where the explicit step is based on the two-dimensional version of the  $S_\alpha^\beta$  schemes presented in Section 17.2.

## 17.5 SUMMARY

The Lax–Wendroff family of schemes has been presented at some length in this chapter, since they play a major role in the development of discretization methods for compressible Euler and Navier–Stokes equations. They are still widely used, in particular under the form of the MacCormack predictor–corrector formulation.

An important feature is the requirement of the addition of artificial dissipation terms in order to remove the oscillations around discontinuities. This requires

good judgement and empiricism and several possible forms have been described, although many others can be defined. A rational method for the determination of artificial dissipation terms will also be presented in Chapter 21, in connection with TVD upwind schemes, leading to a bridge between the central and the upwind methods.

If the one-dimensional form of the Lax-Wendroff schemes is straightforward to apply, a larger variety exists in multidimensions. In this connection, the two-step formulation of  $N_i$  can be recommended as an interesting alternative, in particular when coupled to a multigrid approach. This can actually be generalized to any two-step formulation: the explicit Lax-Wendroff schemes should best be applied with multigrid schemes for stationary problems in order to compensate for the unfavourable CFL limitations on the allowable time step.

Another interesting approach for steady state problems is the implicit version of Lerat, which can be tuned to optimal convergence for high CFL and shows also excellent shock resolution without artificial dissipation, Lerat and Sides (1986, 1988).

## References

- Burstein, S. Z. (1967). 'High order accurate difference methods in hydrodynamics.' In F. Ames (ed.), *Nonlinear Partial Difference Equations*, pp. 279-90, New York: Academic Press.
- Casier, F., Deconinck, H., and Hirsch Ch. (1983). 'A class of central bidiagonal schemes with implicit boundary conditions for the solution of Euler's equations.' *AIAA Paper 83-0126*, AIAA 21st Aerospace Sciences Meeting. See also *AIAA Journal*, Vol. 22, 1556-1563.
- Couston, M., McDonald, P. W., and Smolderen, J. (1975). 'The Damping surface technique for time dependent solutions to fluid dynamics problems.' *Von Karman Institute Report VKI-TN 109*, Brussels, Belgium.
- Daru, V. (1983). 'Contribution à l'étude d'une méthode numérique implicite pour résoudre les équations d'Euler.' Thèse de 3ème cycle, Université de Paris VI.
- Daru, V., and Lerat, A. (1985). 'Analysis of an implicit Euler solver.' In Angrand et al. (eds), *Numerical Methods for the Euler Equations of Fluid Dynamics*. Philadelphia: SIAM Publications.
- Denton, J. (1975). 'A time marching method for two and three dimensional blade to blade flows.' *R & M 3795*, Aeronautical Research Council.
- Denton, J. (1982). 'An improved time marching method for turbomachinery flow calculations.' In P. L. Roe (ed.), *Numerical Methods in Aeronautical Fluid Dynamics*, London: Academic Press.
- Fourmaux, A., and Le Meur, A. (1987). 'Computation of unsteady phenomena in transonic turbines and compression.' *Onera Report TP 131*, Onera, France.
- Hall, M. G. (1985). 'Cell-vertex multigrid schemes for solutions of the Euler equations.' In Proc. IMA Conference on Numerical Methods in Fluids, Oxford: Oxford University Press.
- Harten, A. (1983a). 'On the symmetric form of systems of conservation laws with entropy.' *Journal Computational Physics*, **49**, 151-64.
- Harten, A. (1983b). 'High resolution schemes for hyperbolic conservation laws.' *Journal Computational Physics*, **49**, 357-93.
- Harten, A., and Tal-Ezer, H. (1981). 'On a fourth order accurate implicit scheme for hyperbolic conservation laws.' *Mathematics of Computation*, **36**, 353.

- Jameson, A. (1982). 'Transonic aerofoil calculations using the Euler equations.' In P. L. Roe (ed.), *Numerical Methods in Aeronautical Fluid Dynamics*, New York: Academic Press.
- Jameson, A., Schmidt, W., and Turkel, E. (1981). 'Numerical simulation of the Euler equations by finite volume methods using Runge-Kutta time stepping schemes.' *AIAA Paper 81-1259*, AIAA 5th Computational Fluid Dynamics Conference.
- Klopfer, G. H., and McRae, D. S. (1983). 'Nonlinear truncation error analysis of finite difference schemes for the Euler equations.' *AIAA Journal*, 21, 487-94.
- Koeck, C. (1985). 'Computation of three-dimensional flow using the Euler equations and a multiple-grid scheme.' *Int. Journal for Numerical Methods in Fluids*, 5, 483-500.
- Lax, P. D. (1954). 'Weak solutions of non linear hyperbolic equations and their numerical computation.' *Comm. Pure and Applied Mathematics*, 7, 159-93.
- Lax, P. D. (1957). 'Hyperbolic systems of conservation laws II.' *Comm. Pure and Applied Mathematics*, 10, 537-66.
- Lax, P. D., and Wendroff, B. (1960). 'Systems of conservation laws.' *Comm. Pure and Applied Mathematics*, 13, 217-37.
- Lax, P. D., and Wendroff, B. (1964). 'Difference schemes for hyperbolic equations with high order of accuracy.' *Comm. Pure and Applied Mathematics*, 17, 381-98.
- Lerat, A. (1979). *Une Classe de Schémas aux Différences Implicites pour les Systèmes Hyperboliques de Lois de Conservation*, Vol. 288A, pp. 1033-6, Paris: Comptes Rendus Académie des Sciences.
- Lerat, A. (1981). 'Sur le calcul des solutions faibles des systèmes hyperboliques de lois de conservations à l'aide de schémas aux différences.' *Publication ONERA 1981-1*.
- Lerat, A. (1985). 'Implicit methods of second order accuracy for the Euler equations.' *AIAA Journal*, 23, 33-40.
- Lerat, A., and Peyret, R. (1974). 'Non centered schemes and shock propagation problems.' *Computers and Fluids*, 2, 35-52.
- Lerat, A., and Peyret, R. (1975). 'The problem of spurious oscillations in the numerical solution of the equations of gas dynamics.' *Lecture Notes in Physics*, Vol. 35, pp. 251-256, New York: Springer Verlag.
- Lerat, A., and Sides, J. (1977). 'Calcul numérique d'écoulements transsoniques instationnaires.' *AGARD Conference Proc. CP-226*, pp. 15.1-15.10.
- Lerat, A., and Sides, J. (1982). 'A new finite volume method for the Euler equations with applications to transonic flows.' In P. L. Roe (ed.), *Numerical Methods in Aeronautical Fluid Dynamics*, New York: Academic Press.
- Lerat, A., and Sides, J. (1986). 'Implicit transonic calculations without artificial viscosity or upwinding.' *GAMM Workshop on Numerical Simulation of Compressible Euler Flows*, Vieweg and Sols, Braunschweig. Also, ONERA TP, 87-195.
- Lerat, A., Sides, J., and Daru, V. (1982). 'An implicit finite volume method for solving the Euler equations.' *Lecture Notes in Physics*, Vol. 170, pp. 343-9.
- Lerat, A., Sides, J., and Daru, V. (1985). 'Efficient computation of steady and unsteady transonic flows by an implicit solver.' In W. G. Habashi (ed.), *Advances in Computational Transonics*, London: Pineridge Press.
- Lerat, A., and Sides, J. (1988). 'Efficient solution of the steady Euler equations with a centered implicit method.' In Morton and Baines (eds), *Numerical Methods for Fluid Dynamics III*, 65-86, Clarendon Press, Oxford.
- MacCormack, R. W. (1969). 'The effect of viscosity in hypervelocity impact cratering.' *AIAA Paper 69-354*.
- MacCormack, R. W., and Baldwin, B. S. (1975). 'A numerical method for solving the Navier-Stokes equations with application to shock-boundary layer interaction.' *AIAA Paper 75-1*.
- MacCormack, R. W., and Paullay, A. J. (1972). 'Computational efficiency achieved by time splitting of finite difference operators.' *AIAA Paper 72-154*.
- McDonald, P. W. (1971). 'The computation of transonic flow through two-dimensional gas turbine cascades.' *ASME Paper 71-GT-89*.

- Magnus, R., and Yoshihara, H. (1975). 'Unsteady transonic flows over an airfoil.' *AIAA Journal*, **13**, 1622-8.
- McGuire, G. R., Morris, J. L. (1973). 'A class of second order accurate methods for the solution of systems of conservation laws.' *Journal Computational Physics*, **11**, pp. 531-549.
- Ni, R. N. (1982). 'A multiple grid scheme for solving the Euler equations.' *AIAA Journal*, **20**, 1565-71.
- Palumbo, D. J., and Rubin, D. L. (1972). 'Solution of the two-dimensional unsteady compressible Navier-Stokes equations using a second order accurate numerical scheme.' *Journal Computational Physics*, **9**, 466-95.
- Pulliam, T. H. (1984). 'Euler and thin layer Navier-Stokes codes: ARC2D, ARC3D.' *Proc. Computational Fluid Dynamics User's Workshop*, The University of Tennessee Space Institute, Tullahoma, Tennessee.
- Pulliam, T. H. (1985). 'Artificial dissipation models for the Euler equations.' *AIAA Paper 85-0438*, AIAA 23rd Aerospace Sciences Meeting.
- Pulliam, T. H., and Steger, J. L. (1985). 'Recent improvements in efficiency, accuracy and convergence for implicit approximate factorization algorithms.' *AIAA Paper 85-0360*, AIAA 23rd Aerospace Sciences Meeting.
- Richtmyer, R. D., and Morton, K. W. (1967). *Difference Methods for Initial Value Problems*, 2nd eds, New York: John Wiley and Sons.
- Rizzi, A. W., and Inouye, M. (1973). 'Time split finite volume method for three-dimensional blunt-body flows.' *AIAA Journal*, **11**, 1478-85.
- Roe, P. L. (1981). 'The use of the Riemann Problem in finite difference schemes.' *Lecture Notes in Physics*, Vol. 141, pp. 354-9, Berlin: Springer Verlag.
- Rubin, E. L., Burstein, S. Z. (1967). 'Difference methods for the inviscid and viscous equations of a compressible gas' *Journal Computational Physics*, **2**, pp. 178-196.
- Sides, J. (1985). 'Computation of unsteady transonic flows with an implicit numerical method for solving the Euler equations.' *La Recherche Aerospatiale*, **1985-2**, 17-39.
- Singleton, R. E. (1968). 'Lax-Wendroff difference scheme applied to the transonic airfoil problem.' *AGARD Conference Proc.*, CP-35, 2.1-2.9.
- Steger, J. L. (1978). 'Implicit finite difference simulation of flow about two-dimensional geometries.' *AIAA Journal*, **16**, 679-86.
- Strang, G. (1976). *Linear Algebra and Its Applications*, New York: Academic Press.
- Swanson, R. C., and Turkel, E. (1987). 'Artificial dissipation and central difference schemes for the Euler and Navier-Stokes equations.' *AIAA Paper 87-1107*, *Proc. AIAA 8th Computational Fluid Dynamics Conference*, pp. 55-69.
- Tadmor, E. (1984). 'The large time behaviour of the scalar, genuinely nonlinear Lax-Friedrichs Scheme.' *Mathematics of Computation*, **43**, pp. 353-368.
- Thompkins, W. T., Tong, S. S., Bush, R. H., Usab, W. J., and Norton, R. J. G. (1983). 'Solution procedures for accurate numerical simulations of flow in turbomachinery cascades.' *AIAA Paper 83-0257*, AIAA 21st Aerospace Sciences Meeting.
- Thommen, H. U. (1966). 'Numerical integration of the Navier-Stokes equations.' *ZAMP*, **17**, 369-84.
- Tong, S. S. (1987). 'The impact of smoothing formulations on the stability and accuracy of various time marching schemes.' *AIAA Paper 87-1106*, *Proc. AIAA 8th Computational Fluid Dynamics Conference*, pp. 47-54.
- Turkel, E. (1973). 'Symmetrization of the fluid dynamic matrices with applications.' *Mathematics of Computation*, **27**, 729-36.
- Turkel, E. (1977). 'Symmetric hyperbolic difference schemes and matrix problems.' *Linear Algebra and Applications*, **16**, 109-29.
- Van Hove, W., and Arts, A. (1979). 'Comparison of several finite difference schemes for time marching methods as applied to one dimensional nozzle flow.' *Von Karman Institute Report VKI-TN132*, Brussels, Belgium.
- Von Neumann, J., and Richtmyer, R. D. (1950). 'A method for the numerical calculations of hydrodynamical shocks.' *Journal Mathematical Physics*, **21**.

- Warming, R. F., Kutler, P., Lomax, H. (1973). 'Second and third order non centered difference schemes for non linear hyperbolic equations.' *AIAA Journal*, **11**, pp. 189–195.
- Yanenko, N. N. (1971). *The Method of Fractional Steps*, New York: Springer Verlag.
- Yanenko, N. N., Fedotova, Z. I., Kompaniets, L. A., and Shokin, Yu. I. (1984). 'Classification of difference schemes of gas dynamics by the method of differential approximation—two dimensional case.' *Computers and Fluids*, **12**, 93–119.
- Zeldovich, Y. B., Ranz, Y. P. (1967). *Physics of Shock Waves and High Temperature Hydrodynamic Phenomena*. Academic Press, New York.
- Zwas, G. (1973). 'On two step Lax–Wendroff methods in several dimensions.' *Numerische Mathematik*, **20**, 350–5.

## PROBLEMS

### Problem 17.1

Consider a modified one-dimensional Lax–Friedrichs scheme, applied to the scalar hyperbolic equation  $u_t + f_x = 0$ , instead of (17.1.4) (Tadmor, 1984):

$$u_i^{n+1} = \frac{1}{4}(u_{i+1} + 2u_i + u_{i-1}) - \frac{\tau}{2}(f_{i+1} - f_{i-1})$$

Analyse the stability, error spectrum and truncation error for this scheme. Show that the stability condition is now restricted to  $|\sigma| \leq 1/\sqrt{2}$ .

Derive the expression of the numerical flux  $f^*$  and observe that the above scheme corresponds to the addition of half of the stabilizing dissipation by comparing with equation (17.1.6).

### Problem 17.2

Derive the amplification matrix for the modified Lax–Friedrichs scheme (17.1.30) and show that the conditions (17.1.34) are sufficient for stability in the linear case.

### Problem 17.3

Apply the Lax–Friedrichs scheme in finite volume form to the hexagonal control volume ABCDEF of Figure 6.2.4 in Volume 1 on a Cartesian mesh, and a Lax–Friedrichs averaging over the six nodes. Derive the Von Neumann amplification matrix.

*Hint:* Write

$$\frac{\partial}{\partial t}(U\Omega) + \oint_{ABCDEF} (f dy - g dx) = 0$$

and take average values for the fluxes. For instance,  $f_{AB} = (f_{i+1,j} + f_{i,j-1})/2$ .

Obtain the following scheme, with  $\Omega = 3\Delta x \Delta y$ :

$$\begin{aligned} U_{ij}^{n+1} = & \frac{1}{6}(U_{i+1,j} + U_{i+1,j+1} + U_{i,j+1} + U_{i-1,j} + U_{i-1,j-1} + U_{i,j-1}) \\ & - \frac{1}{6\Delta y}(g_{i+1,j+1} + f_{i,j-1} + 2f_{i+1,j} - 2f_{i-1,j} - f_{i-1,j-1} - f_{i,j+1}) \\ & - \frac{1}{6\Delta y}(g_{i+1,j+1} + 2g_{i,j+1} + g_{i-1,j} - g_{i-1,j-1} - 2g_{i,j-1} - g_{i+1,j}) \end{aligned}$$

**Problem 17.4**

Solve Burger's equation  $u_t + uu_x = 0$  for a stationary discontinuity with the Lax-Friedrichs scheme.

*Hint:* Take  $u_L = 1$  and  $u_R = -1$  where  $u_L$  and  $u_R$  are the value of the solution left and right of the discontinuity. The shock velocity is equal to  $(u_L + u_R)/2$ ; therefore this choice gives a stationary shock.

Consider two cases:

- (1) Shock placed in a mesh point;
- (2) Shock located between two mesh points.

Start with an initial solution, linear over 20 mesh points, and take different CFL numbers, such as 0.2, 0.5, 0.8, 1. Plot and compare the results of these two cases every five time steps.

**Problem 17.5**

Repeat Problem 17.4 for a moving discontinuity by taking  $u_L = 1$ ,  $u_R = -0.8$ . Compare with the case  $u_L = 1$ ,  $u_R = 0.8$ .

**Problem 17.6**

Apply the Lax-Friedrichs scheme to the shock tube problem of Figure 16.5.8. Take  $CFL = 0.95$  and generate plots of the flow variables as a function of  $x$  after 15, 25 and 35 time steps. Compare with the exact solution.

**Problem 17.7**

Apply the Lax-Friedrichs scheme to the diverging nozzle with a shock at  $x = 4$ , shown in Figure 17.2.2. Take the same data and refer to Chapter 19 for the treatment of the boundary conditions. Apply a simple zero-order extrapolation technique for the numerical boundary conditions.

For the physical condition of downstream pressure, take the value of the exact solution.

Generate plots of the flow variables as a function of  $x$  and compare with the exact solution.

**Problem 17.8**

Find the amplification matrix for the two-step Richtmyer schemes (17.2.83) and (17.2.84). Reduce the scheme to a one-step form for the linearized case and compare with the Lax-Wendroff scheme.

*Hint:* Define an intermediate amplification matrix  $\bar{G}$  for the intermediate step by

$$U^{n+1/2} = \bar{G}U^n$$

and

$$U^{n+1} = GU^n$$

Calculate  $\bar{G}$  from the first step and the relation between  $G$  and  $\bar{G}$  from the second step.

**Problem 17.9**

Show that the form (17.2.21) can be obtained also from an analytical derivation of equation (17.2.4) where the flux derivative in the last term is replaced by  $AU_x$ , leading to a term  $(A^2U_x)_x$ .

Calculate directly the matrix  $A^2$  for the conservative variables and compare the discretized form of  $A^2 U_x$  with the expression (17.2.24) taking the right eigenvectors as defined in Chapter 16 and  $\delta w$  as  $w_{i+1} - w_i$ .

*Hint:* Obtain

$$A^2 = \begin{vmatrix} \frac{(\gamma-3)u^2}{2} & (3-\gamma)u & \gamma-1 \\ \left[ \frac{(3\gamma-7)u^2}{2} - c^2 \right] u & 3(2-\gamma)u^2 + c^2 & 3(\gamma-1)u \\ (5\gamma-9)\frac{u^4}{4} - \frac{3+\gamma}{2(\gamma-1)}c^2u^2 & \frac{7-5\gamma}{2}u^3 + \frac{2uc^2}{\gamma-1} & \frac{5\gamma-3}{2}u^2 + c^2 \end{vmatrix}$$

### Problem 17.10

Obtain the amplification matrices (17.2.50) and (17.2.92) for the one-step, two-dimensional Lax-Wendroff scheme and the two-step MacCormack version.

Compare the two expressions, in particular the high-frequency behaviour, and observe that MacCormack's scheme has a stronger damping of the high frequency for the same values of Courant numbers, and obtain the condition (17.2.93).

Write a programme to plot the lines of constant amplification in a diagram  $(\phi_x, \phi_y)$  for a range of values of the  $x$  and  $y$  Courant numbers.

### Problem 17.11

Extend the Lax-Wendroff derivation to the quasi-one-dimensional Euler equations for a nozzle flow (equation (16.4.1)).

Refer to Example 17.2.1 and obtain the following scheme generalizing equation (17.2.10):

$$\begin{aligned} U_i^{n+1} - U_i^n = & -\tau \bar{\delta} f_i^n + \frac{1}{2} \tau^2 \delta^+(A_{i-1/2} \delta^- f_i^n) \\ & + \Delta t \left[ Q_i - \frac{\tau}{2} \bar{\delta}(A_i Q_i) + X_i (\Delta t Q_i - \tau \bar{\delta} f_i) \right] \end{aligned}$$

where  $X = \partial Q / \partial U$  is the Jacobian matrix of the source term (see Problem 16.16).

Work out completely the matrix products of the terms containing the source vector and write out the three components of the additional corrections to  $\Delta t Q$  arising from the Taylor expansion in time.

Compare with the MacCormack formulation of Example 17.2.1 and derive the above result from the two-step version.

### Problem 17.12

Show that constant velocity lines should intersect a flat surface at right angles for an irrotational flow.

*Hint:* Calculate the direction of the constant velocity line  $q = \text{const.}$  as

$$\tan \alpha = \frac{dy}{dx} = -\frac{\partial q / \partial y}{\partial q / \partial x}$$

with the  $x$  direction along the surface.

Introduce the irrotational condition at the wall with  $v = 0$  to show that  $\alpha = 90^\circ$ .

**Problem 17.13**

Write the forward-backward and backward-forward versions of the MacCormack scheme on a Cartesian mesh.

Calculate the amplification factors.

**Problem 17.14**

Write the forward-backward and backward-forward versions of the MacCormack scheme in a finite volume form on an arbitrary mesh, on the control volume ABCD of Figure 17.2.14.

Write out all the terms explicitly and recover the versions of problem 17.13 on a regular mesh.

**Problem 17.15**

Develop the products  $L_x^{(LW)} L_y^{(LW)}$  in the split operator version (17.2.105) of the Lax-Wendroff scheme, assuming that the matrices  $A$  and  $B$  do not commute. Show that one does not recover all the terms of the unsplit version (17.2.48). Show by a Taylor expansion that the split scheme is no longer of second-order accuracy.

**Problem 17.16**

Show, by an explicit calculation, that Lerat's two-dimensional family of schemes reduces to the single-step Lax-Wendroff scheme (17.2.48) for constant matrices  $A, B$  and for all values of  $\alpha_1, \alpha_2, \beta_1, \beta_2$  coefficients.

**Problem 17.17**

Write out in full the Thommen scheme by introducing  $\alpha_1 = \alpha_2 = \beta_1 = \beta_2 = \frac{1}{2}$  in the general family of Lerat's predictor-corrector schemes. Calculate the amplification matrix and show that it is identical to the Lax-Wendroff amplification matrix (17.2.50).

**Problem 17.18**

Solve Burger's equation for the stationary discontinuity of Problem 17.4 with the distributive formulation of Lax and Wendroff. Compare the results with those obtained from the original Lax-Wendroff scheme and with MacCormack's scheme. Test with different Courant numbers.

**Problem 17.19**

Repeat the previous problem for the moving discontinuities of Problem 17.5.

**Problem 17.20**

Obtain the results of Figure 17.2.2 with MacCormack's scheme

Take the same data and refer to Chapter 19 for the treatment of the boundary conditions. Apply a simple zero-order extrapolation technique for the numerical boundary conditions.

For the physical condition of downstream pressure, take the value of the exact solution.

Generate plots of the flow variables as a function of  $x$  and compare with the exact solution. Plot in particular entropy, stagnation temperature and mass flux error in addition to the other variables.

**Problem 17.21**

Solve Problem 17.20 with the  $S_\alpha^\beta$  scheme of Lerat and Peyret. Compare different values of  $(\alpha, \beta)$  and observe that the choice  $\alpha = 1 + \sqrt{5}/2, \beta = \frac{1}{2}$  is indeed optimal.

**Problem 17.22**

Obtain the results of Figure 17.2.3 with MacCormack's scheme.

Take the same data and generate plots of the flow variables as a function of  $x$  and compare with the exact solution after 15, 25 and 35 time steps.

Experiment with other CFL numbers.

Test the alternative scheme (17.2.30).

Note that the expansion shock appears only when the end of the expansion fan is close enough to the sonic value.

**Problem 17.23**

Repeat Problem 17.22 with the  $S_\alpha^\beta$  scheme and compare the results for different values of the parameters  $\alpha, \beta$ .

**Problem 17.24**

Derive a finite volume formulation for the forward-forward version of MacCormack's scheme by considering the triangle PQR for the predictor step and PST for the corrector step, referring to Figure 17.2.14.

Apply the integration formulas (6.2.26) and (6.2.27) in Volume 1 to define average values of the flux derivatives over the triangles.

Show that one recovers the scheme (17.2.91) on a Cartesian mesh.

Obtain the other three versions of the two-dimensional MacCormack scheme by permutation of the triangles. For instance, the forward-backward version is obtained by selecting the triangle PRS for the predictor and PTQ for the corrector.

*Hint:* The integral of  $\partial f / \partial x$  over the triangle PQR leads to a discretization of the average value of this derivative as

$$\overline{\frac{\partial f}{\partial x}} = \frac{1}{\Omega_{PQR}} [f_{i+1,j}(y_{ij} - y_{i,j-1}) - f_{ij}(y_{i+1,j} - y_{i,j-1}) + f_{i,j-1}(y_{i+1,j} - y_{ij})]$$

and similar relations for the other derivatives.

**Problem 17.25**

Show the result (17.3.3) for the normal mode analysis of the stationary part of the Lax-Wendroff scheme.

Repeat the same normal mode analysis for the Lax-Friedrichs scheme.

**Problem 17.26**

Add the artificial viscosity of fourth order (17.3.15) to the Lax-Wendroff scheme applied to Burger's equation for the stationary discontinuity case of Problems 17.4 and 17.18. Compare with the results obtained without artificial dissipation.

**Problem 17.27**

Compare the effects of the artificial viscosity of fourth order with (a) Von Neumann-Richtmyer artificial viscosity and (b) MacCormack-Baldwin artificial viscosity applied to the test case of Problem 17.26.

**Problem 17.28**

Repeat Problem 17.20 by applying (a) Von Neumann–Richtmyer artificial viscosity and (b) MacCormack–Baldwin artificial viscosity, and obtain Figures 17.2.1 and 17.2.4. Experiment with different values of the adjustable coefficient and observe the influence of increasing this parameter.

**Problem 17.29**

Repeat Problem 17.22 by applying (a) Von Neumann–Richtmyer artificial viscosity and (b) MacCormack–Baldwin artificial viscosity, and obtain Figures 17.2.2 and 17.2.3. Compare with the outcome of the MacCormack–Baldwin artificial viscosity.

Experiment with different values of the adjustable coefficient and observe the influence of increasing this parameter.

**Problem 17.30**

Derive the conditions (17.4.4) by following the developments of Section 9.2.1 in Volume 1. Write out explicitly the conditions for the schemes (17.4.2) to be first-, second- and third-order accurate. Compare with the Beam and Warming schemes (18.1.10) and show that one can reproduce only the schemes  $\theta, \xi = 0$ . Explain the reason for this fact.

**Problem 17.31**

Obtain equations (17.4.7) and (17.4.8) and write the schemes explicitly by working out the difference operators.

**Problem 17.32**

Derive the stability conditions (17.4.17) by applying the method presented in Section 8.6.1 in Volume 1.

Obtain also the conditions for dissipation in the sense of Kreiss, by deriving the limit of the amplification matrix  $G$  for  $\phi \rightarrow 0$  and for  $\phi = \pi$ .

**Problem 17.33**

Obtain the equivalent differential equation (17.4.41) of Lerat's implicit schemes, by a Taylor series development of the scheme (17.4.29) following the method described in Chapter 9 in Volume 1.

**Problem 17.34**

Write the scheme (17.4.48) with  $\beta = -1$  as a one-step algorithm for  $U^{n+1}$ .

Observe that in this case the second difference disappears from the right-hand side explicit operator.

Compare and comment on the differences with the Beam and Warming scheme (18.1.10) for  $\xi = 0$  and  $\theta = 1$ .

*Hint:* The Scheme (17.4.48) with  $\beta = -1$  reads

$$U_i^{n+1} - \frac{1}{2}\tau^2 \delta(A_i^{2n} \delta U_i^{n+1}) = U_i^n - \tau \bar{\delta} f_i^n$$

or explicitly

$$U_i^{n+1} - \frac{\tau^2}{2} [A_{i+1/2}^{2n} (U_{i+1}^{n+1} - U_i^{n+1}) - A_{i-1/2}^{2n} (U_i^{n+1} - U_{i-1}^{n+1})] = U_i^n - \frac{\tau}{2} (f_{i+1}^n - f_{i-1}^n)$$

while the Beam and Warming scheme reduces to

$$U_i^{n+1} + \tau \bar{\delta}(A_i^n U_i^{n+1}) = U_i^n - \tau \bar{\delta} f_i^n + \tau \bar{\delta}(A_i^n U_i^n)$$

### Problem 17.35

Solve the inviscid Burger equation for a stationary shock with the implicit Lerat scheme (17.4.48) with  $\beta = -1$  at increasing CFL number  $\sigma$ .

Consider a linear initial distribution and solve for the cases where the shock is on a mesh point and between mesh points.

Observe the shock resolution and the convergence rate with increasing values of Courant number  $\sigma$ .

### Problem 17.36

Repeat Problem 17.35 by replacing the explicit step by the MacCormack two-step scheme.

### Problem 17.37

To the programme developed in Problem 17.28 add an implicit step (17.4.48) using the block tridiagonal solver.

Compare the convergence rate at different CFL values, with  $\beta = -1$ . Observe the effects of increasing the CFL number towards very high values.

Compare with the diagonalized version of equation (17.4.49).

Test different values of  $\beta$  and its influence on the convergence rate.